arXiv:1101.1876v1 [physics.flu-dyn] 7 Jan 2011

Fluctuating pressure correlations in wall turbulence

G. A. GEROLYMOS†, C. LO, D. SENECHAL, I. VALLET

Institut d'Alembert, Université Pierre-et-Marie-Curie (UPMC), 4 place Jussieu, 75005 Paris,
France

(Received 11 January 2011)

The purpose of the present paper is to study the influence of wall-echo on pressure fluctuations p', and on statistical correlations containing p', *viz* redistribution ϕ_{ij} and pressure diffusion $d_{ij}^{(p)}$. We extend the usual analysis of turbulent correlations containing pressure fluctuations in wall-bounded DNS computations [Kim J.: *J. Fluid Mech.* **205** (1989) 421–451], separating p' not only into rapid $p'_{(\mathrm{r})}$ and slow $p'_{(\mathrm{s})}$ parts [Chou P.Y.: *Quart. Appl. Math.* **3** (1945) 38–54], but further into volume (weakly inhomogeneous; $p'_{(\mathrm{r};\mathfrak{V})}$ and $p'_{(\mathrm{s};\mathfrak{V})}$) and surface (strongly inhomogeneous wall-echo; $p'_{(\mathrm{r};w)}$ and $p'_{(\mathrm{s};w)}$) terms. An algorithm, based on a Green's function approach, is developed to compute the above splittings for various correlations containing pressure fluctuations (redistribution, pressure diffusion, velocity/pressure-gradient), in fully developed turbulent plane channel flow. The DNS results are then used to assess several representative second-moment closures for near-wall turbulence. An extended representation basis including a tensor based on the unit vector in the dominant direction of turbulence inhomogeneity is proposed and applied in representing different models in a common framework.

Key Words: turbulence, pressure fluctuations, rapid and slow terms, wall echo, DNS, second-moment closure, Reynolds-stress model

1. Introduction

Understanding the physics of turbulent fluctuations of pressure p' is of major importance, not only because of their direct implication in noise (Hu *et al.* 2002, 2006) and excitation of immersed solid surfaces (Corcos 1964), but also because they appear in correlations present in the transport equations for the Reynolds-stresses and the dissipation tensor (Pope 2000; Jovanović 2004). Traditionally the analysis of p' is based on the Poisson equation for the fluctuating pressure (Chou 1945), which, at the incompressible flow limit ($\rho \approxeq \mathrm{const} = \bar{\rho}\ ; \forall t, x$ and $\mu \approxeq \mathrm{const} = \bar{\mu}\ ; \forall t, x$), in a nonrotating frame-of-reference, reads

$$\frac{1}{\rho}\nabla^2 p' = \frac{1}{\rho}\nabla^2 (p'_{\mathrm{r}} + p'_{\mathrm{s}}) = \underbrace{-2\frac{\partial u'_k}{\partial x_\ell}\frac{\partial \bar{u}_\ell}{\partial x_k}}_{\text{rapid}}\ \underbrace{-\frac{\partial^2}{\partial x_\ell \partial x_k}(u'_k u'_\ell - \overline{u'_k u'_\ell})}_{\text{slow}} \tag{1.1}$$

The incompressible flow Poisson equation (1.1) suggests that (Chou 1945) solenoidal (Hamba 1999) pressure fluctuations, associated with the fluctuating velocity field, are generated by 2 separate mechanisms (Rotta 1951*a*,*b*; Lumley 1978; Piquet 1999; Pope 2000; Jovanović 2004):

---

† Email address for correspondance: georges.gerolymos@upmc.fr

(*a*) the interaction of velocity fluctuations with mean-velocity-gradients called mean-flow/turbulence interaction terms, also termed rapid pressure fluctuations, because they interact immediately with an imposed mean-velocity-gradient, or linear pressure fluctuations, because the corresponding source-term is linear in velocity fluctuations, and

(*b*) the turbulence/turbulence interaction, also termed slow pressure fluctuations, because they react much slower than the rapid ones which are directly driven by mean-velocity-gradients, or nonlinear pressure fluctuations, because the corresponding source-term is quadratic in velocity fluctuations.

This idea of distinguishing between pressure fluctuations associated with mean-flow-gradients ($p'_{(\mathrm{r})}$) and pressure fluctuations associated with turbulence/turbulence interactions only ($p'_{(\mathrm{s})}$) can be applied in general to all correlations which contain the fluctuating pressure (Rotta 1951*a*,*b*; Lumley 1978; Hanjalić 1994; Piquet 1999; Pope 2000; Jovanović 2004).

Chou (1945) pointed out that, because of the linearity in p' of the incompressible flow Poisson equation (1.1), separate solutions can be obtained for each of the 2 source-terms, based on the freespace Green's function for the Poisson equation (Katz & Plotkin 1991)

$$\begin{aligned}\frac{1}{\rho}p'_{(\mathrm{r})}(\vec{x},t) = {} & \underbrace{\frac{1}{2\pi}\iiint_{\mathfrak{V}}\left(\frac{\partial\overline{\mathfrak{u}}_\ell}{\partial\mathfrak{x}_k}\frac{\partial\mathfrak{u}'_k}{\partial\mathfrak{x}_\ell}\right)\frac{d\mathfrak{v}(\vec{\mathfrak{x}},t)}{|\vec{\mathfrak{x}}-\vec{x}|}}_{p'_{(\mathrm{r};\mathfrak{V})}(\vec{x},t)} \\ & + \underbrace{\frac{1}{4\pi\rho}\iint_{\partial\mathfrak{V}}\left(\frac{1}{|\vec{\mathfrak{x}}-\vec{x}|}\frac{\partial\mathfrak{p}'_{\mathrm{r}}}{\partial\mathfrak{n}}-\mathfrak{p}'_{\mathrm{r}}\frac{\partial}{\partial\mathfrak{n}}\left[\frac{1}{|\vec{\mathfrak{x}}-\vec{x}|}\right]\right)d\mathfrak{S}(\vec{\mathfrak{x}},t)}_{p'_{(\mathrm{r};w)}(\vec{x},t)} \qquad (1.2a)\end{aligned}$$

$$\begin{aligned}\frac{1}{\rho}p'_{(\mathrm{s})}(\vec{x},t) = {} & \underbrace{\frac{1}{4\pi}\iiint_{\mathfrak{V}}\left(\frac{\partial^2\mathfrak{u}'_k\mathfrak{u}'_\ell}{\partial\mathfrak{x}_\ell\partial\mathfrak{x}_k}-\frac{\partial^2\overline{\mathfrak{u}'_k\mathfrak{u}'_\ell}}{\partial\mathfrak{x}_\ell\partial\mathfrak{x}_k}\right)\frac{d\mathfrak{v}(\vec{\mathfrak{x}},t)}{|\vec{\mathfrak{x}}-\vec{x}|}}_{p'_{(\mathrm{s};\mathfrak{V})}(\vec{x},t)} \\ & + \underbrace{\frac{1}{4\pi\rho}\iint_{\partial\mathfrak{V}}\left(\frac{1}{|\vec{\mathfrak{x}}-\vec{x}|}\frac{\partial\mathfrak{p}'_{\mathrm{s}}}{\partial\mathfrak{n}}-\mathfrak{p}'_{\mathrm{s}}\frac{\partial}{\partial\mathfrak{n}}\left[\frac{1}{|\vec{\mathfrak{x}}-\vec{x}|}\right]\right)d\mathfrak{S}(\vec{\mathfrak{x}},t)}_{p'_{(\mathrm{s};w)}(\vec{x},t)} \qquad (1.2b)\end{aligned}$$

where $p(\vec{x},t)$ and $\vec{u}(\vec{x},t)$ are the pressure and velocity at point $\vec{x}$, and the volume $d\mathfrak{v}(\vec{\mathfrak{x}},t)$ and surface $d\mathfrak{S}(\vec{\mathfrak{x}},t)$ integrals are taken over all other points $\vec{\mathfrak{x}}$ where the pressure and velocity are $\mathfrak{p}(\vec{\mathfrak{x}},t)$ and $\vec{\mathfrak{u}}(\vec{\mathfrak{x}},t)$. Notice that if (1.2) are multiplied by a function of $\vec{x}$, this function can be entered into the integrals which are over $\vec{\mathfrak{x}}$. In the case of unbounded flow, where $\partial\mathfrak{V}$ is very far (at infinity), only the volume integrals remain. On the other hand, for flow near solid boundaries, the surface integrals indicate that the unsteady pressure field reacts to the presence of the wall (surface integral; $\mathfrak{n}$ is the normal-to-the-wall coordinate, directed outwards from the fluid volume $\mathfrak{V}$). Terms related to the surface integrals are usually called wall-echo terms, also known as wall blockage effect (Hanjalić 1994), since for an isolated infinite plane solid boundary they can be related to reflection from the wall, using the method of images (Shir 1973; Launder *et al.* 1975; Gibson & Launder 1978; Piquet 1999; Pope 2000; Jovanović 2004).

Starting from the seminal paper of Chou (1945) all models (Rotta 1951*a*,*b*; Lumley

1978; Piquet 1999; Pope 2000; Jovanović 2004) for the redistribution tensor ϕ_{ij}, the velocity/pressure-gradient tensor Π_{ij} or the pressure transport $\overline{p'u'_i}$ appearing in the pressure-diffusion tensor $d_{ij}^{(p)}$, are traditionally composed of 4 parts corresponding to the splitting $p' = p'_{(\mathrm{r};\mathfrak{V})} + p'_{(\mathrm{r};w)} + p'_{(\mathrm{s};\mathfrak{V})} + p'_{(\mathrm{s};w)}$ (1.2). There is at present no possibility to separately measure $p'_{(\mathrm{r};\mathfrak{V})}$, $p'_{(\mathrm{r};w)}$, $p'_{(\mathrm{s};\mathfrak{V})}$, and $p'_{(\mathrm{s};w)}$, and the simultaneous measurement of p' and $\partial_{x_j} u'_i$ in the the wall-vicinity is a difficult challenge (Naka *et al.* 2006). Direct numerical simulation (DNS) offers the possibility to directly compute the different terms, experimental uncertainty being replaced by the eventual influence of finite size of the computational box and of convergence of statistics.

Kim (1989), in the context of pseudospectral DNS of incompressible plane channel flow (Kim *et al.* 1987; Moser *et al.* 1999), used a Green's function approach (Ince 1926; Courant & Hilbert 1953; Bender & Orszag 1978; Ockendon *et al.* 2003; Zauderer 2006; Myint-U & Debnath 2007) to solve, as a function of y (normal-to-the-wall coordinate), the incompressible flow Poisson equation for p' (1.1), for each parallel-to-the-wall wavenumber κ_x and κ_z.† The separate solution for each source-term (1.1), permits the separation of slow $p'_{(\mathrm{s})}$ and rapid $p'_{(\mathrm{r})}$ parts. In this way (Kim 1989; Chang *et al.* 1999), the slow and rapid contributions to ϕ_{ij} were computed (Mansour *et al.* 1988). This procedure (Kim 1989) is now used in a standard way in incompressible plane channel flow DNS, at least as far as $\overline{p'^2_{(\mathrm{s})}}$, $\overline{p'^2_{(\mathrm{r})}}$, and $\overline{p'^2_{(\tau)}}$ are concerned, and has also been extended to compressible flow studies (Foysi *et al.* 2004). The term $\overline{p'^2_{(\tau)}}$, usually called Stokes pressure (Mansour *et al.* 1988; Chang *et al.* 1999), corresponds to the separately computed contribution of the wall-boundary condition (Pope 2000, (11.173), p. 439) $[\partial_n p']_w = [\mu \partial^2_{nn} u'_n]_w$, n being the normal-to-the-wall direction. Notice that this boundary-condition is associated with the source-term $\partial^2_{x_i x_j}[\tau'_{ij}]$ in the Poisson equation for p', which is equal to 0 at the incompressible flow limit (Kim *et al.* 1987; Moser *et al.* 1999; Hu & Sandham 2001; Hoyas & Jiménez 2006). This procedure was used by Chang *et al.* (1999) to study the detailed contributions from different locations in the flowfield to wall-pressure wavenumber-frequency spectra.

DNS results for ϕ_{ij}, Π_{ij} and $\overline{p'u'_i}$ are systematically used for the *a priori* and *a posteriori* evaluation of modelling proposals (So *et al.* 1991; Demuren & Sarkar 1993; Moin & Mahesh 1998; Sauret & Vallet 2007; Vallet 2007). Nonetheless, to the authors' knowledge, the detailed 4-part decomposition used in the models has not been studied in detail, nor have DNS data been used to further split $p'_{(\mathrm{s})}$ and $p'_{(\mathrm{r})}$ into volume ($p'_{(\mathrm{r};\mathfrak{V})}$ and $p'_{(\mathrm{s};\mathfrak{V})}$) and wall-echo ($p'_{(\mathrm{r};w)}$ and $p'_{(\mathrm{s};w)}$) terms.

Manceau *et al.* (2001) have studied the wall-echo problem from the specific point-of-view of the so-called elliptic relaxation approach of Durbin (1993), which lumps together all wall-echo effects (both on pressure correlations and on dissipation-rate) into a single tensor, using 2-point correlations (in the physical space) from the DNS data of Moser *et al.* (1999), at wall-friction Reynolds-number $Re_{\tau_w} = 590$. Although that work (Manceau *et al.* 2001) focuses on elliptic relaxation, it does provide information on wall-echo. The method used, although related to classical work on wall pressure spectra (Panton & Linebarger 1974) in that it uses 2-point correlations in physical space, introduces wall-echo by an approximate method of images, one image-channel for the upper wall and another for the lower wall. Furthermore, Manceau *et al.* (2001) neglect Stokes pressure. When analyzed under a formal Green's function framework, the approximation in the method of images used in Manceau *et al.* (2001) is equivalent to using an approximate Green's function, instead of the exact one. Based on this approach we can evaluate the approximation error of the method of images.

---

† Throughout the paper x denotes the streamwise coordinate with corresponding velocity–component u, y denotes the normal-to-the-wall coordinate with corresponding velocity-component v, and z denotes the spanwise coordinate with corresponding velocity-component w. In §2 and in the Appendix, $y = 0$ at the channel centerline, while in §3 and §4 $y = 0$ at the (lower) wall.

The comparative evaluation of different turbulence closures (Patel *et al.* 1985; So *et al.* 1991; Demuren & Sarkar 1993) is essential, not just for the purpose of choosing the best (alternatively eliminating the worse) models, but evenmore, especially in the case of second-moment closures, for evaluating different modelling strategies. This is particularly important for redistribution closures, because there exist several families of models (Schiestel 2007), and many of these, especially models including near-wall effects (So *et al.* 1991), are often presented written in different tensorial bases (Launder *et al.* 1975; Gibson & Launder 1978; Speziale *et al.* 1991; So *et al.* 1996; Suga 2004; Jakirlić *et al.* 2007). Contrary to the case of quasi-homogeneous turbulence, where it is known (Speziale *et al.* 1991; Ristorcelli *et al.* 1995; Gerolymos *et al.* 2010*b*) that a polynomial representation basis of 8 tensors is sufficient for the representation of all known models, very little has been done for the development of representation bases in the inhomogeneous case (Gerolymos *et al.* 2004).

In the present work we are interested in determining the wall-effects on correlations containing the fluctuating pressure. In §2 we revisit the Green's function (§2.2) approach (Kim 1989) applied to DNS computations of incompressible plane channel flow (§2.1), and we develop a procedure for separately evaluating (§2.2.3) the volume ($p'_{(\mathrm{r};\mathfrak{V})}$ and $p'_{(\mathrm{s};\mathfrak{V})}$) and the wall-echo ($p'_{(\mathrm{r};w)}$ and $p'_{(\mathrm{s};w)}$) terms in (1.2). By comparison with these exact results we also quantify the error of the approximate method of images, as a function of the wavenumber (§2.2.4), showing that this method is a high-wavenumber approximation. Analytical details on the Green's functions, with particular emphasis on the singular problem of bulk pressure fluctuations ($\kappa = 0$), are given in the Appendix.

In §3 we apply the algorithm (§2.2) for computing the p'-splitting (1.2) to the study of the contribution of different terms to correlations containing p' in low-Reynolds-number plane channel flow. In §4 we use these results to assess several models, representative of various approaches. We do not include models for pressure-strain redistribution ϕ_{ij} based on the elliptic relaxation approach, as these were studied in Manceau *et al.* (2001), but we study the pressure-diffusion model of Demuren *et al.* (1996) which uses elliptic relaxation for its slow part. The tensorial representations of the different ϕ_{ij} models which were investigated (§4.1), use different bases in the original papers (Launder *et al.* 1975; Gibson & Launder 1978; Speziale *et al.* 1991; So *et al.* 1996; Suga 2004; Jakirlić *et al.* 2007), rendering the critical analysis of the modelling choices complicated. For comparison purposes, the various ϕ_{ij} models are expressed in a common representation basis (§4.2), which extends the usual homogeneous representation bases (Ristorcelli *et al.* 1995; Gerolymos *et al.* 2010*b*) to include an additional tensor based on the unit vector in the dominant direction of turbulence inhomogeneity (§4.2). Contrary to previous work (Gerolymos *et al.* 2004), where a functional (Smith 1971) representation basis had been considered, which did not allow for explicit projection (representation) of various models, a polynomial representation basis (Spencer & Rivlin 1959) was preferred. *A priori* assessment of different ϕ_{ij} closures by comparison with DNS data is then used (§4.3) to highlight strengths and weaknesses of various closure strategies. Finally, several representative models for pressure diffusion $d_{ij}^{(p)}$ (§4.4) are investigated by comparison with DNS data (§4.5).

Re_{τ_w}	$\bar{M}_{\text{CL}}$	$N_x \times N_y \times N_z$	L_x	L_y	L_z	Δx^+	Δy^+_w	$N_{y^+\leq 10}$	Δy^+_{CL}	Δz^+	Δt^+	$t^+_{\text{OBS}_{R_2}}$	$\Delta t^+_{s_{R_2}}$
179	0.34	$193 \times 129 \times 169$	$4\pi\delta$	2δ	$\frac{4}{3}\pi\delta$	11.7	0.22	20	4.9	4.4	6.47×10^{-3}	2329	6.47×10^{-1}
178	0.00	$128 \times 129 \times 128$	$4\pi\delta$	2δ	$\frac{4}{3}\pi\delta$	17.7	0.05	14	4.4	5.9	Moser et al. (1999)		

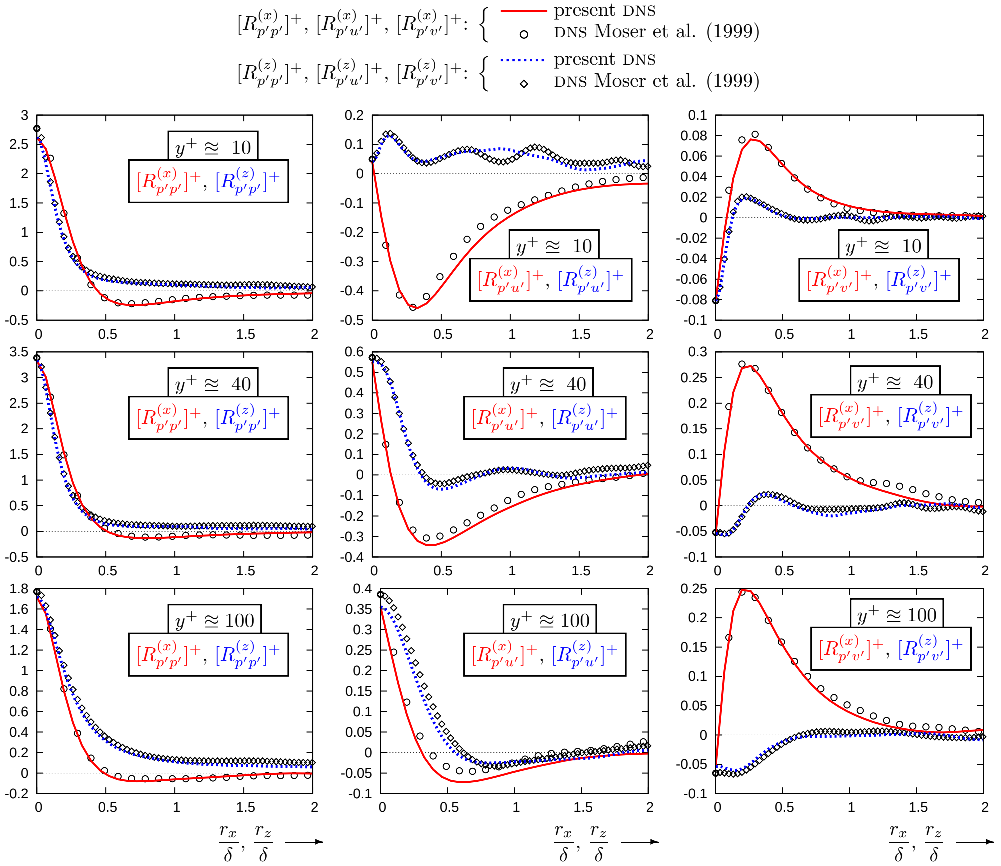

FIGURE 1. Comparison of present DNS-computed ($Re_{\tau_w} = 179$; $\bar{M}_{\text{CL}} = 0.34$; $193 \times 129 \times 169$ grid; Tab. 1) 2-point correlations (2.1) containing the fluctuating pressure in wall-scaling ($[R^{(x)}_{p'p'}]^+$, $[R^{(x)}_{p'u'}]^+$, and $[R^{(x)}_{p'v'}]^+$ in the homogeneous streamwise (x) direction; $[R^{(z)}_{p'p'}]^+$, $[R^{(z)}_{p'u'}]^+$, and $[R^{(z)}_{p'v'}]^+$ in the homogeneous spanwise (z) direction), as a function of distance in outer scaling ($\delta^{-1}r_x$ and $\delta^{-1}r_z$), with reference results of incompressible pseudospectral (Kim *et al.* 1987) DNS computations (Moser *et al.* 1999, $Re_{\tau_w} = 178$, $M_{\text{CL}} = 0$).

2. DNS computations and p'-splitting

2.1. *Plane channel flow configuration and computational method*

In the particular case of plane channel flow, the boundary surface consists of the upper and lower walls ($\mathfrak{W}_l$ at $y = -\frac{1}{2}L_y = -\delta$ and $\mathfrak{W}_u$ at $y = +\frac{1}{2}L_y = +\delta$, respectively), and the periodic boundaries at $x = \pm\frac{1}{2}L_x$ and $z = \pm\frac{1}{2}L_z$. The methodology described in the present paper is independent of the particular DNS solver used. The DNS database was generated for $Re_{\tau_w} := \bar{u}_\tau \delta \nu^{-1} = 180$ (where $2\delta = L_y$ is the channel height, $u_\tau := \sqrt{\bar{\tau}_w \rho^{-1}}$ is the friction velocity and ν the kinematic viscosity) using the DNS solver described and validated in Gerolymos *et al.* (2010*c*), which solves the flow-equations in physical space, with $O(\Delta x^{17})$ discretization of the convective terms (Gerolymos *et al.* 2009). The flow is modelled by the compressible Navier-Stokes equations with air as working medium,

Re_{τ_w}	$\bar{M}_{\text{CL}}$	$N_x \times N_y \times N_z$	L_x	L_y	L_z	Δx^+	Δy_w^+	$N_{y^+\leq 10}$	Δy_{CL}^+	Δz^+	Δt^+	t_{OBS}^+	Δt_s^+	$\Delta t_{s_{R_2}}^+$
179	0.34	$193 \times 129 \times 169$	$4\pi\delta$	2δ	$\frac{4}{3}\pi\delta$	11.7	0.22	20	4.9	4.4	6.47×10^{-3}	2329	6.47×10^{-3}	6.47×10^{-1}
180	0.34	$257 \times 129 \times 385$	$8\pi\delta$	2δ	$4\pi\delta$	17.6	0.23	20	5.0	5.8	6.56×10^{-3}	118	6.57×10^{-3}	6.57×10^{-1}
180	0.34	$129 \times 129 \times 129$	$4\pi\delta$	2δ	$\frac{4}{3}\pi\delta$	17.7	0.23	20	5.0	5.9	6.56×10^{-3}	1539	6.56×10^{-3}	6.56×10^{-1}
184	0.34	$121 \times 161 \times 81$	$4\pi\delta$	2δ	$\frac{4}{3}\pi\delta$	19.3	0.19	25	4.4	9.6	5.50×10^{-3}	1014	5.50×10^{-3}	5.50×10^{-1}

TABLE 1. Parameters of the DNS computations [L_x, L_y, L_z (N_x, N_y, N_z) are the dimensions (number of grid-points) of the computational domain ($x =$ homogeneous streamwise, $y =$ normal-to-the-wall, $z =$ homogeneous spanwise direction); δ is the channel halfheight; Δx^+, Δy_w^+, Δy_{CL}^+, Δz^+ are the mesh-sizes in wall-units; $(\cdot)_w$ denotes wall and $(\cdot)_{\text{CL}}$ centerline values; $N_{y^+\leq 10}$ is the number of grid points between the wall and $y^+ = 10$; $Re_{\tau_w} := \bar{u}_\tau \delta \bar{\nu}_w^{-1}$; $\bar{u}_\tau$ is the friction velocity; δ is the channel halfheight; $\bar{\nu}_w =$ is the kinematic viscosity at the wall; $\bar{M}_{\text{CL}}$ is the centerline Mach-number; Δt^+ is the computational time-step in wall-units; t_{OBS}^+ is the observation period in wall units over which statistics were computed; Δt_s^+ is the sampling time-step for the single-point statistics in wall-units; $\Delta t_{s_{R_2}}^+$ is the sampling time-step for the two-point statistics in wall-units].

but for the quasi-incompressible $\bar{M}_{\text{CL}} \approxeq 0.34$ Mach-number considered in the present work mean density $\bar{\rho}$ variations do not exceed 1.5%, and density fluctuations are negligibly small $\rho'_{\text{rms}} \lessapprox 0.25\%\bar{\rho}$. For this reason the turbulent correlations obtained can be considered as incompressible. This has been verified by systematic comparison with standard incompressible pseudospectral DNS data (Kim *et al.* 1987; Moser *et al.* 1999; del Álamo & Jiménez 2003; del Álamo *et al.* 2004; Hoyas & Jiménez 2006, 2008), both for single point statistics (Gerolymos *et al.* 2010*c*, all SOMs† and TOMs‡ appearing in the Reynolds-stress budgets) and for spectra of velocity fluctuations in the homogeneous streamwise and spanwise directions (Gerolymos *et al.* 2010*c*, Figs. 12–15, pp. 802–805). This very good agreement with pseudospectral incompressible DNS (Kim *et al.* 1987; Hoyas & Jiménez 2008) is also valid for 2-point correlations

$$R_{\mathrm{a'b'}}(\vec{x},\vec{r}) := \overline{\mathrm{a}'(\vec{x},t)\mathrm{b}'(\vec{x}+\vec{r},t)} \tag{2.1}$$

containing the fluctuating pressure p', *viz* $[R_{p'p'}^{(x,z)}]^+$, $[R_{p'u'}^{(x,z)}]^+$, and $[R_{p'v'}^{(x,z)}]^+$ (Fig. 1) and fluctuating pressure spectra¶ $[E_{p'p'}^{(x)}]^+$ and $[E_{p'p'}^{(z)}]^+$ (Fig. 2).

2.2. *Green's function solution of the Poisson equations*

2.2.1. *ODEs for the Fourier transforms*

The solution to (1.1), with Neumann boundary-conditions at the walls (Pope 2000, p. 439) and periodic boundary-conditions in the homogeneous directions, can only be obtained up to an additive function of time t (Ince 1926; Courant & Hilbert 1953; Myint-U & Debnath 2007). We split the fluctuating pressure field as (Kim 1989)

$$p'(x,y,z,t) = p'_{(\mathrm{r})}(x,y,z,t) + p'_{(\mathrm{s})}(x,y,z,t) + p'_{(\tau)}(x,y,z,t) \tag{2.2}$$

---

† second-order moments (Gerolymos *et al.* 2010*c*, $\overline{u'_iu'_j}$: Fig. 7, p. 797, $\overline{p'u'_i}$: Fig. 8, p. 798, $\phi_{ij} := 2\overline{p'S'_{ij}}$: Fig. 10, p. 800, $\varepsilon_{ij}^{(\mu)} := 2\nu\overline{\partial_{x_\ell}u'_i\partial_{x_\ell}u'_j}$: Fig. 11, p. 801)

‡ third-order moments (Gerolymos *et al.* 2010*c*, $\overline{u'_iu'_ju'_k}$: Fig. 9, p. 799)

¶ Notice that the spectra given by Moser *et al.* (1999) are twice the DFT of $R_{p'p'}^+$ (in wall units), and have to be appropriately rescaled (Briggs & Henson 1995) by $(2\pi)^{-1}L_x^+$ or $(2\pi)^{-1}L_z^+$ to get actual 1-D spectra $E_{u_iu_j}^+$ (Pope 2000, (6.206), p. 225), as those given by del Álamo *et al.* (2004).

Re_{τ_w}	$\bar{M}_{\text{CL}}$	$N_x \times N_y \times N_z$	L_x	L_y	L_z	Δx^+	Δy^+_w	$N_{y^+\leq 10}$	Δy^+_{CL}	Δz^+	Δt^+	$t^+_{\text{OBS}_{R_2}}$	$\Delta t^+_{s_{R_2}}$
179	0.34	$193 \times 129 \times 169$	$4\pi\delta$	2δ	$\frac{4}{3}\pi\delta$	11.7	0.22	20	4.9	4.4	6.47×10^{-3}	2329	6.47×10^{-1}
178	0.00	$128 \times 129 \times 128$	$4\pi\delta$	2δ	$\frac{4}{3}\pi\delta$	17.7	0.05	14	4.4	5.9	Moser et al. (1999)		

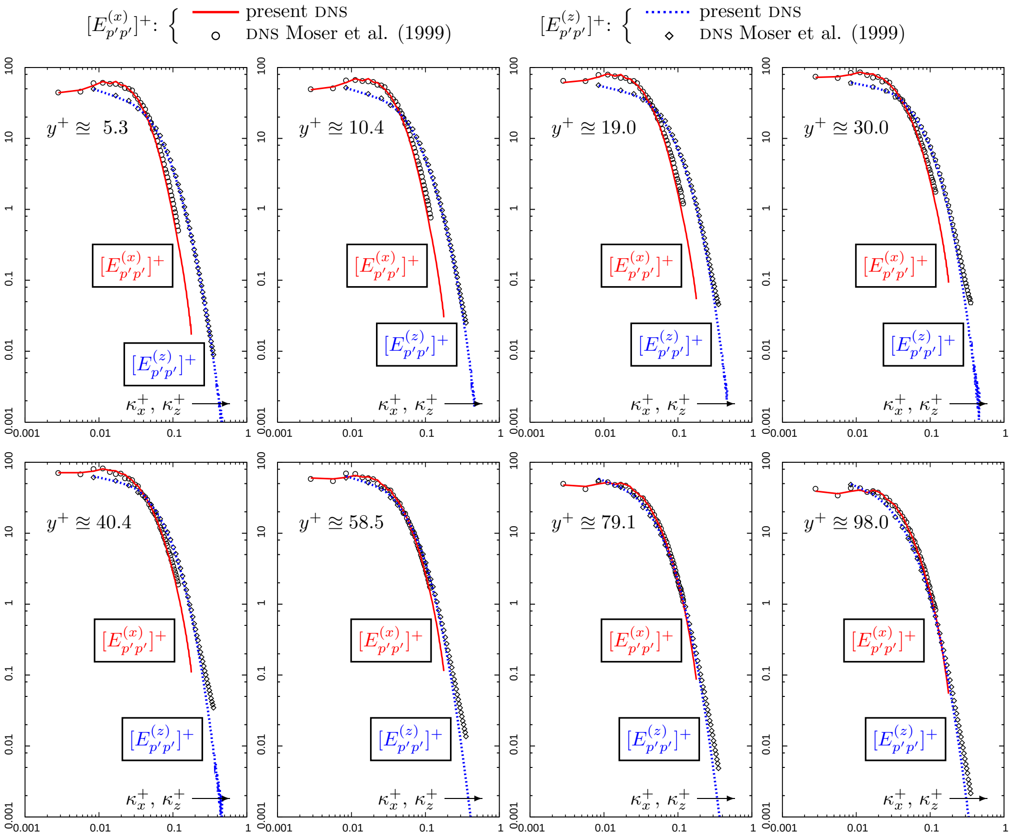

FIGURE 2. Comparison of present DNS-computed ($Re_{\tau_w} = 179$; $\bar{M}_{\text{CL}} = 0.34$; $193 \times 129 \times 169$ grid; Tab. 1) 1-D pressure spectra in wall scaling ($[E^{(x)}_{p'p'}]^+$ and $[E^{(z)}_{p'p'}]^+$ in the homogeneous streamwise (x) and spanwise (z) directions), as a function of wavenumber in wall units (κ^+_x and κ^+_z), with reference results of incompressible pseudospectral (Kim *et al.* 1987) DNS computations (Moser *et al.* 1999, $Re_{\tau_w} = 178$, $M_{\text{CL}} = 0$).

where the rapid $p'_{(\text{r})}$, slow $p'_{(\text{s})}$ and Stokes $p'_{(\tau)}$ pressure fluctuations are solutions of (Kim 1989; Chang *et al.* 1999)

$$\nabla^2 \begin{bmatrix} p'_{(\text{r})} \\ p'_{(\text{s})} \\ p'_{(\tau)} \end{bmatrix} = \begin{bmatrix} Q'_{(\text{r})} \\ Q'_{(\text{s})} \\ Q'_{(\tau)} \end{bmatrix} := \begin{bmatrix} -2\partial_{x_\ell} u'_k \partial_{x_k} \bar{u}_\ell \\ -\partial^2_{x_\ell x_k}(u'_k u'_\ell - \overline{u'_k u'_\ell}) \\ 0 \end{bmatrix} \tag{2.3a}$$

with boundary-conditions (Pope 2000, pp. 390–392, 439–442)

$$\frac{\partial}{\partial y} \begin{bmatrix} p'_{(\text{r})} \\ p'_{(\text{s})} \\ p'_{(\tau)} \end{bmatrix} (x, y = \pm\tfrac{1}{2}L_y, z, t) = \begin{bmatrix} 0 \\ 0 \\ B'_{(\tau)_\pm} \end{bmatrix} := \begin{bmatrix} 0 \\ 0 \\ \mu \partial^2_{yy} v' \end{bmatrix} \tag{2.3b}$$

Since (2.3) is linear in $p'_{(m)}$ ($m \in \{\text{r}, \text{s}, \tau\}$) the 3 problems can be solved independently to compute the 3 fields in (2.2). The last field in the superposition (2.2) is introduced to satisfy the wall boundary-conditions associated with the normal-to-the-wall (y) momentum equation

$$\left.\frac{\partial p'}{\partial y}\right|_{y=\pm\frac{1}{2}L_y}=\left.\frac{\partial \tau'_{y\ell}}{\partial x_\ell}\right|_{y=\pm\frac{1}{2}L_y}=\mu\nabla^2 v'\Big|_{y=\pm\frac{1}{2}L_y}=\left.\mu\frac{\partial^2 v'}{\partial y^2}\right|_{y=\pm\frac{1}{2}L_y} \tag{2.4}$$

because of the no-slip wall boundary-condition $u'_i(x,y=\pm\frac{1}{2}L_y,z,t)=0$. By (2.4) the field $p'_{(\tau)}$ is obviously related to the fluctuating wall-shear-stress, and is usually called Stokes pressure (Mansour *et al.* 1988; Kim 1989; Chang *et al.* 1999) although Pope (2000, p. 439) suggests the alternative term harmonic pressure, because in incompressible flow $\nabla^2 p'_\tau=0$.†

The directions x and z being homogeneous (periodic in the computational model), following Kim (1989), we replace the xz-Fourier-transforms‡ of $p'_{(m)}$, $Q'_{(m)}$ ($m\in\{\mathrm{r},\mathrm{s},\tau\}$) and $B'_{(\tau)\pm}$

$$p'_{(m)}(x,y,z,t)=\int_{-\infty}^{+\infty}\int_{-\infty}^{+\infty}\hat{p}'_{(m)}(\kappa_x,y,\kappa_z,t)\;e^{i\kappa_x x+i\kappa_z z}\;d\kappa_x\;d\kappa_z \tag{2.5a}$$

$$Q'_{(m)}(x,y,z,t)=\int_{-\infty}^{+\infty}\int_{-\infty}^{+\infty}\hat{Q}'_{(m)}(\kappa_x,y,\kappa_z,t)\;e^{i\kappa_x x+i\kappa_z z}\;d\kappa_x\;d\kappa_z \tag{2.5b}$$

$$B'_{(\tau)\pm}(x,z,t)=\int_{-\infty}^{+\infty}\int_{-\infty}^{+\infty}\hat{B}'_{(\tau)\pm}(\kappa_x,\kappa_z,t)\;e^{i\kappa_x x+i\kappa_z z}\;d\kappa_x\;d\kappa_z \tag{2.5c}$$

in the PDE¶ (2.3) to obtain the ODE†

$$\left[\frac{\partial^2}{\partial y^2}-\kappa^2\right]\begin{bmatrix}\hat{p}'_{(\mathrm{r})}\\ \hat{p}'_{(\mathrm{s})}\\ \hat{p}'_{(\tau)}\end{bmatrix}(\kappa_x,y,\kappa_z,t)=\begin{bmatrix}\hat{Q}'_{(\mathrm{r})}\\ \hat{Q}'_{(\mathrm{s})}\\ \hat{0}\end{bmatrix}(\kappa_x,y,\kappa_z,t) \tag{2.6a}$$

$$\frac{\partial\hat{p}'_{(m)}}{\partial y}(\kappa_x,y=\pm\tfrac{1}{2}L_y,\kappa_z,t)=\begin{bmatrix}0\\ 0\\ \hat{B}'_{(\tau)\pm}(\kappa_x,\kappa_z,t)\end{bmatrix} \tag{2.6b}$$

$$\kappa:=\sqrt{\kappa_x^2+\kappa_z^2}\in\mathbb{R}_{\geq 0} \tag{2.6c}$$

The classical solution of (2.6) by Kim (1989), using a Green's function approach, provides detailed information on the structure of the rapid and slow fields, and was extended by Chang *et al.* (1999) to study the detailed influence of the sources, both in type (slow and rapid) and y-location in the channel. In the present work we extend this analysis by identifying and studying the wall-echo influence. Details on the Green's functions, and discussion of the singular case $\kappa=0\overset{(2.6c)}{\Longleftrightarrow}\kappa_x=\kappa_z=0$ are found in the Appendix.

---

† This is however no longer true in the compressible flow case (Foysi *et al.* 2004).

‡ The Fourier-transforms $\hat{p}'_{(m)},\hat{Q}'_{(m)},\hat{B}'_{(m)\pm}\in\mathbb{C}$ are computed using standard DFT (discrete Fourier transform) techniques (Briggs & Henson 1995) in the periodic directions x and z, with maximum computable wavenumbers $\kappa_{x_{\max}}=\pi(\Delta x)^{-1}$ and $\kappa_{z_{\max}}=\pi(\Delta z)^{-1}$.

¶ PDE: partial differential equation; ODE: ordinary differential equation

2.2.2. *Exact solution of* (2.6)

The exact solution to (2.6) is given in Kim (1989), and has been widely used (Mansour *et al.* 1988; Chang *et al.* 1999; Foysi *et al.* 2004). It reads (§A.1.1, §A.2.1)

$$\begin{bmatrix} \hat{p}'_{(\mathrm{r})} \\ \hat{p}'_{(\mathrm{s})} \end{bmatrix}(\kappa_x, y, \kappa_z, t) = \int_{-\frac{1}{2}L_y}^{+\frac{1}{2}L_y} G_{\mathrm{Kim}}(y, Y; \kappa) \begin{bmatrix} \hat{Q}'_{(\mathrm{r})} \\ \hat{Q}'_{(\mathrm{s})} \end{bmatrix}(\kappa_x, Y, \kappa_z, t)\, dY \tag{2.7}$$

where the Green's function $G_{\mathrm{Kim}}(y, Y; \kappa)$ (Tab. 2) is defined by (A 9*b*, A 34), and satisfies the correct homogeneous Neumann boundary-conditions on both walls (Fig. 3), and $\kappa := \sqrt{\kappa_x^2 + \kappa_z^2} \in \mathbb{R}_{\geq 0}$ (2.6*c*). The Stokes pressure is given by

$$\hat{p}'_{(\tau)}(\kappa_x, y, \kappa_z, t) = q_{\mathrm{BC}}(y; \kappa, \hat{B}'_{(\tau)_-}(\kappa_x, \kappa_z, t), \hat{B}'_{(\tau)_+}(\kappa_x, \kappa_z, t)) \tag{2.8}$$

where the function $q_{\mathrm{BC}}(y; \kappa, B_-, B_+)$ (Tab. 2) which solves for the harmonic field $\hat{p}'_{(\tau)}$ is defined by (A 21). As discussed in the Appendix (§A.2), the case $\kappa = 0$ is singular, and a solution exists iff the compatibility conditions

$$L_y \begin{bmatrix} \overline{Q'_{(\mathrm{r})}}^{xyz} \\ \overline{Q'_{(\mathrm{s})}}^{xyz} \end{bmatrix}(t) = \int_{-\frac{1}{2}L_y}^{+\frac{1}{2}L_y} \begin{bmatrix} \hat{Q}'_{(\mathrm{r})} \\ \hat{Q}'_{(\mathrm{s})} \end{bmatrix}(\kappa_x = 0, Y, \kappa_z = 0, t)\, dY = \begin{bmatrix} 0 \\ 0 \end{bmatrix} \tag{2.9a}$$

$$\hat{B}'_{(\tau)_-}(\kappa_x = 0, \kappa_z = 0, t) = \hat{B}'_{(\tau)_-}(\kappa_x = 0, \kappa_z = 0, t) \iff \overline{B'_{(\tau)_-}}^{xz}(t) = \overline{B'_{(\tau)_-}}^{xz}(t) \tag{2.9b}$$

where $\overline{(\cdot)}^{xyz}$ denotes the volume average† (bulk average) and $\overline{(\cdot)}^{xz}$ is the surface average‡ in the homogeneous directions x and z. If the computational box is large enough in the homogeneous directions for the ergodic hypothesis (Monin & Yaglom 1971, p. 243–256) to hold, (2.9) are satisfied, at least approximately. In practice, the compatibility condition (2.9*a*) was enforced when computing the Fourier-transforms (2.5*b*). The form (A 31) of $q_{\mathrm{BC}}(y; \kappa = 0, B_-, B_+)$ (Tab. 2) automatically enforces the compatibility condition, by taking the average gradient $\frac{1}{2}(B_- + B_+)$. In practice $\hat{B}'_{(\tau)_-}(\kappa_x = 0, \kappa_z = 0, t) \approxeq \hat{B}'_{(\tau)_+}(\kappa_x = 0, \kappa_z = 0, t) \approxeq 0$ in (2.9*b*), especially with increasing box size, so that taking the average is a good choice. The additive constant q_{BC_0} up to which (1.1) with Neumann boundary conditions at the walls (Pope 2000, p. 439) can be solved was chosen to satisfy the constraint $p'_{\mathrm{B}}(t) := \overline{p'}^{xyz}(t) = 0$, (*ie* constant bulk pressure) and was included in the Stokes field $p'_{(\tau)}$.

2.2.3. *Volume and wall-echo terms*

The main purpose of the present algorithm is to distinguish in (1.2) the contributions of the volume integral (volume terms denoted by $(\cdot)_{\mathfrak{V}}$) from the contributions of the

---

† $\overline{(\cdot)}^{xyz} := \dfrac{1}{L_x\ L_y\ L_z} \displaystyle\int_{-\frac{1}{2}L_x}^{+\frac{1}{2}L_x} \int_{-\frac{1}{2}L_y}^{+\frac{1}{2}L_y} \int_{-\frac{1}{2}L_z}^{+\frac{1}{2}L_z} (\cdot) dx\ dy\ dz$

‡ $\overline{(\cdot)}^{xz} := \dfrac{1}{L_x\ L_z} \displaystyle\int_{-\frac{1}{2}L_x}^{+\frac{1}{2}L_x} \int_{-\frac{1}{2}L_z}^{+\frac{1}{2}L_z} (\cdot) dx\ dz$

$$\underline{\kappa \neq 0 \ (\S\text{A.1})}$$

$$G_{\mathfrak{V}}(y,Y;\kappa\neq 0) = -\frac{\mathrm{e}^{-\kappa|y-Y|}}{2\kappa} \tag{A 13}$$

$$G_{\mathrm{Kim}}(y,Y;\kappa\neq 0) = -\frac{\cosh[\kappa(L_y-|y-Y|)]+\cosh[\kappa(y+Y)]}{2\kappa\sinh\kappa L_y} \tag{A 9b}$$

$$G_{\pm}(y,Y;\kappa\neq 0) = G_{\mathfrak{V}}(y,Y;\kappa\neq 0) - \frac{\mathrm{e}^{-\kappa(L_y\mp y\mp Y)}}{2\kappa} \tag{A 17}$$

$$q_{\textsc{bc}}(y;\kappa\neq 0,B_-,B_+) = \frac{B_+\cosh[\kappa(\frac{1}{2}L_y+y)]-B_-\cosh[\kappa(\frac{1}{2}L_y-y)]}{\kappa\sinh\kappa L_y} \tag{A 11}$$

$$q_{\textsc{bc}_\pm}(y;\kappa\neq 0,B_\pm) = \pm\frac{B_\pm}{\kappa}\mathrm{e}^{-\kappa(\frac{1}{2}L_y\mp y)} \tag{A 21}$$

$$\underline{\kappa = 0 \overset{(2.6c)}{\iff} \kappa_x=\kappa_z=0 \ (\S\text{A.2})}$$

$$\text{compatibility condition:} \qquad \int_{-\frac{1}{2}L_y}^{+\frac{1}{2}L_y} Q(Y;\kappa=0)dY = 0 \tag{A 24}$$

$$G_{\mathrm{Kim}}(y,Y;\kappa=0) = G_{\pm}(y,Y;\kappa=0) = G_{\mathfrak{V}}(y,Y;\kappa=0) = \frac{|y-Y|}{2} \tag{A 34}$$

$$q_{\textsc{bc}}(y;\kappa=0,B_-,B_+) = \tfrac{1}{2}B_-y+\tfrac{1}{2}B_+y+q_{\textsc{bc}_0} \tag{A 31}$$

$$q_{\textsc{bc}_\pm}(y;\kappa=0,B_\pm) := 0 \tag{A 36}$$

$$\underline{\text{Approximate method of images } (\S\text{A.3})}$$

$$G_{\textsc{mwl}}(y,Y;\kappa\neq 0) = G_{\mathfrak{V}}(y,Y;\kappa\neq 0)+G_{w_-}(y,Y;\kappa\neq 0)+G_{w_+}(y,Y;\kappa\neq 0) \tag{A 41c}$$

$$E_{\textsc{mwl}}(\kappa L_y) := \frac{\mathrm{e}^{-\kappa L_y}(1+\mathrm{e}^{-\kappa L_y})\cosh\kappa L_y}{2\kappa L_y\sinh\kappa L_y} \tag{A 44}$$

Table 2. Green's functions for the solution of the generic modified Helmholtz equation (2.6a), $q''(y;\kappa)-\kappa^2 \ q(y;\kappa) = Q(y;\kappa) \quad \forall y \in (-\frac{1}{2}L_y,+\frac{1}{2}L_y)$, with boundary-conditions (Fig. 3) $q'(y=\pm\frac{1}{2}L_y;\kappa) = B_\pm(\kappa)$ (2.6b), and for the two halfspace problems (Fig. 3) defining the wall-corrections of the method of images (Fig. 3); notice that the solution for $\kappa=0$ is obtained up to an additive constant $q_{\textsc{bc}_0}$ (A 31).

surface integral (wall-echo terms denoted by $(\cdot)_w$), *ie* to extend (2.2) as

$$\begin{aligned} p'(x,y,z,t) =& \underbrace{p'_{(\mathrm{r};\mathfrak{V})}(x,y,z,t)+p'_{(\mathrm{r};w)}(x,y,z,t)}_{p'_{(\mathrm{r})}(x,y,z,t)} \\ &+\underbrace{p'_{(\mathrm{s};\mathfrak{V})}(x,y,z,t)+p'_{(\mathrm{s};w)}(x,y,z,t)}_{p'_{(\mathrm{s})}(x,y,z,t)}+p'_{(\tau)}(x,y,z,t) \end{aligned} \tag{2.10}$$

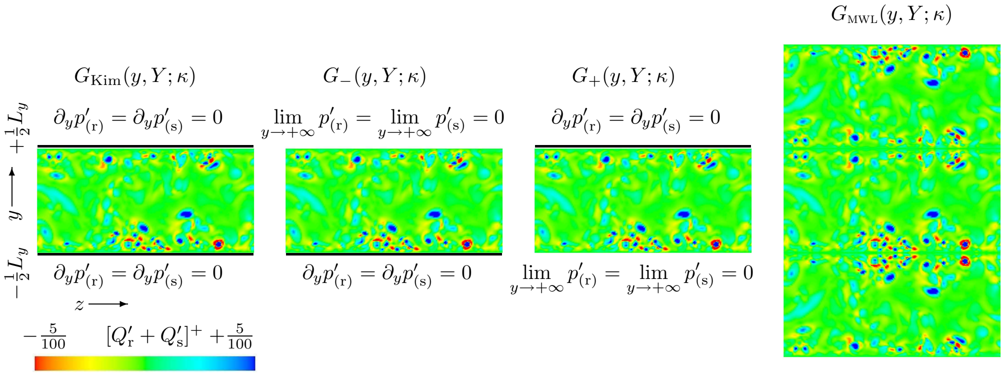

FIGURE 3. Instantaneous pressure fluctuation sources (sum $[Q'_{(\mathrm{r})} + Q'_{(\mathrm{s})}]^{+}$ of rapid and slow sources in wall units) at $x = 0$ (DNS; $Re_{\tau_w} = 179$; $\bar{M}_{\mathrm{CL}} = 0.34$; $193 \times 129 \times 169$ grid; Tab. 1), and boundary conditions for the exact problem (2.6) whose solution (Kim 1989) is given by $G_{\mathrm{Kim}}(y,Y;\kappa)$ (A 9*b*), and for the two virtual halfspace problems with only one wall present defining $G_{\pm}(y,Y;\kappa)$ (A 17), which define the local wall-corrections appearing in the high-wavenumber approximation of the method of images (Manceau *et al.* 2001), corresponding to the approximate Green's function $G_{\mathrm{MWL}}(y,Y;\kappa)$ (A 41*c*).

where $p'_{(\mathrm{r};\mathfrak{V})}$ corresponds to the contribution of the volume integral in (1.2*a*), $p'_{(\mathrm{r};w)}$ corresponds to the contribution of the surface integral in (1.2*a*), $p'_{(\mathrm{s};\mathfrak{V})}$ corresponds to the contribution of the volume integral in (1.2*b*), and $p'_{(\mathrm{s};w)}$ corresponds to the contribution of the surface integral in (1.2*b*). From a modelling point-of-view, the volume terms $p'_{(\mathrm{r};\mathfrak{V})}$ and $p'_{(\mathrm{s};\mathfrak{V})}$ correspond to a quasi-homogeneous (weakly inhomogeneous) part, while the surface terms $p'_{(\mathrm{r};w)}$ and $p'_{(\mathrm{s};w)}$ are the strongly inhomogeneous wall-blockage effect (Hanjalić 1994).

Working directly with the surface integrals in (1.2) would have been a complex task, because they are implicit, *ie* they contain the value of the corresponding field at the wall. On the other hand, it is straightforward to evaluate the volume integrals in (1.2), which contain only the sources and the freespace Green's function $G_{\mathfrak{V}}(y,Y;\kappa)$ which solves (2.6*a*) replacing the boundary-conditions (2.6*b*) by the requirement that $\lim_{|y|\longrightarrow\infty} p'_{(\mathrm{r};\mathfrak{V})} = \lim_{|y|\longrightarrow\infty} p'_{(\mathrm{r};\mathfrak{V})} = 0$, *ie* the solution of the hypothetical problem where p' is generated by a distribution of sources in $y \in [-\frac{1}{2}L_y, +\frac{1}{2}L_y]$ with the walls absent. Straightforward computation (§A.1.3, §A.2.3) gives the freespace Green's function $G_{\mathfrak{V}}(y,Y;\kappa)$ (A 13, A 34) for the 1-D case (Tab. 2) which satisfies

$$\begin{bmatrix} \hat{p}'_{(\mathrm{r};\mathfrak{V})} \\ \hat{p}'_{(\mathrm{s};\mathfrak{V})} \end{bmatrix} (\kappa_x, y, \kappa_z, t) = \int_{-\frac{1}{2}L_y}^{+\frac{1}{2}L_y} G_{\mathfrak{V}}(y,Y;\kappa) \begin{bmatrix} \hat{Q}'_{(\mathrm{r})} \\ \hat{Q}'_{(\mathrm{s})} \end{bmatrix} (\kappa_x, Y, \kappa_z, t)\, dY \tag{2.11}$$

and since by definition (2.10)

$$\begin{bmatrix} \hat{p}'_{(\mathrm{r};w)} \\ \hat{p}'_{(\mathrm{s};w)} \end{bmatrix} (\kappa_x, y, \kappa_z, t) = \begin{bmatrix} \hat{p}'_{(\mathrm{r})} \\ \hat{p}'_{(\mathrm{s})} \end{bmatrix} (\kappa_x, y, \kappa_z, t) - \begin{bmatrix} \hat{p}'_{(\mathrm{r};\mathfrak{V})} \\ \hat{p}'_{(\mathrm{s};\mathfrak{V})} \end{bmatrix} (\kappa_x, y, \kappa_z, t) \tag{2.12}$$

we may readily define, using the Green's functions (Tab. 2) $G_{\mathrm{Kim}}(y,Y;\kappa)$(A 9*b*, A 34) and $G_{\mathfrak{V}}(y,Y;\kappa)$ (A 13, A 34), the wall-echo Green's function

$$G_w(y,Y;\kappa) := G_{\mathrm{Kim}}(y,Y;\kappa) - G_{\mathfrak{V}}(y,Y;\kappa) \tag{2.13}$$

corresponding to the surface integrals (wall-echo) in (1.2)

$$\begin{bmatrix} \hat{p}'_{(\mathrm{r};w)} \\ \hat{p}'_{(\mathrm{s};w)} \end{bmatrix} (\kappa_x, y, \kappa_z, t) = \int_{-\frac{1}{2}L_y}^{+\frac{1}{2}L_y} G_w(y, Y; \kappa) \begin{bmatrix} \hat{Q}'_{(\mathrm{r})} \\ \hat{Q}'_{(\mathrm{s})} \end{bmatrix} (\kappa_x, Y, \kappa_z, t)\, dY \tag{2.14}$$

Notice (Tab. 2) that since $G_{\mathrm{Kim}}(y, Y; \kappa = 0) = G_{\mathfrak{V}}(y, Y; \kappa = 0)$ (A 34) we have $G_w(y, Y; \kappa = 0) = 0$, *ie* wall-echo applies only on fields varying in at least one of the homogeneous directions x and z.

2.2.4. *The approximate method of images*

With the above developments we can directly evaluate the wall-echo terms for the slow and rapid wall-echo terms in each of the correlations containing p' (§3). We study the method of images not only because it has been used by Manceau *et al.* (2001) to analyse the DNS data of Moser *et al.* (1999), in the context of elliptic relaxation models (Durbin 1993), but also because it is often used as a closure-building tool in near-wall turbulence modelling (Shir 1973; Launder *et al.* 1975; Gibson & Launder 1978). By comparing with the exact solution obtained in the present work, it is possible to evaluate the approximation error of the method of images.

The approximate method of images (Manceau *et al.* 2001) simply adds two mirror images of the channel, one above the upper wall and another below the lower wall (Fig. 3), to account for the presence of the walls, postulating that an approximation to the solution is obtained by using the freespace Green's function $G_{\mathfrak{V}}(y, Y; \kappa)$ in the extended domain $y \in [-\frac{3}{2}L_y, +\frac{3}{2}L_y]$. Taking into account the mirror symmetry of the ghost channels with respect to the corresponding wall (Fig. 3), this is equivalent (§A.3) to using an appropriate Green's function $G_{\mathrm{MWL}}(y, Y; \kappa)$ (Tab. 2) on the actual sources between the channel walls, *ie* for $y \in [-\frac{1}{2}L_y, +\frac{1}{2}L_y]$

$$\begin{bmatrix} \hat{p}'_{(\mathrm{r};\mathrm{MWL})}] \\ \hat{p}'_{(\mathrm{s};\mathrm{MWL})}] \end{bmatrix} (\kappa_x, y, \kappa_z, t) = \int_{-\frac{1}{2}L_y}^{+\frac{1}{2}L_y} G_{\mathrm{MWL}}(y, Y; \kappa) \begin{bmatrix} \hat{Q}'_{(\mathrm{r})} \\ \hat{Q}'_{(\mathrm{s})} \end{bmatrix} (\kappa_x, Y, \kappa_z, t)\, dY \tag{2.15}$$

By (A 41*c*)

$$G_{\mathrm{MWL}}(y, Y; \kappa) = G_{\mathfrak{V}}(y, Y; \kappa) + G_{w_-}(y, Y; \kappa) + G_{w_+}(y, Y; \kappa) \tag{2.16}$$

where $G_{w_\pm}(y, Y; \kappa)$ are the wall-echo Green's functions corresponding to the virtual halfspace problems with only one of the walls present (Fig. 3). Notice that this is also the method used in standard wall-echo Reynolds-stress modelling (Gibson & Launder 1978), and (Tab. 2) that the halfspace problems are solved exactly (§A.1.4, §A.2.4). Inherently, this is tantamount to assuming that there is no interaction between the echo effects of the upper and lower walls, since in the case of an isolated wall (halfspace problem; Fig. 3) the method of images yields the exact solution (Pope 2000, pp. 439–442).

The approximation error of the method of images comes from the fact that the direct influence of the upper wall, approximated by the halfspace problem $G_{w_+}(y, Y; \kappa)$ (Fig. 3), induces a nonzero gradient $\partial_y[\hat{p}'_{(\mathrm{r};+)}, \hat{p}'_{(\mathrm{s};+)}]^{\mathrm{T}}(\kappa_x, y = -\frac{1}{2}L_y, \kappa_z, t) \neq 0$ at the lower wall, and that there is no feedback from the lower wall to correct this (and *vice versa*). The nondimensional approximation error can be evaluated (§A.3) by comparison with the exact solution (A 9*b*) of Kim (1989), and is a function of the nondimensional wavenumber $\kappa L_y = 2\kappa\delta$ (A 44). For large nondimensional wavenumbers κL_y, *ie* structures with small streamwise and spanwise extent compared to the channel height, this error is small, and rapidly decreases with increasing wavenumber (Fig. 4).

Let $\ell_\kappa := 2\pi\kappa^{-1}$ be the representative size (wavelength) in the xz plane of structures

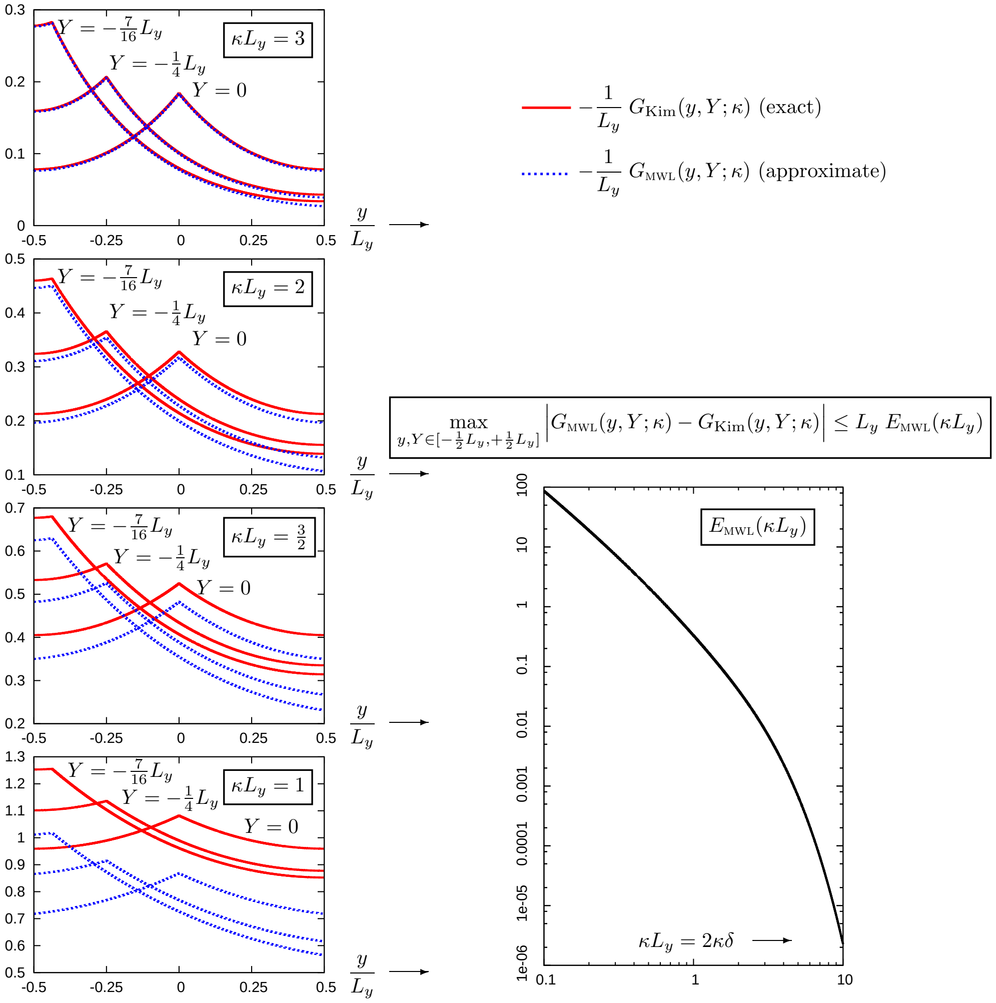

FIGURE 4. Comparison of the exact Green's function (A 9*b*), $G_{\mathrm{Kim}}(y,Y;\kappa)$ (Kim 1989), with the method-of-images approximation (A 41), $G_{\mathrm{MWL}}(y,Y;\kappa)$ (Manceau *et al.* 2001), for $Y \in \{-\frac{7}{16}L_y,-\frac{1}{4}L_y,0\}$ and $\kappa L_y \in \{1,\frac{3}{2},2,3\}$, plotted as a function of yL_y^{-1}, and log-plot of the upper bound estimate of the error made by the method-of-images approximation (A 44) as a function of the nondimensional wavenumber $\kappa L_y = 2\kappa\delta$ ($L_y = 2\delta$ is the channel height).

corresponding to $\kappa := \sqrt{\kappa_x^2+\kappa_z^2}$ (2.6*c*). For $\kappa L_y \gtrapprox 3 \iff \ell_\kappa \lessapprox 4\delta$ the approximation of $G_{\mathrm{Kim}}(y,Y;\kappa)$ by $G_{\mathrm{MWL}}(y,Y;\kappa)$ (Tab. 2) is satisfactory (Fig. 4). For the present case with $Re_{\tau_w} \approxeq 180$ this corresponds roughly to $\kappa^+ \gtrapprox \frac{1}{100}$, which includes the wavenumbers where most of the energy of the p'-spectra is contained (Fig. 2), implying that the method of images is a satisfactory engineering approximation. However, for larger structures, *eg* $\kappa L_y \approxeq \frac{3}{2} \iff \ell_\kappa \approxeq 8\delta$, such as the superstructures observed in higher-Re_{τ_w} wall turbulence (Hutchins & Marusic 2007; Balakumar & Adrian 2007), the approximation error is roughly 10%, and then grows exponentially with increasing size.

2.2.5. *Interaction of wall-echo between walls*

Since the freespace Green's function $G_{\mathfrak{V}}(y,Y;\kappa)$ (A 13, A 34) is the same for all problems (Fig. 3), the differences (Fig. 4) between the exact solution $G_{\mathrm{Kim}}(y,Y;\kappa)$ (A 9*b*) and

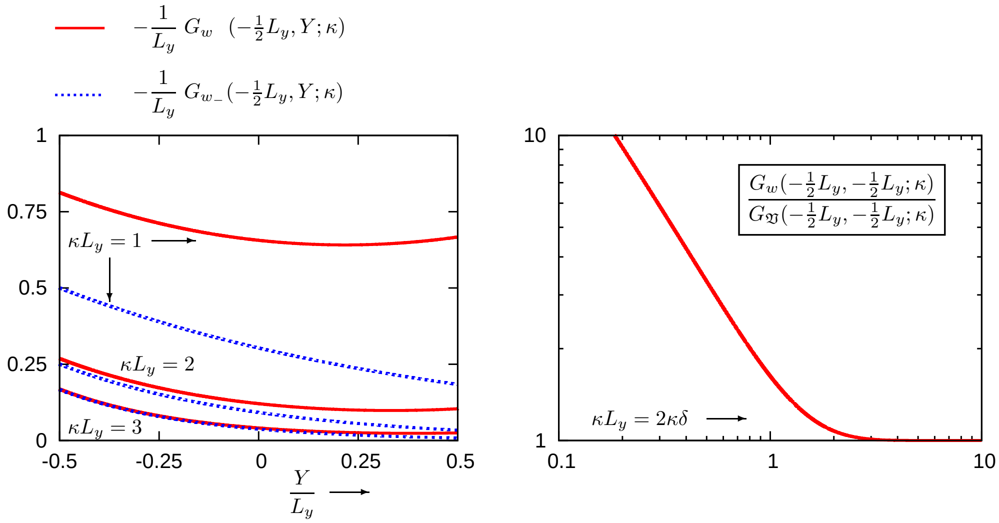

FIGURE 5. Comparison of the exact wall-echo Green's function $G_w(y=-\frac{1}{2}L_y,Y;\kappa)$ (2.16), for the computation of the solution at the lower wall $y=-\frac{1}{2}L_y$, with the wall-echo Green's function $G_{w_-}(y=-\frac{1}{2}L_y,Y;\kappa)$ (A 41), of the corresponding halfspace problem with only the lower wall present (Fig. 3), for $\kappa L_y\in\{1,2,3\}$, plotted as a function of YL_y^{-1}, and log-plot of the ratio at the wall ($y=Y=-\frac{1}{2}L_y$) of the exact wall-echo Green's function $G_w(y=-\frac{1}{2}L_y,Y=-\frac{1}{2}L_y;\kappa)$ (2.16) on the corresponding freespace Green's function $G_{\mathfrak{V}}(y=-\frac{1}{2}L_y,Y=-\frac{1}{2}L_y;\kappa)$ (A 13) plotted against the nondimensional wavenumber $\kappa L_y=2\kappa\delta$ ($L_y=2\delta$ is the channel height).

the method-of-images approximation $G_{\mathrm{MWL}}(y,Y;\kappa)$ (A 41), correspond to increasingly strong interaction between the two walls with decreasing nondimensional wavenumber $\kappa L_y=2\kappa\delta$, leading to amplification of the echo effect. To further explain this phenomenon notice the identity

$$\begin{aligned}G_{\mathfrak{V}}(y=-\tfrac{1}{2}L_y,Y;\kappa\neq 0)\overset{(\mathrm{A\,13})}{=}&-\frac{\mathrm{e}^{\kappa(Y+\frac{1}{2}L_y)}}{2\kappa}\\&\overset{(\mathrm{A\,17}a)}{=}G_-(y=-\tfrac{1}{2}L_y,Y;\kappa\neq 0)-G_{\mathfrak{V}}(y=-\tfrac{1}{2}L_y,Y;\kappa\neq 0)\\&\overset{(\mathrm{A\,41}c)}{=:}G_{w_-}(y=-\tfrac{1}{2}L_y,Y;\kappa\neq 0)\end{aligned}\tag{2.17}$$

which implies by (A 3) that for the halfspace problems (§A.1.4) the wall-echo, at the wall ($y=-\frac{1}{2}L_y$), exactly equals the volume term at the wall.

$$p'_{(\mathrm{s};w_-)}(x,y=-\tfrac{1}{2}L_y,z,t)\overset{(2.17,\ \mathrm{A\,3})}{=}p'_{(\mathrm{s};\mathfrak{V})}(x,y=-\tfrac{1}{2}L_y,z,t)\tag{2.18a}$$

$$p'_{(\mathrm{r};w_-)}(x,y=-\tfrac{1}{2}L_y,z,t)\overset{(2.17,\ \mathrm{A\,3})}{=}p'_{(\mathrm{r};\mathfrak{V})}(x,y=-\tfrac{1}{2}L_y,z,t)\tag{2.18b}$$

This result (2.18) following from the equality of the corresponding Green's functions (2.17) is valid independently of the particular sources $Q(y;\kappa)$ (2.6a).

At high nondimensional wavenumbers κL_y the exact wall-echo Green's function $G_w(y=-\frac{1}{2}L_y,Y;\kappa)$ (2.16), for the computation of p'_w at the lower wall ($y=-\frac{1}{2}L_y$), is approximately equal ($\kappa L_y=3$; Fig. 5) to the wall-echo Green's function $G_{w_-}(y=-\frac{1}{2}L_y,Y;\kappa)$ (A 41) of the halfspace problem with only the lower wall present (Fig. 3), except at the upper part of the channel $Y\in[\frac{1}{4}L_y,\frac{1}{2}L_y]$, where the influence of the upper wall on the Green's function used for the computation of p'_w at the lower wall ($y=-\frac{1}{2}L_y$) is felt. As

Re_{τ_w}	$\bar{M}_{\text{CL}}$	$N_x \times N_y \times N_z$	L_x	L_y	L_z	Δx^+	Δy_w^+	$N_{y^+ \leq 10}$	Δy_{CL}^+	Δz^+	Δt^+	$t^+_{\text{OBS}_{\text{GF}}}$	$\Delta t^+_{s_{\text{GF}}}$
179	0.34	$193 \times 129 \times 169$	$4\pi\delta$	2δ	$\frac{4}{3}\pi\delta$	11.7	0.22	20	4.9	4.4	6.47×10^{-3}	1648	6.47×10^{-1}

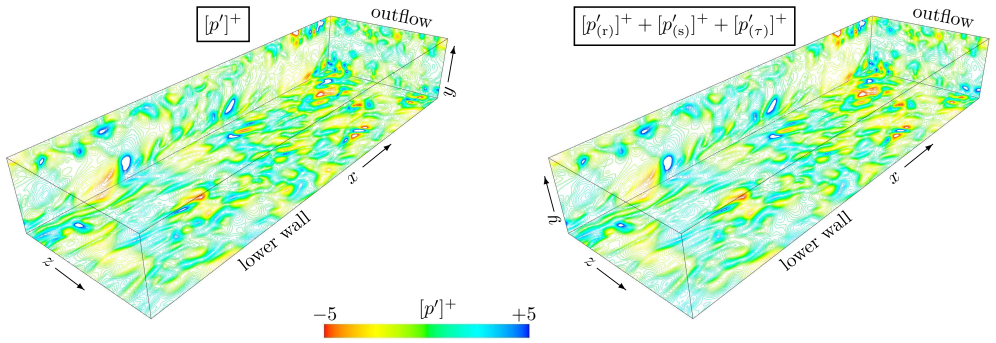

FIGURE 6. Instantaneous fluctuating pressure in wall units $[p']^+$ obtained directly ($Re_{\tau_w} = 179$; $\bar{M}_{\text{CL}} = 0.34$; $193 \times 129 \times 169$ grid; Tab. 1) by the compressible DNS solver (Gerolymos *et al.* 2010*c*) compared to the superposition of the three fields, rapid $[p'_{(\text{r})}]^+$ and slow $[p'_{(\text{s})}]^+$ obtained by the Green's function solution (2.7), and Stokes field $[p'_{(\tau)}]^+$ (2.8), in wall units (50 contours in the range $[-5, +5]$ on the lower wall, the outflow x-periodic interface, and the z-periodicity interface).

the nondimensional wavenumber κL_y further decreases (*ie* the corresponding structure size $\ell_\kappa \delta^{-1} := 2\pi\kappa^{-1}\delta^{-1}$ increases) the influence of the upper wall is felt further down (Fig. 3). Of course there is an analogous effect concerning the influence of the lower wall on the upper wall. As the nondimensional wavenumber κL_y decreases this mutual interaction between the two walls amplifies the echo effect, the amplification growing exponentially with structure size (Fig. 3).

3. Analysis of pressure correlations

The algorithm (§2.2.3) for separating the rapid and slow contributions to p' (§2.2.2) into weakly inhomogeneous ($p'_{(\text{r};\mathfrak{V})}$ and $p'_{(\text{s};\mathfrak{V})}$) and strongly inhomogeneous wall-echo terms ($p'_{(\text{r};w)}$ and $p'_{(\text{s};w)}$), was applied to a low-Reynolds-number ($Re_{\tau_w} \approxeq 180$) well-resolved DNS (grid $193 \times 129 \times 169$; Tab. 1). The simulation was started at $t = t_0$ by interpolation of a well-converged simulation on a coarser grid (grid $129 \times 129 \times 129$; Tab. 1), and continued for $t^+_{\text{GF}_0} - t^+_0 = 681$. During this interval $t^+ \in [t^+_0, t^+_{\text{GF}_0}]$ statistics for $\bar{u}_i$ and $\overline{u'_i u'_j}$, necessary for the computation of the source-terms in (2.3*a*), were computed with sampling at every iteration ($\Delta t^+_s = \Delta t^+ \approxeq 6.47 \times 10^{-3} \iff f^+_s \approxeq 154$). Then the Green's function algorithm for p'-splitting (2.10) was applied, and statistics of pressure correlations were computed for an observation time $t^+_{\text{OBS}_{\text{GF}}} = 1648$, with sampling every 100 iterations ($\Delta t^+_{s_{\text{GF}}} = 100\Delta t^+ \approxeq 6.47 \times 10^{-1} \iff f^+_{s_{\text{GF}}} \approxeq 1.54$).

3.1. *Fluctuating Pressure Field*

The instantaneous fluctuating pressure p'-field reconstructed by the Green's function approach (2.7, 2.8) according to the splitting (2.2) agrees quite well (Fig. 6) with the instantaneous p'-field directly computed (without making use of Green's functions) by the compressible DNS solver (Gerolymos *et al.* 2010*c*).

Both the directly computed p'_{rms} and the rms values ($[p'_{(\text{r})}]_{\text{rms}}$, $[p'_{(\text{s})}]_{\text{rms}}$, $[p'_{(\tau)}]_{\text{rms}}$) of the p'-splitting (2.2) compare satisfactorily (Fig. 7) with standard results from incompressible DNS computations (Kim *et al.* 1987; Hoyas & Jiménez 2008), both in the wall

Re_{τ_w}	$\bar{M}_{\mathrm{CL}}$	$N_x \times N_y \times N_z$	L_x	L_y	L_z	Δx^+	Δy_w^+	$N_{y^+\leq 10}$	Δy_{CL}^+	Δz^+	Δt^+	$t^+_{\mathrm{OBS_{GF}}}$	$\Delta t^+_{s_{\mathrm{GF}}}$
179	0.34	$193 \times 129 \times 169$	$4\pi\delta$	2δ	$\frac{4}{3}\pi\delta$	11.7	0.22	20	4.9	4.4	6.47×10^{-3}	1648	6.47×10^{-1}
178	0.00	$128 \times 129 \times 128$	$4\pi\delta$	2δ	$\frac{4}{3}\pi\delta$	17.7	0.05	14	4.4	5.9	Moser et al. (1999)		
186	0.00	$768 \times 97 \times 340$	$12\pi\delta$	2δ	$4\pi\delta$	8.9	0.10	11	6.1	6.7	Hoyas and Jiménez (2008)		

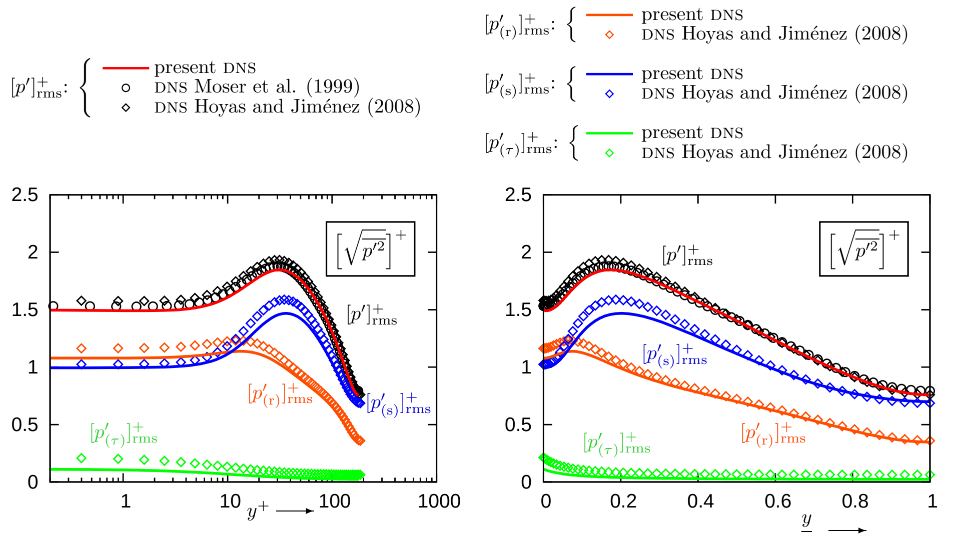

FIGURE 7. Comparison of rms-values $p'_{\mathrm{rms}} := \sqrt{\overline{p'^2}}$ of the fluctuating pressure p' and of the fields $p'_{(\mathrm{r})} + p'_{(\mathrm{s})} + p'_{(\tau)} = p'$ (2.2) from the present DNS computations ($Re_{\tau_w} = 179$; $\bar{M}_{\mathrm{CL}} = 0.34$; $193 \times 129 \times 169$ grid; Tab. 1) with reference results of incompressible pseudospectral (Kim *et al.* 1987) DNS computations of Hoyas & Jiménez (2008, $Re_{\tau_w} = 186$, $M_{\mathrm{CL}} = 0$) and of Moser *et al.* (1999, $Re_{\tau_w} = 178$, $M_{\mathrm{CL}} = 0$), in wall units, plotted against the nondimensional distance-from-the-wall in inner (y^+) and outer ($\delta^{-1}y$) scaling.

and the outer regions (Fig. 7). There is, nonetheless, a difference in the level of Stokes pressure $[p'_{(\tau)}]_{\mathrm{rms}}$ near the wall (Fig. 7), which should be further investigated. However, this discrepancy has no impact on the *a priori* evaluation of various closures (§4), since all models (§4.1, §4.4) neglect the small contributions of the Stokes pressure $p'_{(\tau)}$, although, as discussed in §4.3 the contribution of Stokes pressure to ϕ_{xy} is dominant in the near-wall region ($y^+ \lessapprox 10$).

The new results (Fig. 8) in the present work concern the further splitting ($p' = p'_{(\mathrm{r};\mathfrak{V})} + p'_{(\mathrm{r};w)} + p'_{(\mathrm{s};\mathfrak{V})} + p'_{(\mathrm{s};w)} + p'_{(\tau)}$) into volume and wall-echo terms (2.10). The rms-levels of wall-echo ($[p'_{(\mathrm{r};w)}]_{\mathrm{rms}}$, $[p'_{(\mathrm{s};w)}]_{\mathrm{rms}}$), at the wall ($y = 0$; Fig. 8), are approximately equal to the corresponding volume terms ($[p'_{(\mathrm{r};\mathfrak{V})}]_{\mathrm{rms}}$, $[p'_{(\mathrm{s};\mathfrak{V})}]_{\mathrm{rms}}$). This implies (§2.2.5) that the dominant contributions to the spectra (2.5*b*) of the source-terms $\hat{Q}'_{(\mathrm{r})}R(\kappa_x, y, \kappa_z, t)$ and $\hat{Q}'_{(\mathrm{s})}(\kappa_x, y, \kappa_z, t)$ (2.6*a*) occur at sufficiently high nondimensional wavenumbers $\kappa L_y = 2\kappa\delta$ (Fig. 5), for the interaction between the wall-echo from the upper wall and the wall-echo from the lower wall to be negligibly small. This approximate equality of wall-echo and volume terms holds up to $y^+ \lessapprox 2$ (Fig. 8). Further away from the wall, both wall-echo terms ($[p'_{(\mathrm{r};w)}]_{\mathrm{rms}}$, $[p'_{(\mathrm{s};w)}]_{\mathrm{rms}}$) decay with increasing distance from the wall, always remaining much higher than the Stokes pressure $[p'_{(\tau)}]_{\mathrm{rms}}$ (Fig. 8). In the buffer and outer regions ($y \gtrapprox \frac{5}{100}\delta \overset{Re_{\tau_w}\approxeq 180}{\Longleftrightarrow} y^+ \gtrapprox 10$) the well known predominance of the slow volume term $[p'_{(\mathrm{s};\mathfrak{V})}]_{\mathrm{rms}}$ over the rapid volume term $[p'_{(\mathrm{r};\mathfrak{V})}]_{\mathrm{rms}}$ (Kim 1989; Chang *et al.* 1999) is evident (Fig. 8). Nonetheless, it is essential, from the point-of-view of near-wall modelling,

Re_{τ_w}	$\bar{M}_{\text{CL}}$	$N_x \times N_y \times N_z$	L_x	L_y	L_z	Δx^+	Δy^+_w	$N_{y^+\leq 10}$	Δy^+_{CL}	Δz^+	Δt^+	$t^+_{\text{OBS}_{\text{GF}}}$	$\Delta t^+_{s_{\text{GF}}}$
179	0.34	$193 \times 129 \times 169$	$4\pi\delta$	2δ	$\frac{4}{3}\pi\delta$	11.7	0.22	20	4.9	4.4	6.47×10^{-3}	1648	6.47×10^{-1}
178	0.00	$128 \times 129 \times 128$	$4\pi\delta$	2δ	$\frac{4}{3}\pi\delta$	17.7	0.05	14	4.4	5.9	Moser et al. (1999)		
186	0.00	$768 \times 97 \times 340$	$12\pi\delta$	2δ	$4\pi\delta$	8.9	0.10	11	6.1	6.7	Hoyas and Jiménez (2008)		

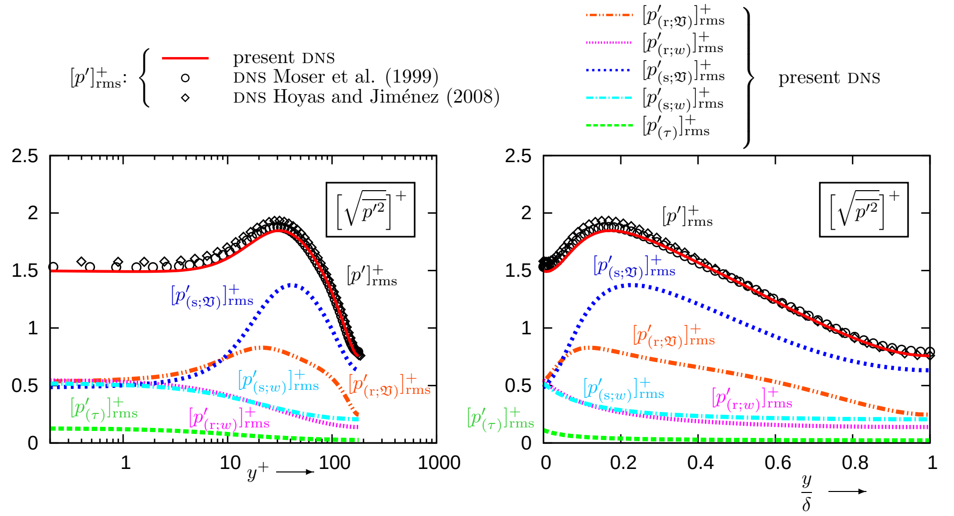

FIGURE 8. Rms-values of the 5 fluctuating pressure fields in the decomposition $p' = p'_{(\text{r};\mathfrak{V})} + p'_{(\text{r};w)} + p'_{(\text{s};\mathfrak{V})} + p'_{(\text{s};w)} + p'_{(\tau)}$ (2.10) from the present DNS computations ($Re_{\tau_w} = 179$; $\bar{M}_{\text{CL}} = 0.34$; $193 \times 129 \times 169$ grid; Tab. 1), plotted against the nondimensional distance-from-the-wall in inner (y^+) and outer ($\delta^{-1}y$) scaling, and p'_{rms} from various DNS databases (Moser *et al.* 1999; Hoyas & Jiménez 2008; Gerolymos *et al.* 2010*c*).

to notice that for $y^+ \lessapprox 10$, $[p'_{(\text{r};\mathfrak{V})}]_{\text{rms}} \approxeq [p'_{(\text{s};\mathfrak{V})}]_{\text{rms}} \approxeq [p'_{(\text{r};w)}]_{\text{rms}} \approxeq [p'_{(\text{s};w)}]_{\text{rms}} > [p'_{(\tau)}]_{\text{rms}}$ (Fig. 8), *ie* for consistent near-wall modelling all of the 4 terms must be accurately modelled.

The above quantitative results (Fig. 8) are also observed qualitatively in the instantaneous levels (Fig. 9) of the 5 terms in the p'-splitting (2.10). Comparison of instantaneous levels of the slow ($p'_{(\text{s})}$) and rapid ($p'_{(\text{r})}$) terms (Fig. 9) clearly shows that both mechanisms of generation of p' (2.3*a*) are of the same magnitude at the wall (lower wall; Fig. 9), while $p'_{(\text{s})}$ is the main mechanism (Chang *et al.* 1999) further away from the wall ($z =$ const plane; Fig. 9). The same observations apply to the corresponding volume terms, $p'_{(\text{r};\mathfrak{V})}$ and $p'_{(\text{s};\mathfrak{V})}$ (Fig. 9). The wall-echo terms, $p'_{(\text{r};w)}$ and $p'_{(\text{s};w)}$, at the wall (lower wall; Fig. 9), are approximately equal to the corresponding volume terms, $p'_{(\text{r};\mathfrak{V})}$ and $p'_{(\text{s};\mathfrak{V})}$, but rapidly decay away from the wall ($z =$ const plane; Fig. 9). Finally, the Stokes pressure $p'_{(\tau)}$ is substantially lower than the other terms and rapidly decays away from the wall (Fig. 9).

The results (Figs. 6–9) on the p'-fields (2.10) provide guidance on the relative importance of each of the 5 p'-fields. Nonetheless, the transposition of these results to the decomposition of correlations containing p' is not always straightforward, especially in the near-wall region ($y^+ \lessapprox 10$). For this reason we study in detail (§3.3, §3.4, §3.5) the correlations containing p' which appear in the transport equations for the Reynolds-stresses (§3.2).

3.2. *Reynolds-stress transport*

The equations governing the Reynolds-stress tensor are central in single-point closure turbulence modelling (Lumley 1978; Hanjalić 1994). The exact transport equations for

Re_{τ_w}	$\bar{M}_{\text{CL}}$	$N_x \times N_y \times N_z$	L_x	L_y	L_z	Δx^+	Δy_w^+	$N_{y^+\leq 10}$	Δy_{CL}^+	Δz^+	Δt^+	$t_{\text{OBS}_{\text{GF}}}^+$	$\Delta t_{s_{\text{GF}}}^+$
179	0.34	$193 \times 129 \times 169$	$4\pi\delta$	2δ	$\frac{4}{3}\pi\delta$	11.7	0.22	20	4.9	4.4	6.47×10^{-3}	1648	6.47×10^{-1}

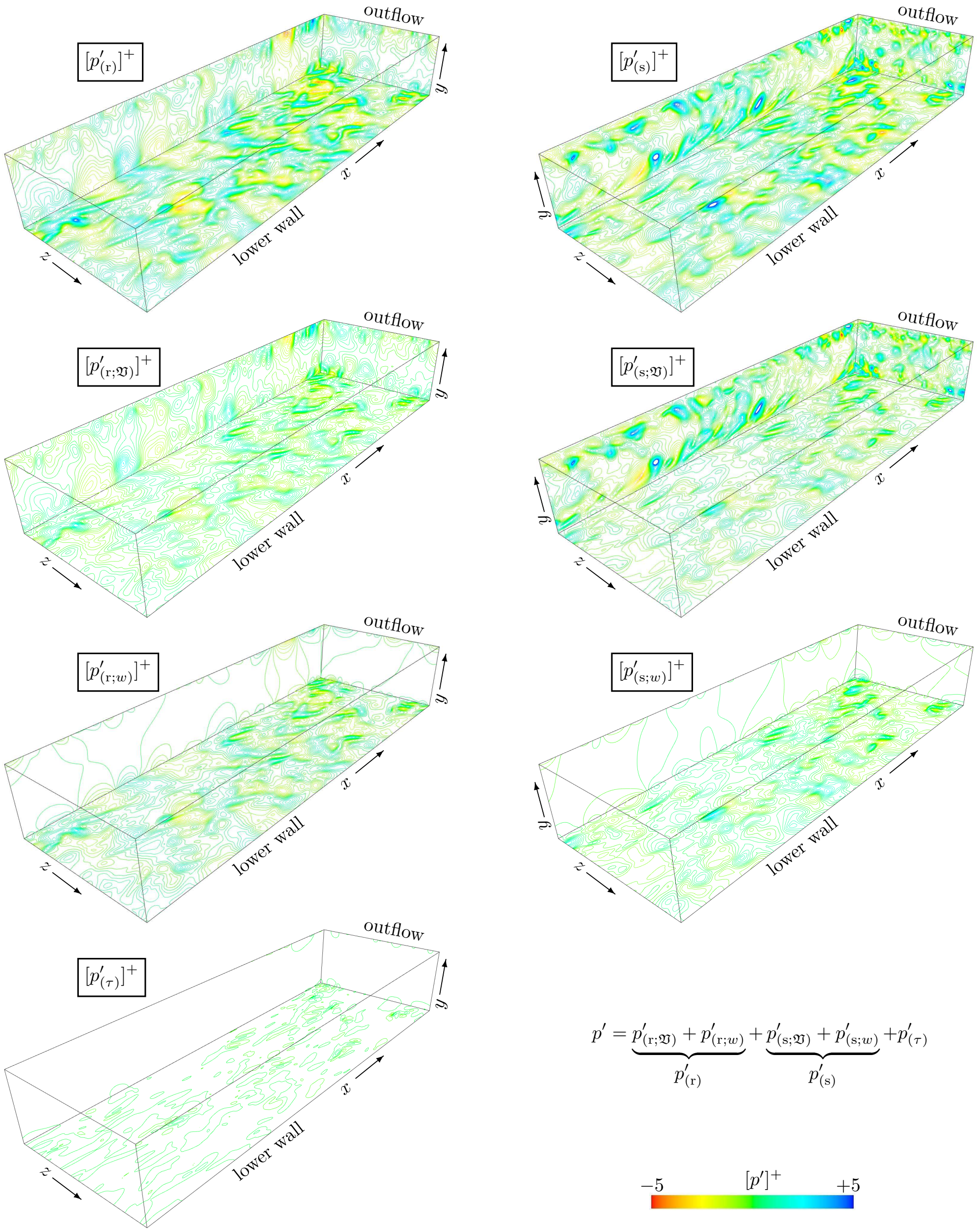

$$p' = \underbrace{p'_{(\text{r};\mathfrak{V})} + p'_{(\text{r};w)}}_{p'_{(\text{r})}} + \underbrace{p'_{(\text{s};\mathfrak{V})} + p'_{(\text{s};w)}}_{p'_{(\text{s})}} + p'_{(\tau)}$$

FIGURE 9. Instantaneous fluctuating pressure fields (2.10) from DNS computations ($Re_{\tau_w} = 179$; $\bar{M}_{\text{CL}} = 0.34$; $193 \times 129 \times 169$ grid; Tab. 1), Stokes $[p'_{(\tau)}]^+$ (2.8), and rapid $[p'_{(\text{r})}]^+$ and slow $[p'_{(\text{s})}]^+$ (2.7), and their decomposition into weakly inhomogeneous volume fields, $[p'_{(\text{r};\mathfrak{V})}]^+$ and $[p'_{(\text{s};\mathfrak{V})}]^+$ (2.11), and strongly inhomogeneous wall-echo fields, $[p'_{(\text{r};w)}]^+$ and $[p'_{(\text{s};w)}]^+$ (2.14), in wall units (50 contours in the range $[-5, +5]$ on the lower wall, the outflow x-periodic interface, and the z-periodicity interface).

the Reynolds-stresses in incompressible flow read (Pope 2000, pp. 315–320)

$$\begin{aligned}\underbrace{\frac{\partial\rho\overline{u'_iu'_j}}{\partial t}+\frac{\partial}{\partial x_\ell}(\rho\overline{u'_iu'_j}\bar{u}_\ell)}_{\text{convection } C_{ij}} &= \underbrace{\frac{\partial}{\partial x_\ell}(-\rho\overline{u'_iu'_ju'_\ell}-\overline{p'u'_j}\delta_{i\ell}-\overline{p'u'_i}\delta_{j\ell}+\overline{u'_i\tau'_{j\ell}+u'_j\tau'_{i\ell}})}_{\text{diffusion } d^{(u)}_{ij}+d^{(p)}_{ij}+d^{(\tau)}_{ij}}\\ &\quad+\underbrace{\overline{p'\left(\frac{\partial u'_i}{\partial x_j}+\frac{\partial u'_j}{\partial x_i}\right)}}_{\text{redistribution } \phi_{ij}}+\underbrace{\left(-\rho\overline{u'_iu'_\ell}\frac{\partial\bar{u}_j}{\partial x_\ell}-\rho\overline{u'_ju'_\ell}\frac{\partial\bar{u}_i}{\partial x_\ell}\right)}_{\text{production } P_{ij}}\\ &\quad-\underbrace{\left(\overline{\tau'_{j\ell}\frac{\partial u'_i}{\partial x_\ell}+\tau'_{i\ell}\frac{\partial u'_j}{\partial x_\ell}}\right)}_{\text{dissipation } \rho\varepsilon^{(\tau)}_{ij}:=2\mu\overline{\partial_{x_\ell}u'_i\partial_{x_\ell}u'_j}+\mu(\overline{\partial_{x_j}u'_\ell\partial_{x_\ell}u'_i}+\overline{\partial_{x_i}u'_\ell\partial_{x_\ell}u'_j})}\end{aligned}\tag{3.1a}$$

Introducing an exact term for the viscous diffusion of the Reynolds-stresses ($d^{(\mu)}_{ij}$) instead of the original term ($d^{(\tau)}_{ij}$), this exact equation is recast in the following mathematically equivalent form, which is actually modelled (Pope 2000, (7.191), p. 319)

$$\begin{aligned}\underbrace{\frac{\partial\rho\overline{u'_iu'_j}}{\partial t}+\frac{\partial}{\partial x_\ell}(\rho\overline{u'_iu'_j}\bar{u}_\ell)}_{\text{convection } C_{ij}} &= \underbrace{\frac{\partial}{\partial x_\ell}(-\rho\overline{u'_iu'_ju'_\ell}-\overline{p'u'_j}\delta_{i\ell}-\overline{p'u'_i}\delta_{j\ell}+\mu\frac{\partial\overline{u'_iu'_j}}{\partial x_\ell})}_{\text{diffusion } d^{(u)}_{ij}+d^{(p)}_{ij}+d^{(\mu)}_{ij}}\\ &\quad+\underbrace{\overline{p'\left(\frac{\partial u'_i}{\partial x_j}+\frac{\partial u'_j}{\partial x_i}\right)}}_{\text{redistribution } \phi_{ij}}+\underbrace{\left(-\rho\overline{u'_iu'_\ell}\frac{\partial\tilde{u}_j}{\partial x_\ell}-\rho\overline{u'_ju'_\ell}\frac{\partial\tilde{u}_i}{\partial x_\ell}\right)}_{\text{production } P_{ij}}\\ &\quad-\underbrace{\left(\frac{\partial}{\partial x_\ell}(\mu\overline{\frac{\partial u'_iu'_j}{\partial x_\ell}})-\overline{(u'_i\frac{\partial\tau'_{j\ell}}{\partial x_\ell}+u'_j\frac{\partial\tau'_{i\ell}}{\partial x_\ell})}\right)}_{\text{dissipation } \bar{\rho}\varepsilon^{(\mu)}_{ij}:=2\mu\overline{\partial_{x_\ell}u'_i\partial_{x_\ell}u'_j}}\end{aligned}\tag{3.1b}$$

Convection C_{ij}, production P_{ij} and viscous diffusion $d^{(\mu)}_{ij}$ are exact terms, while all the other terms ($d^{(u)}_{ij}$, $d^{(p)}_{ij}$, ϕ_{ij}, and $\varepsilon^{(\mu)}_{ij}$) require modelling. Pressure-diffusion $d^{(p)}_{ij}$ and redistribution ϕ_{ij} can be grouped together into the velocity/pressure-gradient correlation tensor Π_{ij}

$$\Pi_{ij}:=-\overline{u'_i\frac{\partial p'}{\partial x_j}}-\overline{u'_j\frac{\partial p'}{\partial x_i}}=\underbrace{\overline{p'\left(\frac{\partial u'_i}{\partial x_j}+\frac{\partial u'_j}{\partial x_i}\right)}}_{\overline{2p'S'_{ij}}}\underbrace{-\left(\overline{\frac{\partial p'u'_i}{\partial x_j}+\frac{\partial p'u'_j}{\partial x_i}}\right)}_{d^{(p)}_{ij}}\overset{(3.1)}{=}\phi_{ij}+d^{(p)}_{ij}\tag{3.2}$$

The velocity/pressure-gradient tensor Π_{ij}, which is the term appearing in most of the original early developments (Chou 1945), tends to 0 as $y\to 0$ (in the viscous sublayer, where $d^{(p)}_{ij}$ and ϕ_{ij} cancel one another). In homogeneous turbulence (HT) $d^{(p)}_{ij}=0 \overset{\text{HT}}{\Longleftrightarrow} \phi_{ij}=\Pi_{ij}$.

Re_{τ_w}	$\bar{M}_{\text{CL}}$	$N_x \times N_y \times N_z$	L_x	L_y	L_z	Δx^+	Δy^+_w	$N_{y^+\leq 10}$	Δy^+_{CL}	Δz^+	Δt^+	$t^+_{\text{OBS}_{\text{GF}}}$	$\Delta t^+_{s_{\text{GF}}}$
179	0.34	$193 \times 129 \times 169$	$4\pi\delta$	2δ	$\frac{4}{3}\pi\delta$	11.7	0.22	20	4.9	4.4	6.47×10^{-3}	1648	6.47×10^{-1}
178	0.00	$128 \times 129 \times 128$	$4\pi\delta$	2δ	$\frac{4}{3}\pi\delta$	17.7	0.05	14	4.4	5.9	Moser et al. (1999)		
186	0.00	$768 \times 97 \times 340$	$12\pi\delta$	2δ	$4\pi\delta$	8.9	0.10	11	6.1	6.7	Hoyas and Jiménez (2008)		

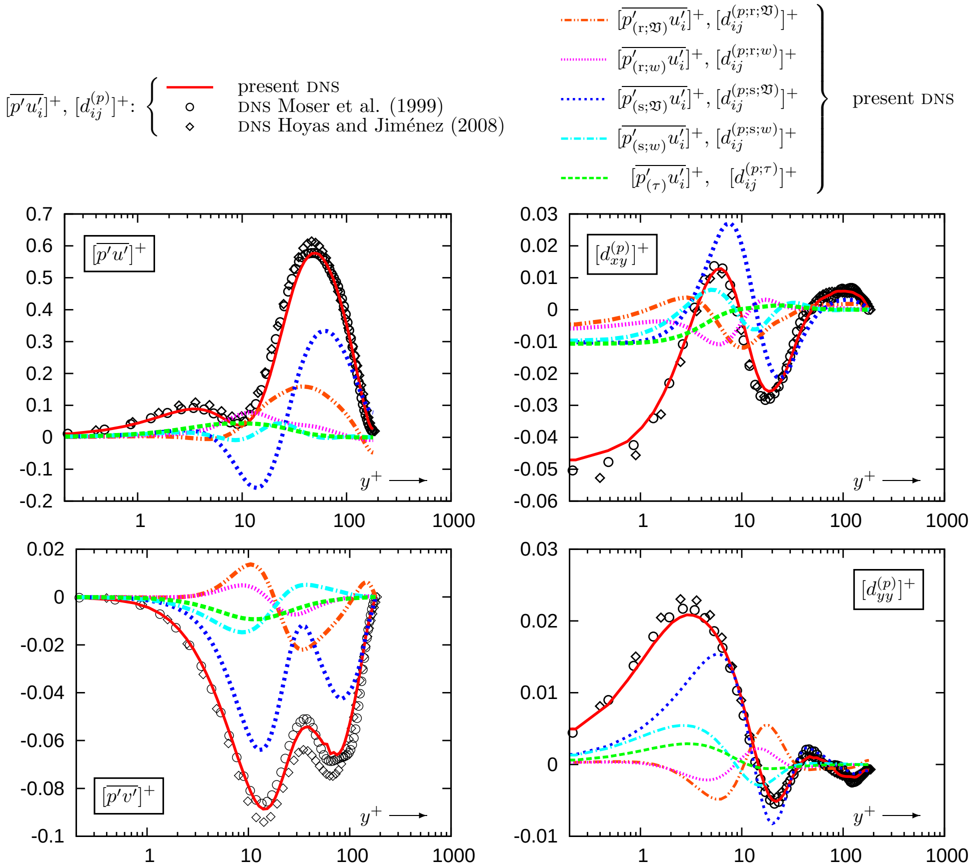

FIGURE 10. Distributions of the 5 terms in the incompressible p'-splitting (2.10) of pressure transport, $\overline{p'_{(\text{r};\mathfrak{V})}u'_i}$, $\overline{p'_{(\text{r};w)}u'_i}$, $\overline{p'_{(\text{s};\mathfrak{V})}u'_i}$, $\overline{p'_{(\text{s};w)}u'_i}$, and $\overline{p'_{(\tau)}u'_i}$, from the present DNS computations ($Re_{\tau_w} = 179$; $\bar{M}_{\text{CL}} = 0.34$; $193 \times 129 \times 169$ grid; Tab. 1), distributions of pressure transport $\overline{p'u'_i}$ from various DNS databases (Moser *et al.* 1999; Hoyas & Jiménez 2008; Gerolymos *et al.* 2010*c*), and corresponding contributions to the pressure-diffusion tensor $d^{(p)}_{ij}$, in wall units, plotted against the nondimensional distance from the wall y^+ (in fully developed incompressible plane channel flow $d^{(p)}_{xx} = d^{(p)}_{yz} = d^{(p)}_{zz} = d^{(p)}_{zx} = 0$).

3.3. *Pressure transport* $\overline{p'u'_i}$ *and pressure diffusion* $d^{(p)}_{ij}$

The p'-splitting (2.10) applied to pressure transport $\overline{p'u'_i}$ and pressure diffusion $d^{(p)}_{ij}$ (3.1, 3.2) indicates (Fig. 10) that the slow volume term $\overline{p'_{(\text{s};\mathfrak{V})}v'}$ is the principal contribution to the normal-to-the-wall transport $\overline{p'v'}$, and evenmore to $d^{(p)}_{yy}$ (for fully developed plane channel flow $d^{(p)}_{yy} \overset{(3.1,\ 3.2)}{=} -2\partial_y\overline{p'v'}$), except in the near-wall region ($y^+ \lessapprox 10$) where all terms are of comparable importance (Fig. 10). Concerning $d^{(p)}_{xy}$ (for fully developed plane channel flow $d^{(p)}_{xy} \overset{(3.1,\ 3.2)}{=} -\partial_y\overline{p'u'}$), again the slow volume term $d^{(p;\text{s};\mathfrak{V})}_{xy}$ is the most

Re_{τ_w}	$\bar{M}_{\text{CL}}$	$N_x \times N_y \times N_z$	L_x	L_y	L_z	Δx^+	Δy_w^+	$N_{y^+\leq 10}$	Δy_{CL}^+	Δz^+	Δt^+	$t^+_{\text{OBS}_{\text{GF}}}$	$\Delta t^+_{s_{\text{GF}}}$
179	0.34	$193 \times 129 \times 169$	$4\pi\delta$	2δ	$\frac{4}{3}\pi\delta$	11.7	0.22	20	4.9	4.4	6.47×10^{-3}	1648	6.47×10^{-1}
178	0.00	$128 \times 129 \times 128$	$4\pi\delta$	2δ	$\frac{4}{3}\pi\delta$	17.7	0.05	14	4.4	5.9	Moser et al. (1999)		
186	0.00	$768 \times 97 \times 340$	$12\pi\delta$	2δ	$4\pi\delta$	8.9	0.10	11	6.1	6.7	Hoyas and Jiménez (2008)		

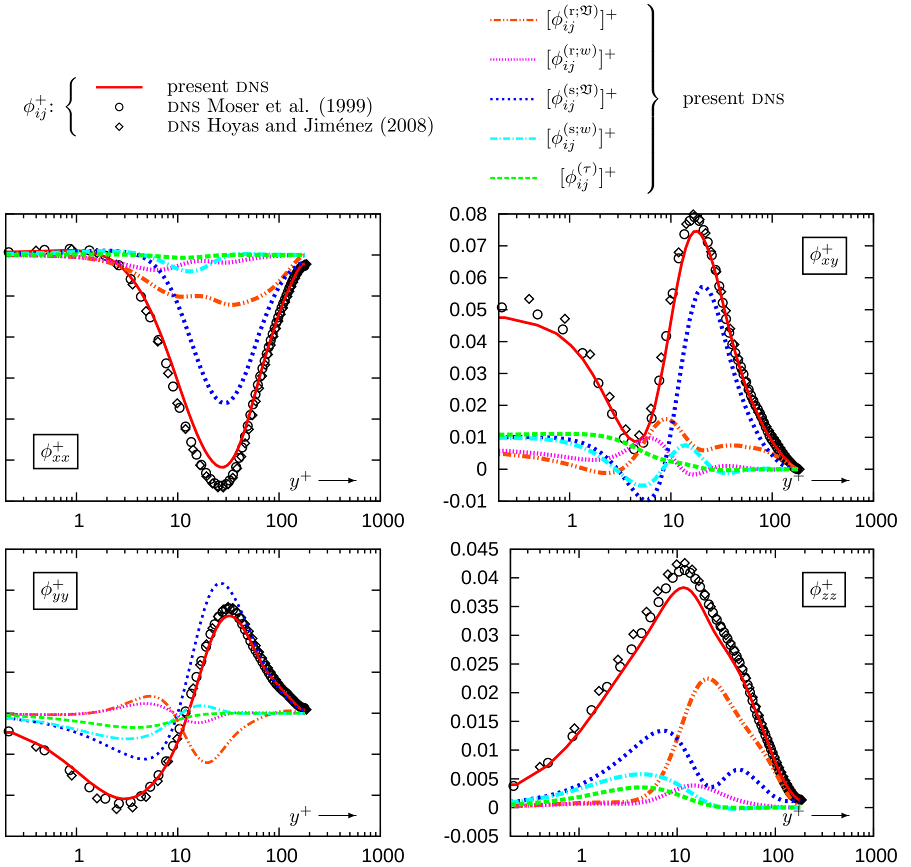

FIGURE 11. Distributions of the 5 terms in the incompressible p'-splitting (2.10) of pressure-strain redistribution, $\phi_{ij}^{(\text{r};\mathfrak{V})}$, $\phi_{ij}^{(\text{r};w)}$, $\phi_{ij}^{(\text{s};\mathfrak{V})}$, $\phi_{ij}^{(\text{s};w)}$, and $\phi_{ij}^{(\tau)}$, from the present DNS computations ($Re_{\tau_w} = 179$; $\bar{M}_{\text{CL}} = 0.34$; $193 \times 129 \times 169$ grid; Tab. 1), and distributions of pressure-strain redistribution ϕ_{ij} from various DNS databases (Moser *et al.* 1999; Hoyas & Jiménez 2008; Gerolymos *et al.* 2010*c*), in wall units, plotted against the nondimensional distance from the wall y^+ (in statistically 2-D plane flow $\phi_{zx} = \phi_{yz} = 0$).

important contribution in the buffer and outer regions, whereas in the near-wall region ($y^+ \lessapprox 10$) all terms are of comparable importance (Fig. 10).

For modelling purposes it is important to notice that, although the slow volume term $d_{ij}^{(p;\text{s};\mathfrak{V})}$ is the main contribution (and a reasonable approximation) to $d_{ij}^{(p)}$ (Fig. 10), in the buffer and outer regions ($y^+ \gtrapprox 10$), this is not the case for pressure transport $\overline{p'u_i'}$, especially for $\overline{p'u'}$ (Fig. 10), where, for $5 \lessapprox y^+ \lessapprox 30$, $\overline{p'_{(\text{s};\mathfrak{V})}u'}$ is of the opposite sign with respect to $\overline{p'u'}$.

These remarks imply that a consistent model for pressure diffusion $d_{ij}^{(p)}$, in the buffer and outer regions ($y^+ \gtrapprox 10$), can be built using only slow volume terms. However, such a model for $d_{ij}^{(p)}$ ($y^+ \gtrapprox 10$), based on $d_{ij}^{(p;\text{s};\mathfrak{V})}$ only, cannot correspond to (or be built from) a satisfactory model for pressure transport $\overline{p'u'_i}$ (Fig. 10). The near-wall modelling of pressure diffusion $d_{ij}^{(p)}$ ($y^+ \lessapprox 10$) is more complex, since (Fig. 10) it must contain rapid terms and wall-echo terms (Fig. 10). To the authors' knowledge (Vallet 2007) no closure for $d_{ij}^{(p)}$ satisfies all of these requirements (Donaldson 1969; Hirt 1969; Daly & Harlow 1970; Lumley 1978; Fu 1993; Demuren *et al.* 1996; Sauret & Vallet 2007; Vallet 2007).

3.4. *Pressure-strain redistribution* ϕ_{ij}

The application of the p'-splitting (2.10) to pressure-strain redistribution ϕ_{ij} (3.1, 3.2) shows again that the volume terms ($\phi_{ij}^{(\mathrm{r};\mathfrak{V})}$ and $\phi_{ij}^{(\mathrm{s};\mathfrak{V})}$) are the dominant contribution to ϕ_{ij} in the buffer and outer regions ($y^+ \gtrapprox 15$; Fig. 11). Notice that $\phi_{zz}^{(\mathrm{r};\mathfrak{V})} > \phi_{zz}^{(\mathrm{s};\mathfrak{V})}$ for $y^+ \gtrapprox 15$ (Fig. 11), contrary to the other components for which the slow volume terms are the more important contributions to ϕ_{ij} in the buffer and outer regions ($y^+ \gtrapprox 15$; Fig. 11).

In the near-wall region ($y^+ \lessapprox 10$) the wall-echo terms ($\phi_{ij}^{(\mathrm{r};w)}$ and $\phi_{ij}^{(\mathrm{s};w)}$) are of the same order-of-magnitude as the corresponding volume terms ($\phi_{ij}^{(\mathrm{r};\mathfrak{V})}$ and $\phi_{ij}^{(\mathrm{s};\mathfrak{V})}$, respectively), satisfying an approximate equality at the wall, which (*cf* §2.2.5) implies that the energy-containing nondimensional wavenumbers of the source-terms (2.3*a*, 2.5*b*, 2.6*a*) are sufficiently high for the interaction between upper and lower wall to be negligible (Fig. 5). Furthermore, for the low-Reynolds-number case studied in the present work ($Re_{\tau_w} \approxeq 180$) the Stokes pressure term $\phi_{ij}^{(\tau)}$ is of the same order-of-magnitude, in the near-wall region ($y^+ \lessapprox 10$; Fig. 11), as the other terms of the p'-splitting (2.10), and is particularly important for the shear component ϕ_{xy} (Fig. 11). At the wall ($y^+ = 0$; Fig. 11) $[\phi_{xy}^{(\tau)}]_{y=0}$ accounts for $\sim 25\%$ of $[\phi_{xy}]_{y=0}$. For a plane wall $\perp \vec{e}_y$, at the wall ($y = 0$), $[\phi_{xy}]_{y=0} \overset{(3.1,\,3.2)}{=} [\overline{p'\partial_y u'}]_{y=0}$ (because $v'_{y=0} = 0 \Longrightarrow [\partial_x v']_{y=0} = 0$). Therefore, the high level of $[\phi_{xy}^{(\tau)}]_{y=0}$ relative to the other terms of the p'-splitting (2.10) implies that at the wall the fluctuating Stokes pressure $[p'_{(\tau)}]_{y=0}$ is well correlated with the fluctuating wall-shear-stress $[\tau'_{xy}]_{y=0} = \mu[\partial_y u']_{y=0}$. Notice that none of known models for ϕ_{ij} (§4.1) gives the correct viscous sublayer behaviour of ϕ_{xy} ($y^+ \lessapprox 5$; Fig. 11).

3.5. *Velocity/pressure-gradient* Π_{ij}

The velocity/pressure-gradient correlation Π_{ij} (3.2) is exactly the sum of pressure diffusion $d_{ij}^{(p)}$ (§3.3) and pressure-strain redistribution ϕ_{ij} (§3.4). By definition (3.2) $[\Pi_{ij}]_{y=0}$ because of the no-slip wall boundary-condition for the fluctuating velocity $[u'_i]_{y=0} = 0$, implying $[\phi_{ij}]_{y=0} = -[d_{ij}^{(p)}]_{y=0}$, so that very near the wall we expect that $\Pi_{ij} := \phi_{ij} + d_{ij}^{(p)}$ will be asymptotically approaching 0. Observation of DNS data ($y^+ \lessapprox 5$; Fig. 12) indicates that the rate at which Π_{zz} approaches 0 as $y^+ \to 0$ is much slower compared to the other components (Π_{xx}, Π_{xy}, and Π_{yy}).

In fully developed incompressible plane channel flow $d_{xx}^{(p)} = d_{zz}^{(p)} = 0$ by (3.2), implying that $\Pi_{xx} = \phi_{xx}$ and $\Pi_{zz} = \phi_{zz}$, but also that $\Pi_{\ell\ell} = d_{yy}^{(p)}$ (since $\phi_{\ell\ell} \overset{(3.2)}{=} 0$ by the incompressible fluctuating continuity equation $\partial_{x_\ell} u'_\ell = 0$). For the three components, Π_{xx}, Π_{xy} and Π_{yy}, the dominant contribution from the mechanisms of the p'-splitting (2.10) comes from the slow volume terms ($\Pi_{xx}^{(\mathrm{s};\mathfrak{V})}$, $\Pi_{xy}^{(\mathrm{s};\mathfrak{V})}$, and $\Pi_{yy}^{(\mathrm{s};\mathfrak{V})}$), the rapid volume terms ($\Pi_{xx}^{(\mathrm{r};\mathfrak{V})}$, $\Pi_{xy}^{(\mathrm{r};\mathfrak{V})}$, and $\Pi_{yy}^{(\mathrm{r};\mathfrak{V})}$) being the main remaining contribution (Fig. 12). On the contrary, all of the 5 mechanisms of p'-generation in (2.10) contribute, with the same order-of-magnitude in the near-wall region ($y^+ \lessapprox 15$; Fig. 12) to Π_{zz} ($= \phi_{zz}$ in fully developed incompressible plane channel flow), this difference between Π_{zz} and the other

Re_{τ_w}	$\bar{M}_{\mathrm{CL}}$	$N_x \times N_y \times N_z$	L_x	L_y	L_z	Δx^+	Δy_w^+	$N_{y^+\leq 10}$	Δy_{CL}^+	Δz^+	Δt^+	$t_{\mathrm{OBS_{GF}}}^+$	$\Delta t_{s_{\mathrm{GF}}}^+$
179	0.34	$193 \times 129 \times 169$	$4\pi\delta$	2δ	$\frac{4}{3}\pi\delta$	11.7	0.22	20	4.9	4.4	6.47×10^{-3}	1648	6.47×10^{-1}
178	0.00	$128 \times 129 \times 128$	$4\pi\delta$	2δ	$\frac{4}{3}\pi\delta$	17.7	0.05	14	4.4	5.9	Moser et al. (1999)		
186	0.00	$768 \times 97 \times 340$	$12\pi\delta$	2δ	$4\pi\delta$	8.9	0.10	11	6.1	6.7	Hoyas and Jiménez (2008)		

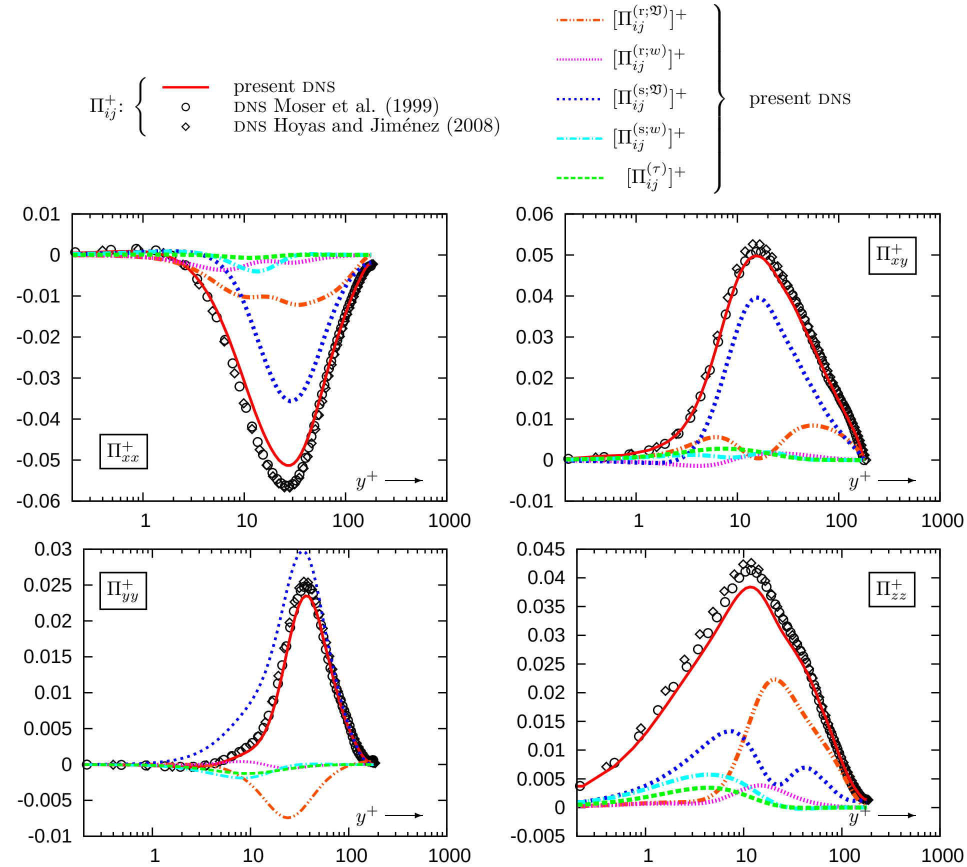

FIGURE 12. Distributions of the 5 terms in the incompressible p'-splitting (2.10) of velocity/pressure-gradient correlation, $\Pi_{ij}^{(\mathrm{r};\mathfrak{V})}$, $\Pi_{ij}^{(\mathrm{r};w)}$, $\Pi_{ij}^{(\mathrm{s};\mathfrak{V})}$, $\Pi_{ij}^{(\mathrm{s};w)}$, and $\Pi_{ij}^{(\tau)}$, from the present DNS computations ($Re_{\tau_w} = 179$; $\bar{M}_{\mathrm{CL}} = 0.34$; $193 \times 129 \times 169$ grid; Tab. 1), and distributions of velocity/pressure-gradient correlation Π_{ij} from various DNS databases (Moser *et al.* 1999; Hoyas & Jiménez 2008; Gerolymos *et al.* 2010*c*), in wall units, plotted against the nondimensional distance from the wall y^+ (in fully developed incompressible plane channel flow $\Pi_{zx} = \Pi_{yz} = 0$, $\Pi_{xx} = \phi_{xx}$, and $\Pi_{zz} = \phi_{zz}$).

components being related to the slower rate at which Π_{zz} goes to 0 as $y^+ \to 0$ ($y^+ \lessapprox 5$; Fig. 12).

4. *A priori* evaluation of SMCs for the pressure correlations

Pressure correlations (3.2) appearing in the Reynolds-stress transport equations (3.1) are of fundamental importance in SMCs (Launder *et al.* 1975; Hanjalić 1994). Evaluation in complex flows around complex geometries (Gerolymos *et al.* 2002, 2010*a*), confirms the generally accepted view (Hanjalić 1994) that the rapid redistribution terms control separation (Vallet 2008), but also suggest that pressure diffusion may be influential not only on the entrainment at the edge of shear layers (Demuren *et al.* 1994; Suga 2004) but also in controling reattachment in the near-wall region (Vallet 2007).

In the present work we assess *a priori* SMCs of the pressure correlations used in RSMs, separately evaluating the closure for the quasi-homogeneous volume terms and the strongly inhomogeneous wall-echo terms, following from the splitting (2.10) of p'

$$\begin{aligned}
\phi_{ij} =& \underbrace{\frac{1}{\pi}\iiint_{\mathfrak{V}} \frac{\partial \bar{\mathfrak{u}}_\ell}{\partial \mathfrak{x}_k} \overline{S'_{ij}\frac{\partial \mathfrak{u}'_k}{\partial \mathfrak{x}_\ell}} \frac{d\mathfrak{v}(\vec{\mathfrak{x}},t)}{|\vec{\mathfrak{x}}-\vec{x}|}}_{\phi_{ij}^{(\mathrm{r};\mathfrak{V})}} + \phi_{ij}^{(\mathrm{r};w)} \\
&+ \underbrace{\frac{1}{2\pi}\iiint_{\mathfrak{V}} \overline{S'_{ij}\frac{\partial^2 \mathfrak{u}'_k\mathfrak{u}'_\ell}{\partial \mathfrak{x}_\ell \partial \mathfrak{x}_k}} \frac{d\mathfrak{v}(\vec{\mathfrak{x}},t)}{|\vec{\mathfrak{x}}-\vec{x}|}}_{\phi_{ij}^{(\mathrm{s};\mathfrak{V})}} + \phi_{ij}^{(\mathrm{s};w)} + \phi_{ij}^{(\tau)} \qquad (4.1a)
\end{aligned}$$

$$\begin{aligned}
\overline{p'u'_i} =& \underbrace{\frac{1}{2\pi}\iiint_{\mathfrak{V}} \frac{\partial \bar{\mathfrak{u}}_\ell}{\partial \mathfrak{x}_k} \overline{u'_i\frac{\partial \mathfrak{u}'_k}{\partial \mathfrak{x}_\ell}} \frac{d\mathfrak{v}(\vec{\mathfrak{x}},t)}{|\vec{\mathfrak{x}}-\vec{x}|}}_{[\overline{p'u'_i}]^{(\mathrm{r};\mathfrak{V})}} + [\overline{p'u'_i}]^{(\mathrm{r};w)} \\
&+ \underbrace{\frac{1}{4\pi}\iiint_{\mathfrak{V}} \overline{u'_i\frac{\partial^2 \mathfrak{u}'_k\mathfrak{u}'_\ell}{\partial \mathfrak{x}_\ell \partial \mathfrak{x}_k}} \frac{d\mathfrak{v}(\vec{\mathfrak{x}},t)}{|\vec{\mathfrak{x}}-\vec{x}|}}_{[\overline{p'u'_i}]^{(\mathrm{s};\mathfrak{V})}} + [\overline{p'u'_i}]^{(\mathrm{s};w)} + [\overline{p'u'_i}]^{(\tau)} \qquad (4.1b)
\end{aligned}$$

where the volume integrals in (4.1) are obtained by multiplying (1.2) by $2S'_{ij}$ (4.1a) or by u'_i (4.1b), and ensemble-averaging.

Every order-2 tensor $\mathbf{A} \in \mathbb{E}^{3\times 3}$ has 3 invariants (Rivlin 1955),

$$\begin{aligned}
\mathrm{I}_{\mathbf{A}} :=& \mathrm{tr}\mathbf{A} && (4.2a) \\
\mathrm{II}_{\mathbf{A}} :=& \tfrac{1}{2}(\mathrm{tr}^2\mathbf{A} - \mathrm{tr}\mathbf{A}^2) = \tfrac{1}{2}\left((A_{\ell\ell})^2 - A_{\ell m}A_{\ell m}\right) \iff \mathrm{tr}\mathbf{A}^2 = \mathrm{I}_{\mathbf{A}}^2 - 2\mathrm{II}_{\mathbf{A}} && (4.2b) \\
\mathrm{III}_{\mathbf{A}} :=& \det\mathbf{A} = \epsilon_{ijk}A_{1i}A_{2j}A_{3k} = \epsilon_{ijk}A_{i1}A_{j2}A_{k3} \\
=& \tfrac{1}{3}\Big(\mathrm{I}_{\mathbf{A}^3} + 3\mathrm{I}_{\mathbf{A}}\mathrm{II}_{\mathbf{A}} - \mathrm{I}_{\mathbf{A}}^3\Big) \\
=& \tfrac{1}{6}\Big(2\mathrm{tr}\mathbf{A}^3 - 3\mathrm{tr}\mathbf{A}\;\mathrm{tr}\mathbf{A}^2 + \mathrm{tr}^3\mathbf{A}\Big) && (4.2c)
\end{aligned}$$

coefficients of its characteristic polynomial $\mathbb{R}[x] \ni p(x;\mathbf{A}) := x^3 - \mathrm{I}_{\mathbf{A}}x^2 + \mathrm{II}_{\mathbf{A}}x - \mathrm{III}_{\mathbf{A}}$. Both for the expression of different models and for the construction of representation bases for redistribution, the following definitions are introduced

$$\begin{aligned}
r_{ij} :=& \overline{u'_i u'_j} \quad ; \quad \mathrm{k} := \tfrac{1}{2}r_{\ell\ell} = \tfrac{1}{2}\overline{u'_\ell u'_\ell} && (4.3a) \\
\varepsilon_{ij}^{(\mu)} :=& 2\nu\overline{\frac{\partial u'_i}{\partial x_\ell}\frac{\partial u'_j}{\partial x_\ell}} \quad ; \quad \varepsilon := \tfrac{1}{2}\varepsilon_{\ell\ell}^{(\mu)} = \nu\overline{\frac{\partial u'_k}{\partial x_\ell}\frac{\partial u'_k}{\partial x_\ell}} && (4.3b) \\
b_{ij} :=& \frac{r_{ij}}{2\mathrm{k}} - \tfrac{1}{3}\delta_{ij} && (4.3c) \\
b_{\varepsilon_{ij}} :=& \frac{\varepsilon_{ij}^{(\mu)}}{2\varepsilon} - \tfrac{1}{3}\delta_{ij} && (4.3d)
\end{aligned}$$

$$\bar{S}_{ij} :=\tfrac{1}{2}\left(\frac{\partial \bar{u}_i}{\partial x_j}+\frac{\partial \bar{u}_j}{\partial x_i}\right) \tag{4.3e}$$

$$\bar{\Omega}_{ij} :=\tfrac{1}{2}\left(\frac{\partial \bar{u}_i}{\partial \bar{x}_j}-\frac{\partial \bar{u}_j}{\partial x_i}\right) \tag{4.3f}$$

$$P_{ij} := -\,\rho\overline{u'_i u'_\ell}\frac{\partial \bar{u}_j}{\partial x_\ell}-\rho\overline{u'_j u'_\ell}\frac{\partial \bar{u}_i}{\partial x_\ell} \quad ; \quad P_{ij}^{(\mathrm{dev})} := P_{ij}-\tfrac{2}{3}P_{\mathrm{k}}\delta_{ij} \tag{4.3g}$$

$$D_{ij} := -\,\rho\overline{u'_i u'_\ell}\frac{\partial \bar{u}_\ell}{\partial x_j}-\rho\overline{u'_j u'_\ell}\frac{\partial \bar{u}_\ell}{\partial x_i} \quad ; \quad D_{ij}^{(\mathrm{dev})} := D_{ij}-\tfrac{2}{3}P_{\mathrm{k}}\delta_{ij} \tag{4.3h}$$

$$P_{\bar{S}_{ij}} := -\,\rho\overline{u'_i u'_\ell}\bar{S}_{j\ell}-\rho\overline{u'_j u'_\ell}\bar{S}_{i\ell} \quad ; \quad P_{\bar{S}_{ij}}^{(\mathrm{dev})} :=P_{\bar{S}_{ij}}-\tfrac{2}{3}P_{\mathrm{k}}\delta_{ij} \tag{4.3i}$$

$$P_{\bar{\Omega}_{ij}} := -\,\rho\overline{u'_i u'_\ell}\bar{\Omega}_{j\ell}-\rho\overline{u'_j u'_\ell}\bar{\Omega}_{i\ell} \quad ; \quad P_{\bar{\Omega}_{ij}}^{(\mathrm{dev})} := P_{\bar{\Omega}_{ij}} \tag{4.3j}$$

where r_{ij} (4.3a) is the symmetric tensor of the second moments of the fluctuating velocities ($-\rho r_{ij}$ are the Reynolds-stresses) with trace $\mathrm{I}_{\mathbf{r}} = 2\mathrm{k}$ (4.3a) and nondimensional deviatoric projection the Reynolds-stress-anisotropy tensor b_{ij} (4.3c), $\varepsilon_{ij}^{(\mu)}$ (4.3b) is the symmetric dissipation-rate tensor (3.1b) with trace $\mathrm{I}_{\boldsymbol{\varepsilon}^{(\mu)}} = 2\varepsilon$ (4.3b) and nondimensional deviatoric projection the dissipation-rate-anisotropy tensor $b_{\varepsilon_{ij}}$ (4.3d), $\bar{S}_{ij}$ (4.3e) is the symmetric deviatoric (in incompressible flow) mean strain-rate tensor, $\bar{\Omega}_{ij}$ (4.3f) is the antisymmetric (hence deviatoric) mean rotation-rate tensor, P_{ij} (4.3g) is the symmetric rate-of-production tensor of the Reynolds-stresses (3.1) with deviatoric projection $P_{ij}^{(\mathrm{dev})}$ (4.3g), the symmetric tensor D_{ij} (4.3h) is the complement of P_{ij} (Naot *et al.* 1970, 1973; Launder *et al.* 1975) with respect to twice the symmetric tensor $P_{\bar{S}_{ij}}$ (4.3i) which is the production by mean strain with deviatoric projection $P_{\bar{S}_{ij}}^{(\mathrm{dev})}$ (4.3i), and the symmetric tensor $P_{\bar{\Omega}_{ij}}$ (4.3j) is the production by mean rotation which is deviatoric[†] so that $P_{\bar{\Omega}_{ij}}^{(\mathrm{dev})} := P_{\bar{\Omega}_{ij}}$ (4.3j). Obviously

$$\frac{\partial \bar{u}_i}{\partial x_j} \overset{(4.3e,\ 4.3f)}{=} \bar{S}_{ij}+\bar{\Omega}_{ij} \tag{4.4a}$$

$$P_{ij} \overset{(4.3g,\ 4.3i,\ 4.3j,\ 4.4a)}{=} P_{\bar{S}_{ij}}+P_{\bar{\Omega}_{ij}} \tag{4.4b}$$

$$D_{ij} \overset{(4.3h,\ 4.3i,\ 4.3j,\ 4.4a)}{=} P_{\bar{S}_{ij}}-P_{\bar{\Omega}_{ij}} = 2P_{\bar{S}_{ij}}-P_{ij} = P_{ij}-2P_{\bar{\Omega}ij} \tag{4.4c}$$

$$(4.3) \Longrightarrow \begin{cases} \mathrm{I}_{\mathbf{P}} = \mathrm{I}_{\mathbf{D}} = \mathrm{I}_{\mathbf{P}_{\bar{S}}} = 2P_{\mathrm{k}} \\ \mathrm{I}_{\mathbf{P}_{\bar{\Omega}}} = 0 \end{cases} \tag{4.4d}$$

By (4.4c) D_{ij} is better interpreted as the difference between production by mean strain and production by mean rotation. In (4.3, 4.4) k (4.3a) is the kinetic energy of turbulence, ε (4.3b) is its dissipation rate, and P_{k} (4.4d) is its production rate. Following Lumley (1978) the invariants (4.2) $\mathrm{II}_{\mathbf{b}}$ and $\mathrm{III}_{\mathbf{b}}$ of the Reynolds-stress-anisotropy tensor (4.3c) play a major role in turbulence modelling. More recently (Jakirlić & Hanjalić 2002) the invariants $\mathrm{II}_{\mathbf{b}_\varepsilon}$ and $\mathrm{III}_{\mathbf{b}_\varepsilon}$ were also considered. Both r_{ij} (4.3a) and $\varepsilon_{ij}^{(\mu)}$ (4.3b) are positive semidefinite (their diagonal components are always nonnegative and they have 3 nonnegative eigenvalues), so that they have the same realizability triangle, and we may define the corresponding Lumley's flatness parameters (Lumley 1978)

[†] $P_{\bar{\Omega}_{ii}} \overset{(4.3j)}{=} -2\rho\overline{u'_i u'_\ell}\bar{\Omega}_{i\ell} \overset{(4.3f)}{=} +2\rho\overline{u'_i u'_\ell}\bar{\Omega}_{\ell i} = +2\rho\overline{u'_j u'_k}\bar{\Omega}_{jk} = +2\rho\overline{u'_i u'_\ell}\bar{\Omega}_{i\ell} \overset{(4.3j)}{=} -P_{\bar{\Omega}_{ii}} \Longrightarrow P_{\bar{\Omega}_{ii}} = 0$

$$A := 1 + 27\mathrm{III}_{\mathbf{b}} + 9\mathrm{II}_{\mathbf{b}} \tag{4.5a}$$

$$A_\varepsilon := 1 + 27\mathrm{III}_{\mathbf{b}_\varepsilon} + 9\mathrm{II}_{\mathbf{b}_\varepsilon} \tag{4.5b}$$

Both A (4.5*a*) and A_ε (4.5*b*) vary in $[0, 1]$ with $A = 0$ denoting 2-C turbulence (Simonsen & Krogstad 2005), $A = 1$ denoting isotropic turbulence, $A_\varepsilon = 0$ denoting 2-C dissipation and $A_\varepsilon = 1$ denoting isotropic dissipation.

4.1. *Typical models for* ϕ_{ij}

It is beyond the scope of the present work to make an exhaustive review of existing models. We concentrate instead on models representative of widely used families of closures (LRR: Launder *et al.* 1975; GL: Gibson & Launder 1978; SSG: Speziale *et al.* 1991; SAYS: So *et al.* 1996; S: Suga 2004; JEJK: Jakirlić *et al.* 2007). These models are briefly summarised in the following, using the forms given in the original papers,† before proceeding to their representation in a common basis.

4.1.1. Launder *et al.* 1975, LRR

The LRR model (Launder *et al.* 1975) is an early attempt to apply tensorial representations for the closure of the order-4 tensor defined by the volume integrals in (4.1), leading to the same tensorial representation of ϕ_{ij} as the one which was obtained by Naot *et al.* (1970, 1973) applying a closure for the 2-point correlations in (4.1). It reads

$$[\phi_{ij}]_{\mathrm{LRR}} := [\phi_{ij}^{(\mathrm{s};\mathfrak{V})}]_{\mathrm{LRR}} + [\phi_{ij}^{(\mathrm{s};w)}]_{\mathrm{LRR}} + [\phi_{ij}^{(\mathrm{r};\mathfrak{V})}]_{\mathrm{LRR}} + [\phi_{ij}^{(\mathrm{r};w)}]_{\mathrm{LRR}} \tag{4.6a}$$

$$[\phi_{ij}^{(\mathrm{s};\mathfrak{V})}]_{\mathrm{LRR}} := -2c_{\mathrm{LRR}_1}\rho\varepsilon b_{ij} \tag{4.6b}$$

$$\begin{aligned}[\phi_{ij}^{(\mathrm{r};\mathfrak{V})}]_{\mathrm{LRR}} :=& -(\tfrac{60}{55}c_{\mathrm{LRR}_2} - \tfrac{4}{55})\rho \mathrm{k}\bar{S}_{ij}\\ & -(\tfrac{1}{11}c_{\mathrm{LRR}_2} + \tfrac{8}{11})P_{ij}^{(\mathrm{dev})} - (\tfrac{8}{11}c_{\mathrm{LRR}_2} - \tfrac{2}{11})D_{ij}^{(\mathrm{dev})}\end{aligned} \tag{4.6c}$$

$$[\phi_{ij}^{(\mathrm{s};w)}]_{\mathrm{LRR}} := +2c_{\mathrm{LRR}_3}f_{\mathrm{GL}_w}\rho\varepsilon b_{ij} \tag{4.6d}$$

$$[\phi_{ij}^{(\mathrm{r};w)}]_{\mathrm{LRR}} := +c_{\mathrm{LRR}_4}f_{\mathrm{GL}_w}(P_{ij} - D_{ij}) \tag{4.6e}$$

$$c_{\mathrm{LRR}_1} = 1.5 \quad ; \quad c_{\mathrm{LRR}_2} = 0.4 \quad ; \quad c_{\mathrm{LRR}_3} = \tfrac{25}{80} \quad ; \quad c_{\mathrm{LRR}_4} = \tfrac{3}{80} \tag{4.6f}$$

where $P_{ij}^{(\mathrm{dev})}$ (4.3*g*) is the deviatoric projection of the production tensor (3.1*a*), $D_{ij}^{(\mathrm{dev})}$ (4.3*h*) is the deviatoric projection of the difference between production by strain minus production by rotation (4.4*c*). The wall-echo terms (4.6*d*, 4.6*e*) do not use the tensor $e_{n_i}e_{n_j}$ ($\vec{e}_n$ being the unit normal-to-the-wall vector; *cf* §4.1.2), but only a wall-proximity function f_{GL_w} (4.7*f*), which is inversely proportional to the distance-from-the-wall n made nondimensional by the turbulence lengthscale ℓ_{T} (4.7*f*), and which discussed in further detail in §4.1.2. Although superseded by more recent models (Hanjalić 1994) the LRR proposal is included here as a baseline reference, not only because it is one of the most widely known closures, but also because it can be used to highlight the problems encountered when using a linear model with constant coefficients.

---

† Several models (*eg* S: Suga 2004; JEJK: Jakirlić *et al.* 2007) are written using $a_{ij} := 2b_{ij}$ to denote an alternative anisotropy tensor (4.3*c*), and the traces $A_2 := \mathrm{tr}\mathbf{a}^2 = a_{ij}a_{ij} = 4b_{ij}b_{ij} = -8\mathrm{II}_{\mathbf{b}}$ and $A_3 := \mathrm{tr}\mathbf{a}^3 = a_{ij}a_{jk}a_{ki} = 8b_{ij}b_{jk}b_{ki} = 24\mathrm{III}_{\mathbf{b}}$. These substitutions were directly made in the model expressions. Lumley's flatness parameter (Lumley 1978) is the same in both bases, *viz* $A \overset{(4.5a)}{:=} 1 + 27\mathrm{III}_{\mathbf{b}} + 9\mathrm{II}_{\mathbf{b}} = 1 - \frac{9}{8}(A_2 - A_3)$.

4.1.2. Gibson & Launder 1978, GL

The Gibson-Launder model introduces the modern form (Hanjalić 1994) for the wall-echo terms, by applying the ideas of Daly & Harlow (1970) and Shir (1973) to include both slow and rapid wall-echo terms. It uses the isotropisation-of-production (IP) model (Naot *et al.* 1970; Reynolds 1974) for the quasi-homogeneous part of rapid pressure-strain, along with the linear return-to-isotropy (RI) model of Rotta (1951*a*) for the quasi-homogeneous part of slow pressure-strain, and reads

$$
\begin{aligned}
[\phi_{ij}]_{\text{GL}} :=& [\phi_{ij}^{(\text{s};\mathfrak{V})}]_{\text{GL}} + [\phi_{ij}^{(\text{s};w)}]_{\text{GL}} + [\phi_{ij}^{(\text{r};\mathfrak{V})}]_{\text{GL}} + [\phi_{ij}^{(\text{r};w)}]_{\text{GL}} && (4.7a)\\
[\phi_{ij}^{(\text{s};\mathfrak{V})}]_{\text{GL}} :=& -2c_{\text{GL}_1}\rho\varepsilon b_{ij} && (4.7b)\\
[\phi_{ij}^{(\text{r};\mathfrak{V})}]_{\text{GL}} :=& -c_{\text{GL}_2}P_{ij}^{(\text{dev})} && (4.7c)\\
[\phi_{ij}^{(\text{s};w)}]_{\text{GL}} :=& c'_{\text{GL}_1} f_{\text{GL}_w} \frac{\rho\varepsilon}{\text{k}} \left(\overline{u'_k u'_m} e_{n_k} e_{n_m} \delta_{ij} - \tfrac{3}{2}\overline{u'_k u'_i} e_{n_k} e_{n_j} - \tfrac{3}{2}\overline{u'_k u'_j} e_{n_k} e_{n_i}\right)\\
=& -\tfrac{3}{2}c'_{\text{GL}_1} f_{\text{GL}_w} \frac{\rho\varepsilon}{\text{k}} \left(\overline{u'_k u'_i} e_{n_k} e_{n_j} + \overline{u'_k u'_j} e_{n_k} e_{n_i} - \tfrac{2}{3}\overline{u'_k u'_m} e_{n_k} e_{n_m} \delta_{ij}\right) && (4.7d)\\
[\phi_{ij}^{(\text{r};w)}]_{\text{GL}} :=& c'_{\text{GL}_2} f_{\text{GL}_w} \left([\phi_{km}^{(\text{r};\mathfrak{V})}]_{\text{GL}} e_{n_k} e_{n_m} \delta_{ij} - \tfrac{3}{2}[\phi_{ki}^{(\text{r};\mathfrak{V})}]_{\text{GL}} e_{n_k} e_{n_j} - \tfrac{3}{2}[\phi_{kj}^{(\text{r};\mathfrak{V})}]_{\text{GL}} e_{n_k} e_{n_i}\right)\\
=& -\tfrac{3}{2}c'_{\text{GL}_2} f_{\text{GL}_w} \Big([\phi_{ki}^{(\text{r};\mathfrak{V})}]_{\text{GL}} e_{n_k} e_{n_j} + [\phi_{kj}^{(\text{r};\mathfrak{V})}]_{\text{GL}} e_{n_k} e_{n_i}\\
& \qquad - \tfrac{2}{3}[\phi_{km}^{(\text{r};\mathfrak{V})}]_{\text{GL}} e_{n_k} e_{n_m} \delta_{ij}\Big) && (4.7e)
\end{aligned}
$$

$$
\begin{gathered}
c_{\text{GL}_1} = 1.8 \quad ; \quad c_{\text{GL}_2} = 0.6 \quad ; \quad c'_{\text{GL}_1} = 0.5 \quad ; \quad c'_{\text{GL}_2} = 0.3\\
f_{\text{GL}_w} := \frac{\alpha_s^{\frac{3}{2}}}{\kappa_{\text{VK}}} \frac{\ell_{\text{T}}}{n} \quad ; \quad \alpha_s = 0.3 \quad ; \quad \kappa_{\text{VK}} = 0.41 \quad ; \quad \ell_{\text{T}} := \frac{\text{k}^{\frac{3}{2}}}{\varepsilon} \qquad (4.7f)
\end{gathered}
$$

The tensor $e_{n_i} e_{n_j}$ ($\vec{e}_n$ being the unit normal-to-the-wall vector) was introduced by Shir (1973), following earlier attempts to modelling the surface integrals in (1.2) by Daly & Harlow (1970), to account for the wall-suppression effect (Shir 1973, p. 1329) which increases near-wall anisotropy (Daly & Harlow 1970, p. 2638), and has since been generalized in near-wall modelling (Hanjalić 1994). The function f_{GL_w} (4.7*d*, 4.7*e*) is a wall-proximity indicator, which activates the wall-echo terms near solid boundaries. Daly & Harlow (1970, (20–22), p. 2638) have suggested that this wall-proximity function should be inversely proportional to the the distance-from-the-wall n made nondimensional by the turbulence lengthscale ℓ_{T}, and this was also adopted in the definition of f_{GL_w} (4.7*f*) by Gibson & Launder (1978). As shown in Gibson & Launder (1978) the constant in the definition (4.7*f*) of f_{GL_w} can be related to the von Kàrmàn constant κ_{VK} and to the value of the equilibrium structural parameter $\alpha_s := \text{k}^{-1}(-\overline{u'v'})$ for simple shear flow (Townsend 1956). Although the LRR model (Launder *et al.* 1975) includes an IP variant (LRR–IP), the GL proposal (Gibson & Launder 1978) includes the general tensorial formulation for both slow (4.7*d*) and rapid (4.7*e*) wall-echo terms, and has certainly been much more influential in modern near-wall modelling work (Shima 1988; Launder & Shima 1989; Shima 1993*a*,*b*; Hanjalić & Jakirlić 1993; Hanjalić 1994; Hanjalić & Jakirlić 1998; Gerolymos & Vallet 2001, 2002; Jakirlić & Hanjalić 2002; Gerolymos *et al.* 2004; Jakirlić *et al.* 2007).

4.1.3. Jakirlić *et al.* 2007, JEJK

The JEJK model (Jakirlić *et al.* 2007) is included as a typical representative of the family of quite successful models (Shima 1988; Launder & Shima 1989; Shima 1993*a*,*b*;

Hanjalić & Jakirlić 1993; Hanjalić 1994; Hanjalić & Jakirlić 1998; Gerolymos & Vallet 2001, 2002; Jakirlić & Hanjalić 2002; Gerolymos *et al.* 2004) which have been developed using a quasilinear isotropisation-of-production (IP) tensorial formulation for the rapid volume part $\phi_{ij}^{(\mathrm{r};\mathfrak{V})}$, with a corresponding wall-echo term $\phi_{ij}^{(\mathrm{r};w)}$ using a tensorial form based on a unit vector (Shir 1973; Gibson & Launder 1978) pointing in the dominant direction of turbulence inhomogeneity. The dependence of the coefficient-functions of these models on the invariants of the anisotropy tensor (4.2, 4.5) is the key element which greatly enhances their accuracy and physical consistency (Sambasivam *et al.* 2004). Furthermore, the JEJK (Jakirlić *et al.* 2007) model, follows the suggestion of Hanjalić & Jakirlić (1993) to include not only the invariants of b_{ij} (4.3*c*) but also those of $b_{\varepsilon_{ij}}$ (4.3*d*) in the definition of the coefficient-functions (Hanjalić & Jakirlić 1993, 1998; Jakirlić & Hanjalić 2002). It reads

$$
\begin{aligned}
[\phi_{ij}]_{\mathrm{JEJK}} :=& [\phi_{ij}^{(\mathrm{s};\mathfrak{V})}]_{\mathrm{JEJK}} + [\phi_{ij}^{(\mathrm{s};w)}]_{\mathrm{JEJK}} + [\phi_{ij}^{(\mathrm{r};\mathfrak{V})}]_{\mathrm{JEJK}} + [\phi_{ij}^{(\mathrm{r};w)}]_{\mathrm{JEJK}} && (4.8a)\\
[\phi_{ij}^{(\mathrm{s};\mathfrak{V})}]_{\mathrm{JEJK}} :=& -\rho\varepsilon\Big(2c_{\mathrm{JEJK}_1} b_{ij} - 4c'_{\mathrm{JEJK}_1}(b_{ik}b_{kj} + \tfrac{2}{3}\mathrm{II}_{\mathbf{b}}\delta_{ij})\Big) && (4.8b)\\
[\phi_{ij}^{(\mathrm{r};\mathfrak{V})}]_{\mathrm{JEJK}} :=& -c_{\mathrm{JEJK}_2} P_{ij}^{(\mathrm{dev})} && (4.8c)\\
[\phi_{ij}^{(\mathrm{s};w)}]_{\mathrm{JEJK}} :=& c_{\mathrm{JEJK}_1}^{(w)} f_{\mathrm{JEJK}_w} \frac{\varepsilon}{\mathrm{k}}\Big(\overline{u'_k u'_m} e_{\eta_{\mathrm{JEJK}_k}} e_{\eta_{\mathrm{JEJK}_m}} \delta_{ij} - \tfrac{3}{2}\overline{u'_k u'_i} e_{\eta_{\mathrm{JEJK}_k}} e_{\eta_{\mathrm{JEJK}_j}}\\
& \qquad - \tfrac{3}{2}\overline{u'_k u'_j} e_{\eta_{\mathrm{JEJK}_k}} e_{\eta_{\mathrm{JEJK}_i}}\Big) && (4.8d)\\
[\phi_{ij}^{(\mathrm{r};w)}]_{\mathrm{JEJK}} :=& c_{\mathrm{JEJK}_2}^{(w)} f_{\mathrm{JEJK}_w} \Big([\phi_{km}^{(\mathrm{r};\mathfrak{V})}]_{\mathrm{JEJK}} e_{\eta_{\mathrm{JEJK}_k}} e_{\eta_{\mathrm{JEJK}_m}} \delta_{ij} - \tfrac{3}{2}[\phi_{ki}^{(\mathrm{r};\mathfrak{V})}]_{\mathrm{JEJK}} e_{\eta_{\mathrm{JEJK}_k}} e_{\eta_{\mathrm{JEJK}_j}}\\
& \qquad - \tfrac{3}{2}[\phi_{kj}^{(\mathrm{r};\mathfrak{V})}]_{\mathrm{JEJK}} e_{\eta_{\mathrm{JEJK}_k}} e_{\eta_{\mathrm{JEJK}_i}}\Big) && (4.8e)
\end{aligned}
$$

$$
\begin{aligned}
c_{\mathrm{JEJK}} := 2.5A\Big(\min(\tfrac{6}{10}, -8\mathrm{II}_{\mathbf{b}})\Big)^{\frac{1}{4}} \min\left(\left(\frac{Re_{\mathrm{T}}}{150}\right)^{\frac{3}{2}}, 1\right) \quad ; \quad Re_{\mathrm{T}} := \frac{\mathrm{k}^2}{\nu\varepsilon}\\
\vec{e}_{\eta_{\mathrm{JEJK}}} := \frac{\mathrm{grad}(A\ell_{\mathrm{T}})}{|\mathrm{grad}(A\ell_{\mathrm{T}})|} \quad ; \quad f_{\mathrm{JEJK}_w} := \min\big(f_{\mathrm{GL}_w}, \tfrac{7}{5}\big)\\
c_{\mathrm{JEJK}_1} := c_{\mathrm{JEJK}} + \sqrt{A}\, A_{\varepsilon}^2 \quad ; \quad c'_{\mathrm{JEJK}_1} = \max\big(-\tfrac{64}{10}\mathrm{II}_{\mathbf{b}}, \tfrac{1}{2}\big)c_{\mathrm{JEJK}_1}\\
c_{\mathrm{JEJK}_2} := \tfrac{6}{10}\sqrt{A} \quad ; \quad c_{\mathrm{JEJK}_1}^{(w)} := \max\Big(\tfrac{9}{10} - \tfrac{7}{10}c_{\mathrm{JEJK}}, \tfrac{3}{10}\Big) \quad ; \quad c_{\mathrm{JEJK}_2}^{(w)} := \min\big(A, \tfrac{3}{10}\big) \qquad (4.8f)
\end{aligned}
$$

The JEJK (Jakirlić *et al.* 2007) model uses a unit vector $\vec{e}_{\eta_{\mathrm{JEJK}}}$ (4.8*f*) pointing in the dominant direction of turbulence inhomogeneity (Gerolymos *et al.* 2004), and although the wall-proximity function f_{JEJK_w} (4.8*f*) is based on the wall-proximity function f_{GL_w} (4.7*f*) of the GL (Gibson & Launder 1978) model, and hence contains the distance-from-the-wall n, it could easily be made fully wall-normal-free by appropriate redefinition of the wall-proximity function.

4.1.4. Speziale *et al.* 1991, SSG

The SSG (Speziale *et al.* 1991) model is based on general tensorial representation approaches, and was developed as a closure for homogeneous turbulence. It is therefore interpreted here as a closure for the quasi-homogeneous volume part of redistribution

$\phi_{ij}^{(\mathfrak{W})}$ (4.1) and reads

$$
\begin{aligned}
[\phi_{ij}]_{\text{SSG}} :=& [\phi_{ij}^{(\mathfrak{W})}]_{\text{SSG}} := [\phi_{ij}^{(s;\mathfrak{W})}]_{\text{SSG}} + [\phi_{ij}^{(r;\mathfrak{W})}]_{\text{SSG}} && (4.9a)\\
[\phi_{ij}^{(s;\mathfrak{W})}]_{\text{SSG}} :=& - c_{\text{SSG}_1} \rho \varepsilon b_{ij} + c_{\text{SSG}_2} \rho \varepsilon (b_{ik} b_{kj} + \tfrac{2}{3} \mathrm{II}_{\mathbf{b}} \delta_{ij}) && (4.9b)\\
[\phi_{ij}^{(r;\mathfrak{W})}]_{\text{SSG}} :=& - c^{*}_{\text{SSG}_1} P_{\mathrm{k}} b_{ij}\\
& + \Big(c_{\text{SSG}_3} - c^{*}_{\text{SSG}_3} \sqrt{-2\mathrm{II}_{\mathbf{b}}}\Big) \rho \mathrm{k} \bar{S}_{ij}\\
& + c_{\text{SSG}_4} \rho \mathrm{k} (b_{ik} \bar{S}_{kj} + \bar{S}_{ik} b_{kj} - \tfrac{2}{3} \mathrm{I}_{\mathbf{bS}} \delta_{ij})\\
& + c_{\text{SSG}_5} \rho \mathrm{k} (b_{ik} \bar{\Omega}_{jk} + b_{jk} \bar{\Omega}_{ik}) && (4.9c)\\
& && (4.9d)
\end{aligned}
$$

$$
\begin{array}{llllllll}
c_{\text{SSG}_1} = 3.4 & ; & c_{\text{SSG}_2} = 4.2 & ; & c_{\text{SSG}_3} = \frac{4}{5} & ; & c_{\text{SSG}_4} = 1.25 & \\
c^{*}_{\text{SSG}_1} = 1.8 & ; & & & c^{*}_{\text{SSG}_3} = 1.30 & ; & c_{\text{SSG}_5} = 0.40 &
\end{array}
\qquad (4.9e)
$$

The term $-c^{*}_{\text{SSG}_1} P_{\mathrm{k}} b_{ij}$ (4.9c) depends on mean velocity gradients because of the presence of P_{k} (4.4d, 4.3g) and is therefore included in the rapid part $\phi_{ij}^{(r;\mathfrak{W})}$ (Shih & Lumley 1993; Ristorcelli *et al.* 1995).

4.1.5. So *et al.* 1996, SAYS

As mentioned above (§4.1.4) the SSG model for ϕ_{ij} was designed for quasi-homogeneous flows (Speziale *et al.* 1991). So *et al.* (1996) developed a near-wall version of the SSG model, by adding wall-echo terms to it. Incidentally, they used $P_{ij}^{(\mathrm{dev})}$ (4.3g) and $D_{ij}^{(\mathrm{dev})}$ (4.3h) for an equivalent with (4.9c) tensorial representation of $[\phi_{ij}^{(\mathrm{r};\mathfrak{W})}]_{\text{SAYS}} = [\phi_{ij}^{(\mathrm{r};\mathfrak{W})}]_{\text{SSG}}$. The model reads

$$
\begin{aligned}
[\phi_{ij}]_{\text{SAYS}} :=& [\phi_{ij}^{(\mathrm{s};\mathfrak{W})}]_{\text{SAYS}} + [\phi_{ij}^{(\mathrm{s};w)}]_{\text{SAYS}} + [\phi_{ij}^{(\mathrm{r};\mathfrak{W})}]_{\text{SAYS}} + [\phi_{ij}^{(\mathrm{r};w)}]_{\text{SAYS}} && (4.10a)\\
[\phi_{ij}^{(\mathrm{s};\mathfrak{W})}]_{\text{SAYS}} =& [\phi_{ij}^{(s;\mathfrak{W})}]_{\text{SSG}} \overset{(4.9b)}{=} -c_{\text{SSG}_1} \rho \varepsilon b_{ij} + c_{\text{SSG}_2} \rho \varepsilon (b_{ik} b_{kj} + \tfrac{2}{3} \mathrm{II}_{\mathbf{b}} \delta_{ij}) && (4.10b)\\
[\phi_{ij}^{(r;\mathfrak{W})}]_{\text{SAYS}} :=& [\phi_{ij}^{(r;\mathfrak{W})}]_{\text{SSG}} \overset{(4.9c,\ 4.3g,\ 4.3h)}{=} -c^{*}_{\text{SSG}_1} P_{\mathrm{k}} b_{ij}\\
& + \Big(c_{\text{SSG}_3} - \tfrac{2}{3} c_{\text{SSG}_4} - c^{*}_{\text{SSG}_3} \sqrt{-2\mathrm{II}_{\mathbf{b}}}\Big) \rho \mathrm{k} \bar{S}_{ij}\\
& - \tfrac{1}{4} (c_{\text{SSG}_4} + c_{\text{SSG}_5}) P_{ij}^{(\mathrm{dev})}\\
& - \tfrac{1}{4} (c_{\text{SSG}_4} - c_{\text{SSG}_5}) D_{ij}^{(\mathrm{dev})} && (4.10c)\\
[\phi_{ij}^{(\mathrm{s};w)}]_{\text{SAYS}} =& - [\phi_{ij}^{(s;\mathfrak{W})}]_{\text{SAYS}}\, f_{\text{SAYS}_w} \overset{(4.10b)}{=} -[\phi_{ij}^{(s;\mathfrak{W})}]_{\text{SSG}}\, f_{\text{SAYS}_w} && (4.10d)\\
[\phi_{ij}^{(r;w)}]_{\text{SAYS}} :=& \Big(- c^{*}_{\text{SSG}_1} P_{\mathrm{k}} b_{ij} + \alpha^{*}_{\text{SAYS}}\, P_{ij}^{(\mathrm{dev})} + 2\gamma^{*}_{\text{SAYS}}\, \mathrm{k} \bar{S}_{ij}\Big)\, f_{\text{SAYS}_w} && (4.10e)
\end{aligned}
$$

$$
\begin{array}{lll}
\frac{1}{4}(c_{\text{SSG}_4} + c_{\text{SSG}_5}) =: \alpha_{\text{SAYS}_1} = \frac{33}{80} & ; & c_{\text{SSG}_3} - \frac{2}{3} c_{\text{SSG}_4} =: -2\gamma_{\text{SAYS}_1} = \frac{1}{30}\\
\frac{1}{4}(c_{\text{SSG}_4} - c_{\text{SSG}_5}) =: \beta_{\text{SAYS}_1} = \frac{17}{80} & ; & f_{\text{SAYS}_w} := \mathrm{e}^{-\left(\frac{Re_{\mathrm{T}}}{200}\right)^2}\\
\alpha^{*}_{\text{SAYS}} = -0.29 & ; & \gamma^{*}_{\text{SAYS}} = 0.065
\end{array}
\qquad (4.10f)
$$

The wall-echo terms (4.10d, 4.10e) use a wall-proximity function f_{SAYS_w} (4.10f) which is based on the turbulence Reynolds-number Re_{T} (4.8f) only.

4.1.6. Suga 2004, Suga

This closure for ϕ_{ij} (Suga 2004) is one of the recent representatives of the so-called two-component-limit (TCL) closures, which are based on the representation for the quasi-homogeneous part $\phi_{ij}^{(\mathfrak{V})}$ developed by Fu (1988), to which inhomogeneous terms were added (Craft & Launder 1996; Craft 1998; Batten *et al.* 1999; Suga 2004; Al-Sharif *et al.* 2010), these variants differing mainly on the particular choice for the free coefficient-function c'_{S_2} which multiplies in (4.11*c*) the tensor $F_{\mathrm{TCL}_{ij}}$ (4.11*f*) and on the model for the inhomogeneous terms. A systematic study of the differences in results between variants of the TCL has not yet been conducted. The S (Suga 2004) variant of the TCL model uses a simplified representation for the inhomogeneous terms, following Batten *et al.* (1999). It reads†

$$
\begin{aligned}
[\phi_{ij}]_{\mathrm{S}} :=& [\phi_{ij}^{(\mathrm{s};\mathfrak{V})}]_{\mathrm{S}} + [\phi_{ij}^{(\mathrm{s};w)}]_{\mathrm{S}} + [\phi_{ij}^{(\mathrm{r};\mathfrak{V})}]_{\mathrm{S}} + [\phi_{ij}^{(\mathrm{r};w)}]_{\mathrm{S}} && (4.11a)\\
[\phi_{ij}^{(\mathrm{s};\mathfrak{V})}]_{\mathrm{S}} =& -2(c_{\mathrm{S}_1} + c''_{\mathrm{S}_1})\rho\varepsilon b_{ij} - 4c_{\mathrm{S}_1} c'_{\mathrm{S}_1}\rho\varepsilon(b_{ik}b_{kj} + \tfrac{2}{3}\mathrm{II}_{\mathbf{b}}\delta_{ij}) && (4.11b)\\
[\phi_{ij}^{(\mathrm{r};\mathfrak{V})}]_{\mathrm{S}} =& -0.6P_{ij}^{(\mathrm{dev})} + 1.2P_{\mathrm{k}}b_{ij}\\
& -0.2\frac{1}{\mathrm{k}}\Big(\overline{u'_k u'_j}\;\overline{u'_\ell u'_i}2\bar{S}_{k\ell} - \overline{u'_\ell u'_k}\big(\overline{u'_i u'_k}\frac{\partial\bar{u}_j}{\partial x_\ell} + \overline{u'_j u'_k}\frac{\partial\bar{u}_i}{\partial x_\ell}\big)\Big)\\
& -4c_{\mathrm{S}_2}\Big(-2\mathrm{II}_{\mathbf{b}}(P_{ij} - D_{ij}) + 3b_{im}(P_{mn} - D_{mn})b_{nj}\Big) + c'_{\mathrm{S}_2}F_{\mathrm{TCL}_{ij}} && (4.11c)\\
[\phi_{ij}^{(\mathrm{s};w)}]_{\mathrm{S}} =& f_{\mathrm{S}_{w_1}}\frac{\varepsilon}{\mathrm{k}}\Big(\overline{u'_\ell u'_k}d_\ell^{(A)}d_k^{(A)}\delta_{ij} - \tfrac{3}{2}\overline{u'_i u'_k}d_j^{(A)}d_k^{(A)} - \tfrac{3}{2}\overline{u'_j u'_k}d_i^{(A)}d_k^{(A)}\Big)\\
& + f_{\mathrm{S}_{w_2}}\frac{\varepsilon}{\mathrm{k}^2}\Big(\overline{u'_m u'_n}\;\overline{u'_\ell u'_m}d_\ell^{(A)}d_n^{(A)}\delta_{ij} - \tfrac{3}{2}\overline{u'_i u'_m}\;\overline{u'_\ell u'_m}d_\ell^{(A)}d_j^{(A)}\\
& \qquad\qquad\qquad\qquad - \tfrac{3}{2}\overline{u'_j u'_m}\;\overline{u'_\ell u'_m}d_\ell^{(A)}d_i^{(A)}\Big) && (4.11d)\\
[\phi_{ij}^{(\mathrm{r};w)}]_{\mathrm{S}} =& f_{\mathrm{S}_I}\mathrm{k}\frac{\partial\bar{u}_\ell}{\partial x_n}d_\ell d_n\Big(d_i d_j - \tfrac{1}{3}d_k d_k\delta_{ij}\Big) && (4.11e)
\end{aligned}
$$

$$
\begin{aligned}
F_{\mathrm{TCL}_{ij}} :=& (\tfrac{7}{15} + 2\mathrm{II}_{\mathbf{b}})P_{ij}^{(\mathrm{dev})} + \tfrac{2}{10}P_{\mathrm{k}}\Big(2b_{ij} - 4(b_{ik}b_{kj} + \tfrac{2}{3}\mathrm{II}_{\mathbf{b}}\delta_{ij})\Big)\\
& - \tfrac{2}{10}(b_{\ell k}P_{\ell k})b_{ij} + \tfrac{1}{10}\frac{1}{\mathrm{k}}\Big(\overline{u'_i u'_m}P_{mj} + \overline{u'_j u'_m}P_{mi} - \tfrac{2}{3}\overline{u'_\ell u'_m}P_{\ell m}\delta_{ij}\Big)\\
& + \tfrac{1}{10}\frac{1}{\mathrm{k}^2}\big(\overline{u'_\ell u'_i}\;\overline{u'_k u'_j} - \tfrac{1}{3}\overline{u'_\ell u'_m}\;\overline{u'_k u'_m}\delta_{ij}\big)\big(6D_{\ell k} + 26\mathrm{k}\bar{S}_{\ell k}\big)\\
& + \tfrac{2}{10}\frac{\overline{u'_\ell u'_i}\;\overline{u'_k u'_j}}{\mathrm{k}^2}(D_{\ell k} - P_{\ell k}) && (4.11f)
\end{aligned}
$$

$$
d_i := \frac{\partial_{x_i}\ell_{\mathrm{T}}}{\tfrac{1}{2} + \sqrt{[\partial_{x_k}\ell_{\mathrm{T}}][\partial_{x_k}\ell_{\mathrm{T}}]}} \quad ; \quad d_i^{(A)} := \frac{\partial_{x_i}(\ell_{\mathrm{T}}\sqrt{A})}{\tfrac{1}{2} + \sqrt{[\partial_{x_k}(\ell_{\mathrm{T}}\sqrt{A})][\partial_{x_k}(\ell_{\mathrm{T}}\sqrt{A})]}} \qquad (4.11g)
$$

---

† In the present paper we conformed to the usual definitions of strain-rate (4.3*e*) $\bar{S}_{ij}$ and rotation-rate (4.3*f*) $\bar{\Omega}_{ij}$ tensors, which are also adopted in the more recent papers on the TCL (two–component-limit) model (*eg* Al-Sharif *et al.* 2010). The equations are identical with those of earlier papers on TCL (Fu 1988; Craft & Launder 1996; Fu & Wang 1997; Craft 1998; Batten *et al.* 1999), including Suga (2004), where $[\bar{S}_{ij}]_{\mathrm{TCL}} := 2\bar{S}_{ij}$ and $[\bar{\Omega}_{ij}]_{\mathrm{TCL}} := 2\bar{\Omega}_{ij}$ are used instead, with appropriate multiplicative modification of coefficients.

$$
\begin{aligned}
c_{\mathrm{S}_1} &= 3.2\sqrt{-8\mathrm{II}_{\mathbf{b}}}f_{\mathrm{S}_A}\min\big((\tfrac{1}{200}Re_{\mathrm{T}})^2,1\big)\\
f_{\mathrm{S}_A} &= \begin{cases}\sqrt{\tfrac{1}{14}A} & A\leq\tfrac{5}{100}\\ \sqrt{\tfrac{10}{7}}A & \tfrac{5}{100}<A<\tfrac{7}{10}\\ \sqrt{A} & A\geq\tfrac{7}{10}\end{cases}\\
c'_{\mathrm{S}_1} &= \tfrac{11}{10}\quad;\quad c''_{\mathrm{S}_1}=\sqrt{A}\\
c_{\mathrm{S}_2} &= \min\left\{\tfrac{55}{100}\Big(1-\exp\big(\frac{-A^{\frac{3}{2}}Re_{\mathrm{T}}}{100}\big)\Big),\frac{\tfrac{32}{10}A}{1+\dfrac{\mathrm{k}}{\varepsilon}\sqrt{-8\mathrm{II}_{\bar{\mathbf{S}}}}}\right\}\\
c'_{\mathrm{S}_2} &= \min\big(\tfrac{6}{10},\sqrt{A}\big)+\frac{\tfrac{35}{10}\dfrac{\mathrm{k}}{\varepsilon}\Big(\sqrt{-8\mathrm{II}_{\bar{\mathbf{S}}}}-\sqrt{-8\mathrm{II}_{\bar{\mathbf{\Omega}}}}\Big)}{3+\dfrac{\mathrm{k}}{\varepsilon}\Big(\sqrt{-8\mathrm{II}_{\bar{\mathbf{S}}}}+\sqrt{-8\mathrm{II}_{\bar{\mathbf{\Omega}}}}\Big)}-4\sqrt{6}\min\left(\frac{3\mathrm{III}_{\bar{\mathbf{S}}}}{(-2\mathrm{II}_{\bar{\mathbf{S}}})^{\frac{3}{2}}},0\right)\\
f_{\mathrm{S}_{w_1}} &= 3\Big(1-\sqrt{A}\Big)\min\Big(1,\max\big(0,1-\frac{Re_{\mathrm{T}}-55}{70}\big)\Big)\\
f_{\mathrm{S}_{w_2}} &= -\tfrac{24}{5}\mathrm{II}_{\mathbf{b}}\big(1-\sqrt{A}\big)\min\Big(1,\max\big(0,1-\frac{Re_{\mathrm{T}}-50}{200}\big)\Big)+\tfrac{1}{10}\\
f_{\mathrm{S}_I} &= 3f_{\mathrm{S}_A}
\end{aligned}
\tag{4.11h}
$$

The above equations are presented in their original form (Suga 2004) and can be reduced by projection on an irreducible basis (*cf* §4.2). Notice also that the presence of the invariants of $\bar{\mathbf{S}}$ and $\bar{\mathbf{\Omega}}$ in the definition of c'_{S_2} (4.11*h*), in particular the fraction which forms the second term of the three-term-sum expression of c'_{S_2} (4.11*h*), make the TCL model for $[\phi_{ij}^{(\mathrm{r};\mathfrak{V})}]_{\mathrm{S}}$ (4.11*c*) weakly nonlinear with mean velocity gradients, contrary to the usually applied linearity constraint (Launder *et al.* 1975; Lumley 1978; Ristorcelli *et al.* 1995) implied by (4.1*a*).

4.2. *Tensorial representations for ϕ_{ij} including wall-echo*

To compare different models and analyse differences between them, it is necessary to project (represent) these models in a common tensorial basis (Spencer & Rivlin 1959; Smith 1971). This is obviously not the case for the models considered in the present work (§4.1). Several of these models (LRR: Launder *et al.* 1975; GL: Gibson & Launder 1978; SSG: Speziale *et al.* 1991; SAYS: So *et al.* 1996) represent the closure for the quasi-homogeneous part of redistribution $\phi_{ij}^{(\mathfrak{V})}\overset{(4.1a)}{=}\phi_{ij}^{(\mathrm{s};\mathfrak{V})}+\phi_{ij}^{(\mathrm{r};\mathfrak{V})}$ as a linear combination of the tensors b_{ij} (4.3*c*), $\bar{S}_{ij}$ (4.3*e*), P_{ij} (4.3*g*), and D_{ij} (4.3*h*), and their products which are linear in mean velocity gradients. The SSG model (Speziale *et al.* 1991) was written using the tensors b_{ij} (4.3*c*), $\bar{S}_{ij}$ (4.3*e*), and $\bar{\Omega}_{ij}$ (4.3*f*), and their products which are linear in mean velocity gradients, but can also be expressed using the previous tensors (b_{ij}, $\bar{S}_{ij}$, P_{ij}, D_{ij}), which are the expressions used in the SAYS model (So *et al.* 1996), which uses SSG (Speziale *et al.* 1991) for the quasi-homogeneous part of the model (4.10*c*). Finally the models of the TCL family (Fu 1988; Craft & Launder 1996; Fu & Wang 1997; Craft 1998; Batten *et al.* 1999; Suga 2004) use (4.11) all these tensors (b_{ij}, $\bar{S}_{ij}$, P_{ij}, D_{ij}, $\bar{\Omega}_{ij}$), but also r_{ij} (4.3*a*), and their products which are linear in mean velocity gradients. It is established (Ristorcelli *et al.* 1995) that the most general model developed from (4.1*a*) assuming homogeneity (Lumley 1978) is expressible in the irreducible polynomial (Spencer & Rivlin 1959) representation basis of isotropic symmetric deviatoric tensor-valued functions of the 3 tensors b_{ij} (4.3*c*), $\bar{S}_{ij}$ (4.3*e*), and $\bar{\Omega}_{ij}$ (4.3*f*), which is formed by

8† tensors (*eg* Ristorcelli *et al.* 1995, (42), p. 131), and this is the classical representation basis $\mathfrak{B}[\mathbf{b},\bar{\mathbf{S}},\bar{\mathbf{\Omega}}]$ (Gerolymos *et al.* 2010*b*). Alternatively (Gerolymos *et al.* 2010*b*) we can construct a basis of 8 symmetric deviatoric tensors $\mathfrak{B}_{(P)}[\mathbf{b},\mathbf{S},\mathbf{P}_{\bar{\Omega}};\mathbf{P}_{\bar{S}}]$, where we use explicitly $P_{\bar{\Omega}_{ij}} \overset{(4.3j)}{=} \frac{1}{2}\mathrm{k}\big(b_{i\ell}\bar{\Omega}_{\ell j}-\bar{\Omega}_{i\ell}b_{\ell j}\big)$ and its products with b_{ij} (4.3*c*) to express $\mathbf{b}\bar{\mathbf{\Omega}}-\bar{\mathbf{\Omega}}\mathbf{b}$, $\mathbf{b}^2\bar{\mathbf{\Omega}}-\bar{\mathbf{\Omega}}\mathbf{b}^2$, and $\mathbf{b}^2\bar{\mathbf{\Omega}}\mathbf{b}-\mathbf{b}\bar{\mathbf{\Omega}}\mathbf{b}^2$, and $P_{\bar{S}_{ij}} \overset{(4.3i)}{=} -\frac{1}{2}\mathrm{k}\big(b_{i\ell}\bar{S}_{\ell j}+\bar{S}_{i\ell}b_{\ell j}-\frac{2}{3}\mathrm{I}_{\mathbf{b}\bar{\mathbf{S}}}\big)-\frac{2}{3}\mathrm{k}\bar{S}_{ij}$ and its products with b_{ij} (4.3*c*) to express $\mathbf{b}\bar{\mathbf{S}}+\bar{\mathbf{S}}\mathbf{b}-\frac{2}{3}\mathrm{I}_{\mathbf{b}\bar{\mathbf{S}}}\mathbf{I}_3$ and $\mathbf{b}^2\bar{\mathbf{S}}+\bar{\mathbf{S}}\mathbf{b}^2-\frac{2}{3}\mathrm{I}_{\mathbf{b}^2\bar{\mathbf{S}}}\mathbf{I}_3$. Passage matrices $\in \mathbb{R}^{8\times 8}$ from (to) $\mathfrak{B}[\mathbf{b},\bar{\mathbf{S}},\bar{\mathbf{\Omega}}]$ to (from) $\mathfrak{B}_{(P)}[\mathbf{b},\mathbf{S},\mathbf{P}_{\bar{\Omega}};\mathbf{P}_{\bar{S}}]$ are quite simple (Gerolymos *et al.* 2010*b*, Tabs. I and II, p. 2). We will represent each model for the quasi-homogeneous volume-terms

$$[\phi_{ij}^{(\mathfrak{V})}]_{\mathrm{M}} := \underbrace{\rho\varepsilon\sum_{n=1}^{2}c_{\mathrm{M}_n}^{(\phi^{\mathrm{s};\mathfrak{V}})}\overset{\star}{H}_{(n)ij}}_{\sim\,\left(\phi_{ij}^{(\mathrm{s};\mathfrak{V})}-\chi_{\mathrm{M}_\varepsilon}2\rho\varepsilon b_{\varepsilon_{ij}}\right)} \underbrace{+\rho\varepsilon\sum_{n=1}^{8}c_{\mathrm{M}_n}^{(\phi^{\mathrm{r};\mathfrak{V}})}\overset{\star}{H}_{(n)ij}}_{\sim\,\phi_{ij}^{(\mathrm{r};\mathfrak{V})}} \tag{4.12}$$

where the slow part of the model eventually ($\chi_{\mathrm{M}_\varepsilon}=1$) but not necessarily ($\chi_{\mathrm{M}_\varepsilon}=0$) contains the dissipation anisotropy (Lumley 1978), and the symmetric deviatoric basis tensors

$$\overset{\star}{H}_{(1)ij} := b_{ij} \tag{4.13a}$$

$$\overset{\star}{H}_{(2)ij} := b_{i\ell}b_{\ell j}+\tfrac{2}{3}\mathrm{II}_{\mathbf{b}}\,\delta_{ij} \tag{4.13b}$$

$$\overset{\star}{H}_{(3)ij} := \overset{\star}{S}_{ij} := \frac{\mathrm{k}}{\varepsilon}\bar{S}_{ij} \tag{4.13c}$$

$$\overset{\star}{H}_{(4)ij} := \overset{\star}{P}_{\bar{S}_{ij}} := \frac{1}{\rho\varepsilon}\big(P_{\bar{S}_{ij}}-\tfrac{2}{3}P_{\mathrm{k}}\delta_{ij}\big) \tag{4.13d}$$

$$\overset{\star}{H}_{(5)ij} := \overset{\star}{P}_{\bar{\Omega}_{ij}} := \frac{1}{\rho\varepsilon}P_{\bar{\Omega}_{ij}} \tag{4.13e}$$

$$\overset{\star}{H}_{(6)ij} := b_{i\ell}\overset{\star}{P}_{\bar{S}_{\ell j}}+\overset{\star}{P}_{\bar{S}_{i\ell}}b_{\ell j}-\tfrac{2}{3}\mathrm{I}_{\mathbf{b}\overset{\star}{\mathbf{P}}_{\bar{S}}}\ \delta_{ij} \tag{4.13f}$$

$$\overset{\star}{H}_{(7)ij} := b_{i\ell}\overset{\star}{P}_{\bar{\Omega}_{\ell j}}+\overset{\star}{P}_{\bar{\Omega}_{i\ell}}b_{\ell j} \tag{4.13g}$$

$$\overset{\star}{H}_{(8)ij} := b_{ik}b_{k\ell}\overset{\star}{P}_{\bar{\Omega}_{\ell j}}+\overset{\star}{P}_{\bar{\Omega}_{i\ell}}b_{\ell k}b_{kj} \tag{4.13h}$$

were made nondimensional by scaling with powers of k (4.3*a*) and ε (4.3*b*). The representation of different models for the quasi-homogeneous part of redistribution in $\mathfrak{B}[\mathbf{b},\mathbf{S},\mathbf{\Omega}]$ is available in the literature (Speziale *et al.* 1991; Ristorcelli *et al.* 1995; Fu & Wang 1997), and it is straightforward to project these representations on $\mathfrak{B}_{(P)}[\mathbf{b},\mathbf{S},\mathbf{P}_{\bar{\Omega}};\mathbf{P}_{\bar{S}}]$ (Gerolymos *et al.* 2010*b*), with the exception of the tensor $F_{\mathrm{TCL}_{ij}}$ (4.11*c*), which is invariably given in the reducible form (4.11*f*). Its expression in $\mathfrak{B}_{(P)}[\mathbf{b},\mathbf{S},\mathbf{P}_{\bar{\Omega}};\mathbf{P}_{\bar{S}}]$ is obtained after straightforward albeit lengthy calculations, which require the use of the Cayley-Hamilton theorem (Rivlin 1955, (4.24), p. 689) and its extensions (Rivlin 1955, (4.21) and (4.22), p. 688), as

---

† These can be reduced to 7 using RE-projection (Rivlin & Ericksen 1955, pp. 380–382) to express $\mathbf{b}^2\bar{\mathbf{\Omega}}\mathbf{b}-\mathbf{b}\bar{\mathbf{\Omega}}\mathbf{b}^2$ as a linear combination of the other basis tensors, thus obtaining a functional representation basis (Smith 1971), *ie* a basis where isotropic tensor-valued functions are represented with coefficients which are rational (not necessarily continuous) functions of the invariants.

$$\frac{F_{\mathrm{TC}_{ij}}}{\rho\varepsilon} := \frac{-\frac{4}{15}P_{\mathrm{k}} + \mathrm{I}_{\mathbf{bP}}}{\rho\varepsilon}\overset{\star}{H}_{(1)ij} + \frac{2P_{\mathrm{k}}}{\rho\varepsilon}\overset{\star}{H}_{(2)ij} + \Big(\tfrac{52}{5}(\tfrac{1}{3} + \mathrm{II}_{\mathbf{b}}) - \tfrac{24}{5}(\tfrac{8}{27} + \tfrac{2}{3}\mathrm{II}_{\mathbf{b}} - \mathrm{III}_{\mathbf{b}})\Big)\overset{\star}{H}_{(3)ij}$$
$$+(\tfrac{23}{15} + 2\mathrm{II}_{\mathbf{b}})\overset{\star}{H}_{(4)ij} + (\tfrac{7}{45} + 6\mathrm{II}_{\mathbf{b}})\overset{\star}{H}_{(5)ij} - \tfrac{13}{5}\overset{\star}{H}_{(6)ij} - \tfrac{17}{15}\overset{\star}{H}_{(7)ij} + 4\overset{\star}{H}_{(8)ij} \qquad (4.14)$$

Since in the present work we are interested in wall effects, we must also include inhomogeneous terms in the representation. Current and past modelling status (Shir 1973; Launder *et al.* 1975; Gibson & Launder 1978; Gerolymos & Vallet 2001) usually† includes a unit vector pointing in the dominant direction where turbulence inhomogeneity is the highest. In wall-topology-dependent models this unit vector is simply the normal-to-the-wall (Shir 1973; Launder *et al.* 1975; Gibson & Launder 1978), $\vec{e}_n$, while in wall-topology-free models (Gerolymos & Vallet 2001; Gerolymos *et al.* 2004) this a unit vector $\vec{e}_{\mathrm{I}}$ determined from gradients of the local state of turbulence (length and time scales and anisotropy invariants; Gerolymos *et al.* 2004, (3), p. 410), or in the context of elliptic blending models by the gradient of the blending parameter (Oceni *et al.* 2008). Several wall-normal-free models which contain inhomogeneous terms (Craft & Launder 1996; Craft 1998; Batten *et al.* 1999; Suga 2004) contain such inhomogeneity-direction-unit-vectors, although this is not always stated explicitly, and in some instances 2 or 3 different vectors are used (Craft & Launder 1996; Craft 1998; Suga 2004). Let us for the time assume that the modelling strategy includes a single unit-vector. Smith (1971) develops representations making explicit use of vectors, and application of this approach leads to the functional representation basis in Gerolymos *et al.* (2004, (31), p.4 28), built from b_{ij}, $\bar{S}_{ij}$, $\bar{\Omega}_{ij}$ and $\vec{e}_{\mathrm{I}}$. Obviously this basis, written using explicitly $\vec{e}_{\mathrm{I}}$, can be rewritten using the deviatoric projection of the symmetric tensor $\vec{e}_{\mathrm{I}} \otimes \vec{e}_{\mathrm{I}}$

$$\boldsymbol{\eta} := \vec{e}_\eta \otimes \vec{e}_\eta - \tfrac{1}{3}\mathbf{I}_3 := \begin{cases} \vec{e}_n \otimes \vec{e}_n - \tfrac{1}{3}\mathbf{I}_3 & \text{geometric normals} \\ \vec{e}_{\mathrm{I}} \otimes \vec{e}_{\mathrm{I}} - \tfrac{1}{3}\mathbf{I}_3 & \text{WNF models} \end{cases} \qquad (4.15a)$$

which, being the deviatoric projection of the tensor product of a unit vector ($\vec{e}_\eta$) by itself satisfies

$$\boldsymbol{\eta}^2 \overset{(4.15)}{=} (e_{\eta_i}e_{\eta_\ell} - \tfrac{1}{3}\delta_{i\ell})(e_{\eta_\ell}e_{\eta_j} - \tfrac{1}{3}\delta_{\ell j})\vec{e}_i \otimes \vec{e}_j$$
$$= (e_{\eta_i}\underbrace{e_{\eta_\ell}e_{\eta_\ell}}_{=1}e_{\eta_j} - \tfrac{2}{3}e_{\eta_i}e_{\eta_j} + \tfrac{1}{9}\delta_{i\ell}\delta_{\ell j})\vec{e}_i \otimes \vec{e}_j = \tfrac{1}{3}\boldsymbol{\eta} + \tfrac{2}{9}\mathbf{I}_3 \qquad (4.15b)$$

$$\boldsymbol{\eta}^3 = \boldsymbol{\eta}\boldsymbol{\eta}^2 \overset{(4.13a)}{=} \tfrac{1}{3}\boldsymbol{\eta}^2 + \tfrac{2}{9}\boldsymbol{\eta} \overset{(4.13a)}{=} \tfrac{1}{3}\Big(\tfrac{1}{3}\boldsymbol{\eta} + \tfrac{2}{9}\mathbf{I}_3\Big) + \tfrac{2}{9}\boldsymbol{\eta} = \tfrac{1}{3}\boldsymbol{\eta}\tfrac{2}{27}\mathbf{I}_3 \qquad (4.15c)$$

$$\mathrm{I}_{\boldsymbol{\eta}} \overset{(4.2a)}{=} 0 \qquad (4.15d)$$

$$\mathrm{II}_{\boldsymbol{\eta}} \overset{(4.2b)}{=} -\tfrac{1}{3} \qquad (4.15e)$$

$$\mathrm{III}_{\boldsymbol{\eta}} \overset{(4.2c)}{=} \tfrac{2}{27} \qquad (4.15f)$$

As a consequence the basis should only contain elements linear in $\boldsymbol{\eta}$, since all higher powers are expressible using (4.15*b*, 4.15*c*) and relations derived from these. The functional representation basis (Gerolymos *et al.* 2004, (31), p. 428) is not very practical, because the representation of, *eg*, the classical echo-term of the isotropisation-of-production rapid closure (Gibson & Launder 1978), cannot be represented explicitly (Gerolymos *et al.*

---

† As stated in §1 the alternative approach of applying elliptic relaxation to the quasi-homogeneous model to account for wall-blockage (Durbin 1993) has already been studied by Manceau *et al.* (2001), and is not investigated in the present work.

2004), this being a recurent problem with functional representation bases (Ristorcelli *et al.* 1995; Wallin & Johansson 2000). For this reason, we use a polynomial basis, constructed following Spencer & Rivlin (1959), who worked directly with tensors. The polynomial representation basis constructed (Spencer & Rivlin 1959, Theorem 1, p. 320) by adding $\boldsymbol{\eta}$ (4.15*a*) to the tensors generating $\mathfrak{B}_{(P)}[\mathbf{b}, \mathbf{S}, \mathbf{P}_{\bar{\Omega}}; \mathbf{P}_{\bar{S}}]$, *viz* b_{ij} (4.3*c*), $\bar{S}_{ij}$ or $P_{\bar{S}_{ij}}$ (4.3*e*), and $P_{\bar{\Omega}_{ij}}$ (4.3*f*), to construct $\mathfrak{B}_{(P)}[\mathbf{b}, \mathbf{S}, \mathbf{P}_{\bar{\Omega}}, \boldsymbol{\eta}; \mathbf{P}_{\bar{S}}]$. Since the representation must be linear in mean velocity gradients, and because of (4.15*b*, 4.15*c*), terms

(*a*) nonlinear in $\overset{\star}{\mathbf{S}}$ and/or $\overset{\star}{\boldsymbol{\Omega}}$ (*ie* terms containing $[\overset{\star}{\mathbf{S}}]^{n_1}[\overset{\star}{\boldsymbol{\Omega}}]^{n_2}$ with $n_1 + n_2 > 1$)
(*b*) nonlinear in $\boldsymbol{\eta}$

are omitted. This leads to adding to the 8 tensors of the representation basis (4.13) the tensors

$$\overset{\star}{H}_{(\eta;\ 1)ij} := \eta_{ij} \tag{4.16a}$$

$$\overset{\star}{H}_{(\eta;\ 2)ij} := b_{i\ell}\eta_{\ell j} + \eta_{i\ell}b_{\ell j} - \tfrac{2}{3}\mathrm{I}_{\boldsymbol{\eta}\mathbf{b}}\ \delta_{ij} \tag{4.16b}$$

$$\overset{\star}{H}_{(\eta;\ 3)ij} := b_{i\ell}b_{\ell k}\eta_{kj} + \eta_{i\ell}b_{\ell k}b_{kj} - \tfrac{2}{3}\mathrm{I}_{\mathbf{b}^2\boldsymbol{\eta}}\ \delta_{ij} \tag{4.16c}$$

$$\overset{\star}{H}_{(\eta;\ 4)ij} := \eta_{i\ell}\overset{\star}{S}_{\ell j} + \overset{\star}{S}_{i\ell}\eta_{\ell j} - \tfrac{2}{3}\mathrm{I}_{\boldsymbol{\eta}\overset{\star}{\mathbf{S}}}\ \delta_{ij} \tag{4.16d}$$

$$\overset{\star}{H}_{(\eta;\ 5)ij} := \eta_{i\ell}\overset{\star}{P}_{\bar{S}_{\ell j}} + \overset{\star}{P}_{\bar{S}_{i\ell}}\eta_{\ell j} - \tfrac{2}{3}\mathrm{I}_{\boldsymbol{\eta}\overset{\star}{\mathbf{P}}_{\bar{S}}}\ \delta_{ij} \tag{4.16e}$$

$$\overset{\star}{H}_{(\eta;\ 6)ij} := \eta_{i\ell}\overset{\star}{P}_{\bar{\Omega}_{\ell j}} + \overset{\star}{P}_{\bar{\Omega}_{i\ell}}\eta_{\ell j} - \tfrac{2}{3}\mathrm{I}_{\boldsymbol{\eta}\overset{\star}{\mathbf{P}}_{\bar{\Omega}}}\ \delta_{ij} \tag{4.16f}$$

$$\overset{\star}{H}_{(\eta;\ 7)ij} := \eta_{i\ell}b_{\ell k}\overset{\star}{P}_{\bar{S}_{kj}} + \overset{\star}{P}_{\bar{S}_{i\ell}}b_{\ell k}\eta_{kj} - \tfrac{2}{3}\mathrm{I}_{\boldsymbol{\eta}\mathbf{b}\overset{\star}{\mathbf{P}}_{\bar{S}}}\ \delta_{ij} \tag{4.16g}$$

$$\overset{\star}{H}_{(\eta;\ 8)ij} := \eta_{i\ell}\overset{\star}{P}_{\bar{S}_{\ell k}}b_{kj} + b_{i\ell}\overset{\star}{P}_{\bar{S}_{\ell k}}\eta_{kj} - \tfrac{2}{3}\mathrm{I}_{\boldsymbol{\eta}\mathbf{b}\overset{\star}{\mathbf{P}}_{\bar{S}}}\ \delta_{ij} \tag{4.16h}$$

$$\overset{\star}{H}_{(\eta;\ 9)ij} := \eta_{i\ell}b_{\ell k}\overset{\star}{P}_{\bar{\Omega}_{kj}} + \overset{\star}{P}_{\bar{\Omega}_{i\ell}}b_{\ell k}\eta_{kj} - \tfrac{2}{3}\mathrm{I}_{\boldsymbol{\eta}\mathbf{b}\overset{\star}{\mathbf{P}}_{\bar{\Omega}}}\ \delta_{ij} \tag{4.16i}$$

$$\overset{\star}{H}_{(\eta;10)ij} := \eta_{i\ell}\overset{\star}{P}_{\bar{\Omega}_{\ell k}}b_{kj} + b_{i\ell}\overset{\star}{P}_{\bar{\Omega}_{\ell k}}\eta_{kj} - \tfrac{2}{3}\mathrm{I}_{\boldsymbol{\eta}\mathbf{b}\overset{\star}{\mathbf{P}}_{\bar{\Omega}}}\ \delta_{ij} \tag{4.16j}$$

$$\overset{\star}{H}_{(\eta;11)ij} := \eta_{i\ell}b_{\ell k}b_{km}\overset{\star}{P}_{\bar{S}_{mj}} + \overset{\star}{P}_{\bar{S}_{i\ell}}b_{\ell k}b_{km}\eta_{mj} - \tfrac{2}{3}\mathrm{I}_{\boldsymbol{\eta}\mathbf{b}^2\overset{\star}{\mathbf{P}}_{\bar{S}}}\ \delta_{ij} \tag{4.16k}$$

$$\overset{\star}{H}_{(\eta;12)ij} := \eta_{i\ell}\overset{\star}{P}_{\bar{S}_{\ell k}}b_{km}b_{mj} + b_{i\ell}b_{\ell m}\overset{\star}{P}_{\bar{S}_{mk}}\eta_{kj} - \tfrac{2}{3}\mathrm{I}_{\boldsymbol{\eta}\mathbf{b}^2\overset{\star}{\mathbf{P}}_{\bar{S}}}\ \delta_{ij} \tag{4.16l}$$

$$\overset{\star}{H}_{(\eta;13)ij} := \eta_{i\ell}b_{\ell m}b_{mk}\overset{\star}{P}_{\bar{\Omega}_{kj}} + \overset{\star}{P}_{\bar{\Omega}_{i\ell}}b_{\ell m}b_{mk}\eta_{kj} - \tfrac{2}{3}\mathrm{I}_{\boldsymbol{\eta}\mathbf{b}^2\overset{\star}{\mathbf{P}}_{\bar{\Omega}}}\ \delta_{ij} \tag{4.16m}$$

$$\overset{\star}{H}_{(\eta;14)ij} := \eta_{i\ell}\overset{\star}{P}_{\bar{\Omega}_{\ell k}}b_{km}b_{mj} + b_{i\ell}b_{\ell m}\overset{\star}{P}_{\bar{\Omega}_{mk}}\eta_{kj} - \tfrac{2}{3}\mathrm{I}_{\boldsymbol{\eta}\mathbf{b}^2\overset{\star}{\mathbf{P}}_{\bar{\Omega}}}\ \delta_{ij} \tag{4.16n}$$

If more than one inhomogeneity-direction vectors are used (*eg* Craft & Launder 1996; Craft 1998; Suga 2004) then one can either repeat (4.16) for each η, or attempt a RE-projection (Rivlin & Ericksen 1955, pp. 380–382) of all η's on a selected one, using as a second tensor, *eg* $\mathbf{b}$, but also keeping in mind that the projection may fail if the 2 selected tensors are not linearly independent, for the particular case of interest. In practice only a few of the tensors in (4.16) are used (*viz* $\overset{\star}{H}_{(\eta;\ 1)ij}$, $\overset{\star}{H}_{(\eta;\ 2)ij}$, $\overset{\star}{H}_{(\eta;\ 4)ij}$, $\overset{\star}{H}_{(\eta;\ 5)ij}$ and $\overset{\star}{H}_{(\eta;\ 6)ij}$). All models for wall-echo considered in the present work (§4.1)

model	$c_1^{(\phi^{\mathrm{s};\mathfrak{V}})}$	$c_2^{(\phi^{\mathrm{s};\mathfrak{V}})}$	$c_1^{(\phi^{\mathrm{s};w})}$	$c_2^{(\phi^{\mathrm{s};w})}$	$\vec{e}_\eta$	$c_{(\eta;1)}^{(\phi^{\mathrm{s};w})}$	$c_{(\eta;2)}^{(\phi^{\mathrm{s};w})}$	$c_{(\eta;3)}^{(\phi^{\mathrm{s};w})}$	χ_ε
LRR	$-2c_{\mathrm{LRR}_1}$	0	$2c_{\mathrm{LRR}_3} f_{\mathrm{GL}_w}$	0	—	—	—	—	1
GL	$-2c_{\mathrm{GL}_1}$	0	$-2c'_{\mathrm{GL}_1} f_{\mathrm{GL}_w}$	0	$\vec{e}_n$	$-2c'_{\mathrm{GL}_1} f_{\mathrm{GL}_w}$	$-3c'_{\mathrm{GL}_1} f_{\mathrm{GL}_w}$	0	1
JEJK	$-2c_{\mathrm{JEJK}_1}$	$4c'_{\mathrm{JEJK}_1}$	$-2c^{(w)}_{\mathrm{JEJK}_1} f_{\mathrm{JEJK}_w}$	0	$\dfrac{\mathrm{grad}(A\ell_{\mathrm{T}})}{\lvert\mathrm{grad}(A\ell_{\mathrm{T}})\rvert}$	$-2c^{(w)}_{\mathrm{JEJK}_1} f_{\mathrm{JEJK}_w}$	$-3c^{(w)}_{\mathrm{JEJK}_1} f_{\mathrm{JEJK}_w}$	0	0
SSG	$-c_{\mathrm{SSG}_1}$	c_{SSG_2}	—	—	—	—	—	—	1
SAYS	$-c_{\mathrm{SSG}_1}$	c_{SSG_2}	$c_{\mathrm{SSG}_1} f_{\mathrm{SAYS}_w}$	$-c_{\mathrm{SSG}_2} f_{\mathrm{SAYS}_w}$	—	—	—	—	0
S	$-2(c_{\mathrm{S}_1} + c''_{\mathrm{S}_1})$	$-4c_{\mathrm{S}_1} c'_{\mathrm{S}_1}$	$\dfrac{(-2f_{\mathrm{S}_{w_1}} - \frac{8}{3} f_{\mathrm{S}_{w_2}})\lvert\mathrm{grad}(\ell_{\mathrm{T}}\sqrt{A})\rvert^2}{\big(\frac{1}{2} + \lvert\mathrm{grad}(\ell_{\mathrm{T}}\sqrt{A})\rvert\big)^2}$	$\dfrac{-4f_{\mathrm{S}_{w_2}} \lvert\mathrm{grad}(\ell_{\mathrm{T}}\sqrt{A})\rvert^2}{\big(\frac{1}{2} + \lvert\mathrm{grad}(\ell_{\mathrm{T}}\sqrt{A})\rvert\big)^2}$	$\dfrac{\mathrm{grad}(\ell_{\mathrm{T}}\sqrt{A})}{\lvert\mathrm{grad}(\ell_{\mathrm{T}}\sqrt{A})\rvert}$	$\dfrac{(-2f_{\mathrm{S}_{w_1}} - \frac{4}{3} f_{\mathrm{S}_{w_2}})\lvert\mathrm{grad}(\ell_{\mathrm{T}}\sqrt{A})\rvert^2}{\big(\frac{1}{2} + \lvert\mathrm{grad}(\ell_{\mathrm{T}}\sqrt{A})\rvert\big)^2}$	$\dfrac{(-3f_{\mathrm{S}_{w_1}} - 4f_{\mathrm{S}_{w_2}})\lvert\mathrm{grad}(\ell_{\mathrm{T}}\sqrt{A})\rvert^2}{\big(\frac{1}{2} + \lvert\mathrm{grad}(\ell_{\mathrm{T}}\sqrt{A})\rvert\big)^2}$	$\dfrac{-6f_{\mathrm{S}_{w_2}} \lvert\mathrm{grad}(\ell_{\mathrm{T}}\sqrt{A})\rvert^2}{\big(\frac{1}{2} + \lvert\mathrm{grad}(\ell_{\mathrm{T}}\sqrt{A})\rvert\big)^2}$	0

model	$c_1^{(\phi^{\mathrm{r};\mathfrak{V}})}$	$c_2^{(\phi^{\mathrm{r};\mathfrak{V}})}$	$c_3^{(\phi^{\mathrm{r};\mathfrak{V}})}$	$c_4^{(\phi^{\mathrm{r};\mathfrak{V}})}$	$c_5^{(\phi^{\mathrm{r};\mathfrak{V}})}$	$c_6^{(\phi^{\mathrm{r};\mathfrak{V}})}$	$c_7^{(\phi^{\mathrm{r};\mathfrak{V}})}$	$c_8^{(\phi^{\mathrm{r};\mathfrak{V}})}$
LRR	0	0	$-\big(\frac{60}{55} c_{\mathrm{LRR}_2} - \frac{4}{55}\big)$	$-\big(\frac{9}{11} c_{\mathrm{LRR}_2} + \frac{6}{11}\big)$	$+\big(\frac{7}{11} c_{\mathrm{LRR}_2} - \frac{10}{11}\big)$	0	0	0
GL	0	0	0	$-c_{\mathrm{GL}_2}$	$-c_{\mathrm{GL}_2}$	0	0	0
JEJK	0	0	0	$-c_{\mathrm{JEJK}_2}$	$-c_{\mathrm{JEJK}_2}$	0	0	0
SSG	$-c^*_{\mathrm{SSG}_1} \dfrac{P_{\mathrm{k}}}{\rho\varepsilon}$	0	$\big(c_{\mathrm{SSG}_3} - \frac{2}{3} c_{\mathrm{SSG}_4} - c^*_{\mathrm{SSG}_3} \sqrt{-2\mathrm{II}_{\mathbf{b}}}\big)$	$-\frac{1}{2} c_{\mathrm{SSG}_4}$	$-\frac{1}{2} c_{\mathrm{SSG}_5}$	0	0	0
SAYS	$-c^*_{\mathrm{SSG}_1} \dfrac{P_{\mathrm{k}}}{\rho\varepsilon}$	0	$\big(c_{\mathrm{SSG}_3} - \frac{2}{3} c_{\mathrm{SSG}_4} - c^*_{\mathrm{SSG}_3} \sqrt{-2\mathrm{II}_{\mathbf{b}}}\big)$	$-\frac{1}{2} c_{\mathrm{SSG}_4}$	$-\frac{1}{2} c_{\mathrm{SSG}_5}$	0	0	0
S	$\big(\frac{6}{5} - \frac{4}{15} c'_{\mathrm{S}_2}\big) \dfrac{P_{\mathrm{k}}}{\rho\varepsilon} + \mathrm{I}_{\mathbf{b}\overset{\star}{\mathbf{P}}} c'_{\mathrm{S}_2}$	$2c'_{\mathrm{S}_2} \dfrac{P_{\mathrm{k}}}{\rho\varepsilon}$	$\frac{4}{5}\big(\frac{1}{3} + \mathrm{II}_{\mathbf{b}}\big)\big(-4 + 13c'_{\mathrm{S}_2}\big) - \frac{24}{5}\big(\frac{8}{27} + \frac{2}{3}\mathrm{II}_{\mathbf{b}} - \mathrm{III}_{\mathbf{b}}\big) c'_{\mathrm{S}_2}$	$-\frac{7}{5} + \big(\frac{23}{15} + 2\mathrm{II}_{\mathbf{b}}\big) c'_{\mathrm{S}_2}$	$-\frac{13}{15} + 40\mathrm{II}_{\mathbf{b}} c_{\mathrm{S}_2} + \big(\frac{7}{45} + 6\mathrm{II}_{\mathbf{b}}\big) c'_{\mathrm{S}_2}$	$\frac{6}{5} - \frac{13}{5} c'_{\mathrm{S}_2}$	$-\frac{2}{5} - \frac{17}{15} c'_{\mathrm{S}_2}$	$24c_{\mathrm{S}_2} + 4c'_{\mathrm{S}_2}$

model	$c_1^{(\phi^{\mathrm{r};w})}$	$c_3^{(\phi^{\mathrm{r};w})}$	$c_4^{(\phi^{\mathrm{r};w})}$	$c_5^{(\phi^{\mathrm{r};w})}$	$\vec{e}_\vartheta$	$c_{(\vartheta;1)}^{(\phi^{\mathrm{r};w})}$	$c_{(\vartheta;5)}^{(\phi^{\mathrm{r};w})}$	$c_{(\vartheta;6)}^{(\phi^{\mathrm{r};w})}$
LRR	0	0	0	$2c_{\mathrm{LRR}_4} f_{\mathrm{GL}_w}$	—	—	—	—
GL	0	0	$c_{\mathrm{GL}_2} c'_{\mathrm{GL}_2} f_{\mathrm{GL}_w}$	$c_{\mathrm{GL}_2} c'_{\mathrm{GL}_2} f_{\mathrm{GL}_w}$	$\vec{e}_n$	0	$\frac{3}{2} c_{\mathrm{GL}_2} c'_{\mathrm{GL}_2} f_{\mathrm{GL}_w}$	$\frac{3}{2} c_{\mathrm{GL}_2} c'_{\mathrm{GL}_2} f_{\mathrm{GL}_w}$
JEJK	0	0	$c_{\mathrm{JEJK}_2} c^{(w)}_{\mathrm{JEJK}_2} f_{\mathrm{JEJK}_w}$	$c_{\mathrm{JEJK}_2} c^{(w)}_{\mathrm{JEJK}_2} f_{\mathrm{JEJK}_w}$	$\dfrac{\mathrm{grad}(A\ell_{\mathrm{T}})}{\lvert\mathrm{grad}(A\ell_{\mathrm{T}})\rvert}$	0	$\frac{3}{2} c_{\mathrm{JEJK}_2} c^{(w)}_{\mathrm{JEJK}_2} f_{\mathrm{JEJK}_w}$	$\frac{3}{2} c_{\mathrm{JEJK}_2} c^{(w)}_{\mathrm{JEJK}_2} f_{\mathrm{JEJK}_w}$
SSG	—	—	—	—	—	—	—	—
SAYS	$-c^*_{\mathrm{SSG}_1} \dfrac{P_{\mathrm{k}}}{\rho\varepsilon} f_{\mathrm{SAYS}_w}$	$2\gamma^*_{\mathrm{SAYS}} f_{\mathrm{SAYS}_w}$	$\alpha^*_{\mathrm{SAYS}} f_{\mathrm{SAYS}_w}$	$\alpha^*_{\mathrm{SAYS}} f_{\mathrm{SAYS}_w}$	—	—	—	—
S	0	0	0	0	$\dfrac{\mathrm{grad}\ell_{\mathrm{T}}}{\lvert\mathrm{grad}\ell_{\mathrm{T}}\rvert}$	$f_{\mathrm{S}_I} \mathrm{I}_{\overset{\star}{\mathbf{S}}\boldsymbol{\vartheta}} \dfrac{\lvert\mathrm{grad}\ell_{\mathrm{T}}\rvert^4}{\big(\frac{1}{2} + \lvert\mathrm{grad}\ell_{\mathrm{T}}\rvert\big)^4}$	0	0

TABLE 3. Coefficients of the tensorial representation of redistribution closures (4.13, 4.15, 4.16, 4.17) (for $[\phi_{ij}^{(\mathrm{r};\mathfrak{V})}]_{\mathrm{M}}$ (4.12) only coefficients which are $\neq 0$ for at least one of the models are tabulated), for the models considered in the present work (LRR: Launder *et al.* 1975; GL: Gibson & Launder 1978; SSG: Speziale *et al.* 1991; SAYS: So *et al.* 1996; S: Suga 2004; JEJK: Jakirlić *et al.* 2007) with reference to the coefficients of the original representations (§4.1), and indicator $\chi_{\mathrm{M}_\varepsilon}$ (4.12) of the inclusion ($\chi_{\mathrm{M}_\varepsilon} = 1$) of the anisotropy of dissipation in the slow volume part (Lumley 1978) of the model (recall that the SSG model is quasi-homogeneous and that the SAYS model is its near-wall extension).

can be represented as

$$[\phi_{ij}^{(w)}]_{\mathrm{M}} := \underbrace{\rho\varepsilon\Big(\sum_{n=1}^{2} c_{\mathrm{M}_n}^{(\phi^{\mathrm{s};w})} \overset{\star}{H}_{(n)ij} + \sum_{n=1}^{3} c_{\mathrm{M}_{(\eta;n)}}^{(\phi^{\mathrm{s};w})} \overset{\star}{H}_{(\eta;n)ij}\Big)}_{\sim\, \phi_{ij}^{(\mathrm{s};w)}}$$
$$+ \underbrace{\rho\varepsilon\Big(\sum_{n=1}^{8} c_{\mathrm{M}_n}^{(\phi^{\mathrm{r};w})} \overset{\star}{H}_{(n)ij} + \sum_{n=1}^{14} c_{\mathrm{M}_{(\vartheta;n)}}^{(\phi^{\mathrm{r};w})} \overset{\star}{H}_{(\vartheta;n)ij}\Big)}_{\sim\, \phi_{ij}^{(\mathrm{r};w)}} \tag{4.17}$$

where a different tensor $\boldsymbol{\vartheta} =: \overset{\star}{\mathbf{H}}_{(\vartheta;1)}$, based on the unit vector $\vec{e}_\vartheta$ (4.15*a*), was used in the rapid term, to accommodate the different inhomogeneity direction used in the S (Suga 2004) model (4.11*e*) for the slow and rapid terms.

All the models studied in the present work (§4.1) can be represented by (4.12, 4.17), with coefficients (Tab. 3) which are readily obtained by straightforward computation from the original form of the model. Alternative equivalent representation bases (Gerolymos *et al.* 2010*b*) can be used, the coefficients in these different bases being easily computed using basis-change matrices (Gerolymos *et al.* 2010*b*).

4.3. A priori *assessment of typical models for* ϕ_{ij}

A priori assessment of the various models for the rapid part of pressure-strain redistribution (Fig. 13) indicates that the two more recent models (S: Suga 2004; JEJK: Jakirlić *et al.* 2007) give the best estimate of $\phi_{ij}^{(\mathrm{r})}$ both globally and for the individual volume ($\phi_{ij}^{(\mathrm{r};\mathfrak{V})}$) and wall-echo ($\phi_{ij}^{(\mathrm{r};w)}$) terms (Fig. 13). The prediction of the $\phi_{yy}^{(\mathrm{r})}$ component is the most unsatisfactory, both these models (S and JEJK) predicting the wrong sign (Fig. 13), indicating that the much more complicated TCL representation used for the S (Suga 2004) model is not sufficient to correct this discrepancy, common to all of the models studied (§4.1), with exception of the GL (Gibson & Launder 1978) proposal. Nonetheless, even in this case, the separate assessment of the volume ($\phi_{ij}^{(\mathrm{r};\mathfrak{V})}$) and wall-echo ($\phi_{ij}^{(\mathrm{r};w)}$) terms (Fig. 13) shows unsatisfactory prediction of the *yy*-component for all models, the GL (Gibson & Launder 1978) closure overestimating wall-echo by an order of magnitude, and thus overcorrecting the equally overestimated volume term (Fig. 13). In general, both legacy models (LRR: Launder *et al.* 1975; GL: Gibson & Launder 1978), which have constant model coefficients (not functions of the invariants), often exhibit an order-of-magnitude difference with respect to the DNS data, especially when examining individually the volume ($\phi_{ij}^{(\mathrm{r};\mathfrak{V})}$) and wall-echo ($\phi_{ij}^{(\mathrm{r};w)}$) terms (Fig. 13). Nonetheless, observation of the shear component of wall-echo $\phi_{xy}^{(\mathrm{r};w)}$ (Fig. 13) shows a fundamental difference between the wall-echo approaches, of GL (Gibson & Launder 1978) based on the general tensorial formulation (4.7*e*), and of LRR (Launder *et al.* 1975) which simply uses a wall-proximity function approach (4.6*e*). The directionality information present in the GL (Gibson & Launder 1978) closure predicts the correct form of $\phi_{xy}^{(\mathrm{r};w)}$, contrary to the LRR (Launder *et al.* 1975) model (Fig. 13). The quasi-homogeneous SSG (Speziale *et al.* 1991) largely overpredicts $\phi_{ij}^{(\mathrm{r};\mathfrak{V})}$, and the corresponding near-wall model (SAYS: So *et al.* 1996) has to introduce overpredicted wall-echo terms to correct this discrepancy (Fig. 13).

When assessing the models for the slow part $\phi_{ij}^{(\mathrm{s})}$ (Fig. 14) we included in the DNS data the pressure-strain redistribution tensor (3.2) augmented by the anisotropy of dissipation (4.4*d*), $\phi_{ij} - 2\rho\varepsilon b_{\varepsilon_{ij}}$, since several closures follow the suggestion of Lumley (1978)

Re_{τ_w}	$\bar{M}_{\text{CL}}$	$N_x \times N_y \times N_z$	L_x	L_y	L_z	Δx^+	Δy^+_w	$N_{y^+\leq 10}$	Δy^+_{CL}	Δz^+	Δt^+	$t^+_{\text{OBS}_{\text{GF}}}$	$\Delta t^+_{s_{\text{GF}}}$
179	0.34	$193 \times 129 \times 169$	$4\pi\delta$	2δ	$\frac{4}{3}\pi\delta$	11.7	0.22	20	4.9	4.4	6.47×10^{-3}	1648	6.47×10^{-1}

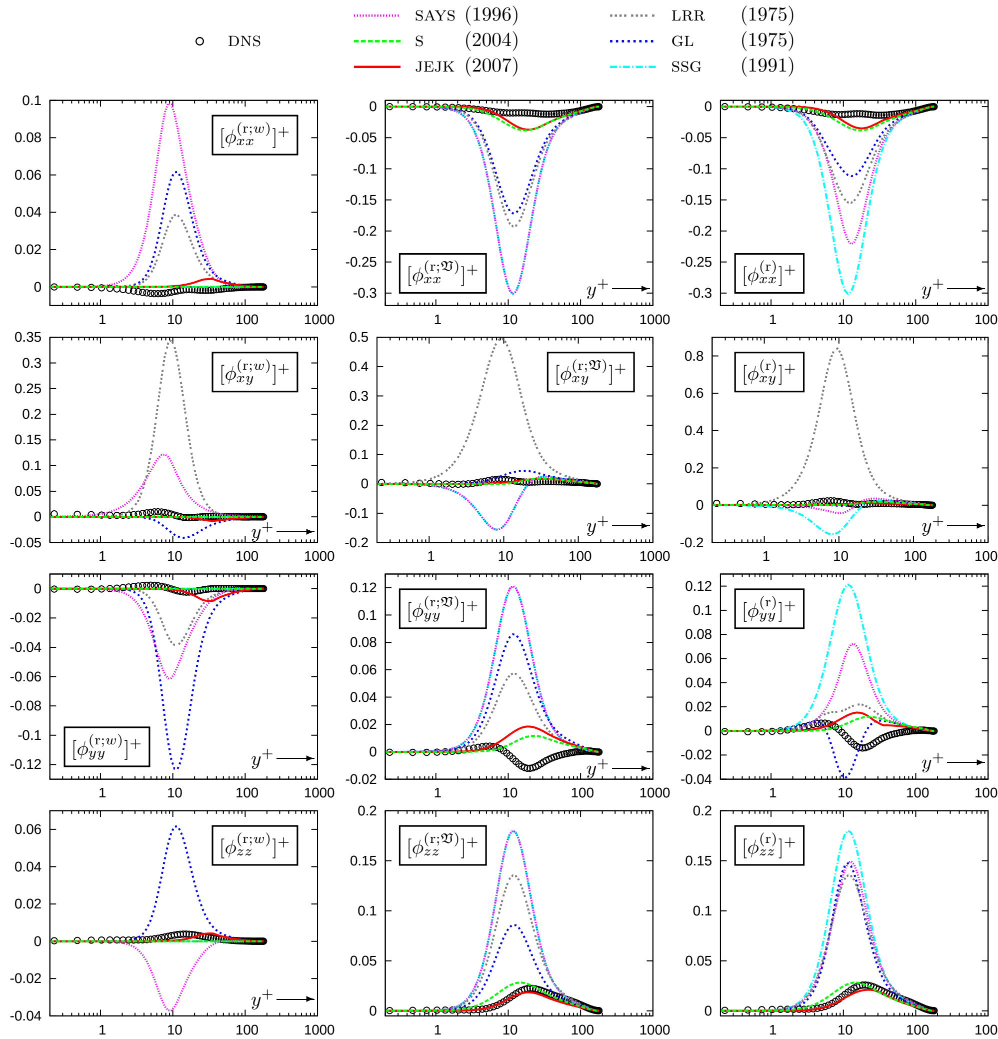

FIGURE 13. *A priori* comparison of various models (LRR: Launder *et al.* 1975; GL: Gibson & Launder 1978; SSG: Speziale *et al.* 1991; SAYS: So *et al.* 1996; S: Suga 2004; JEJK: Jakirlić *et al.* 2007) for the rapid pressure-strain redistribution $\phi^{(\text{r})}_{ij} = \phi^{(\text{r};\mathfrak{V})}_{ij} + \phi^{(\text{r};w)}_{ij}$ with present DNS results for the volume $\phi^{(\text{r};\mathfrak{V})}_{ij}$ and the wall-echo $\phi^{(\text{r};w)}_{ij}$ terms, in wall units, plotted against the nondimensional distance from the wall y^+ (in fully developed incompressible plane channel flow $\phi_{yz} = \phi_{zx}$).

to include the anisotropy of dissipation into the model for the slow part of ϕ_{ij}. This suggestion was motivated by the fact (Lumley 1978) that, in the context of SMCs, both $\phi^{(\text{s})}_{ij}$ and $b_{\varepsilon_{ij}}$ are modelled by a quasilinear combination of b_{ij} and $b_{im}b_{mj} + \frac{2}{3}\text{II}_{\mathbf{b}}\delta_{ij}$ (4.12, 4.13). Obviously (Fig. 14) the LRR (Launder *et al.* 1975), GL (Gibson & Launder 1978), and SSG (Speziale *et al.* 1991) proposals include the anisotropy of dissipation into the model for the slow volume part $\phi^{(\text{s};\mathfrak{V})}_{ij} - 2\rho\varepsilon b_{\varepsilon_{ij}}$, while the JEJK (Jakirlić *et al.* 2007) closure models $\phi^{(\text{s};\mathfrak{V})}_{ij}$ alone. Examination of the S (Suga 2004) closure shows that in

Re_{τ_w}	$\bar{M}_{\text{CL}}$	$N_x \times N_y \times N_z$	L_x	L_y	L_z	Δx^+	Δy_w^+	$N_{y^+\leq 10}$	Δy_{CL}^+	Δz^+	Δt^+	$t^+_{\text{OBS}_{\text{GF}}}$	$\Delta t^+_{s_{\text{GF}}}$
179	0.34	$193 \times 129 \times 169$	$4\pi\delta$	2δ	$\frac{4}{3}\pi\delta$	11.7	0.22	20	4.9	4.4	6.47×10^{-3}	1648	6.47×10^{-1}

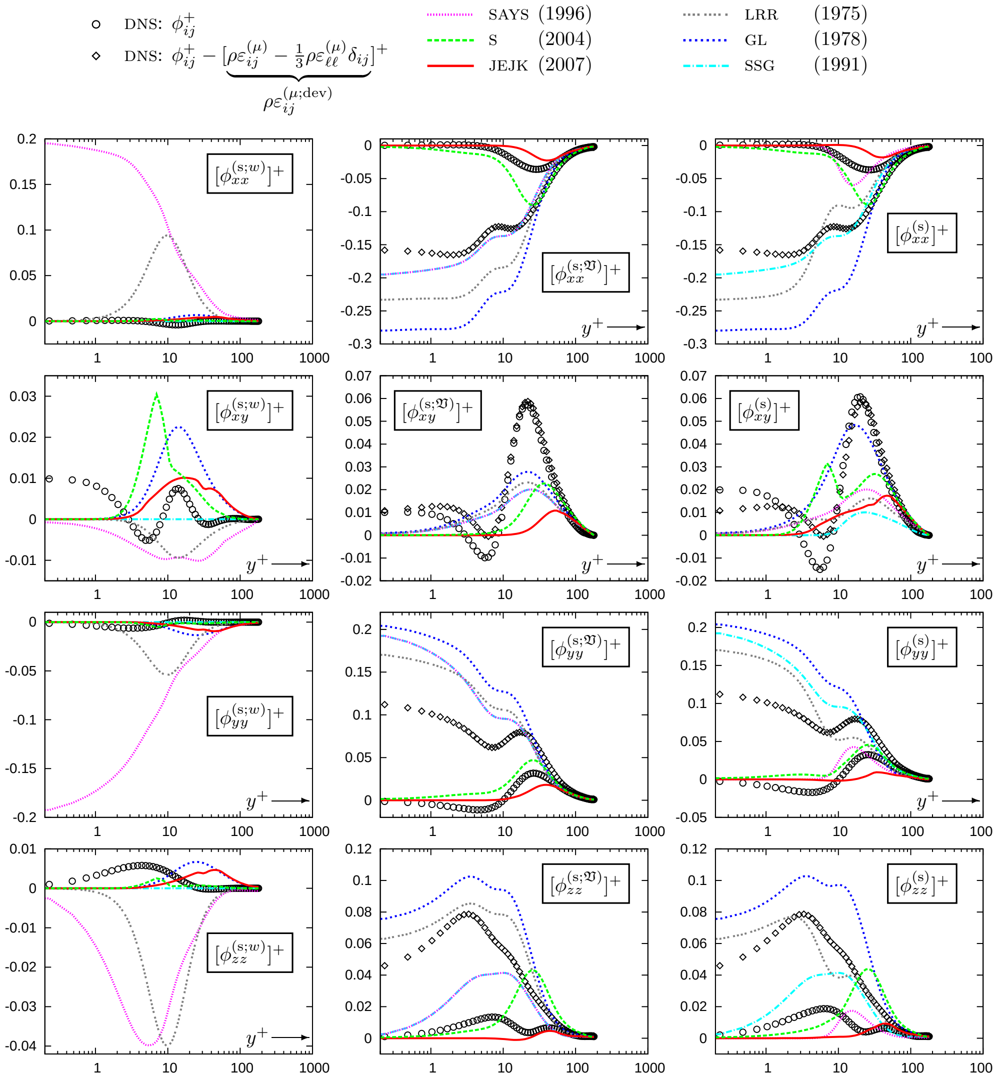

FIGURE 14. *A priori* comparison of various models (LRR: Launder *et al.* 1975; GL: Gibson & Launder 1978; SSG: Speziale *et al.* 1991; SAYS: So *et al.* 1996; S: Suga 2004; JEJK: Jakirlić *et al.* 2007) for the slow pressure-strain redistribution $\phi_{ij}^{(\text{s})} = \phi_{ij}^{(\text{s};\mathfrak{V})} + \phi_{ij}^{(\text{s};w)}$ with present DNS results for the volume $\phi_{ij}^{(\text{s};\mathfrak{V})}$ and the wall-echo $\phi_{ij}^{(\text{s};w)}$ terms, and slow redistribution augmented by the anisotropy of dissipation $\phi_{ij}^{(\text{s})} - \rho\varepsilon_{ij}^{(\mu;\text{dev})}$, in wall units, plotted against the nondimensional distance from the wall y^+ (in fully developed incompressible plane channel flow $\phi_{yz} = \phi_{zx}$).

the buffer and outer regions ($y^+ \gtrapprox 20$; Fig. 14) it overpredicts $\phi_{ij}^{(\text{s};\mathfrak{V})}$ but closely fits $\phi_{ij}^{(\text{s};\mathfrak{V})} - 2\rho\varepsilon b_{\varepsilon_{ij}}$, while near the wall ($y^+ \lessapprox 10$; Fig. 14) it closely fits $\phi_{ij}^{(\text{s};\mathfrak{V})}$ alone, as it respects the two-component-limit (TCL) for $A \to 0$. This behaviour is particularly visible for the xx-component (Fig. 14). Concerning the global prediction of $\phi_{ij}^{(\text{s})}$ (Fig. 14) the

Re_{τ_w}	$\bar{M}_{\text{CL}}$	$N_x \times N_y \times N_z$	L_x	L_y	L_z	Δx^+	Δy_w^+	$N_{y^+ \leq 10}$	Δy_{CL}^+	Δz^+	Δt^+	t_{OBS}^+	Δt_s^+
179	0.34	$193 \times 129 \times 169$	$4\pi\delta$	2δ	$\frac{4}{3}\pi\delta$	11.7	0.22	20	4.9	4.4	6.47×10^{-3}	2329	6.47×10^{-3}

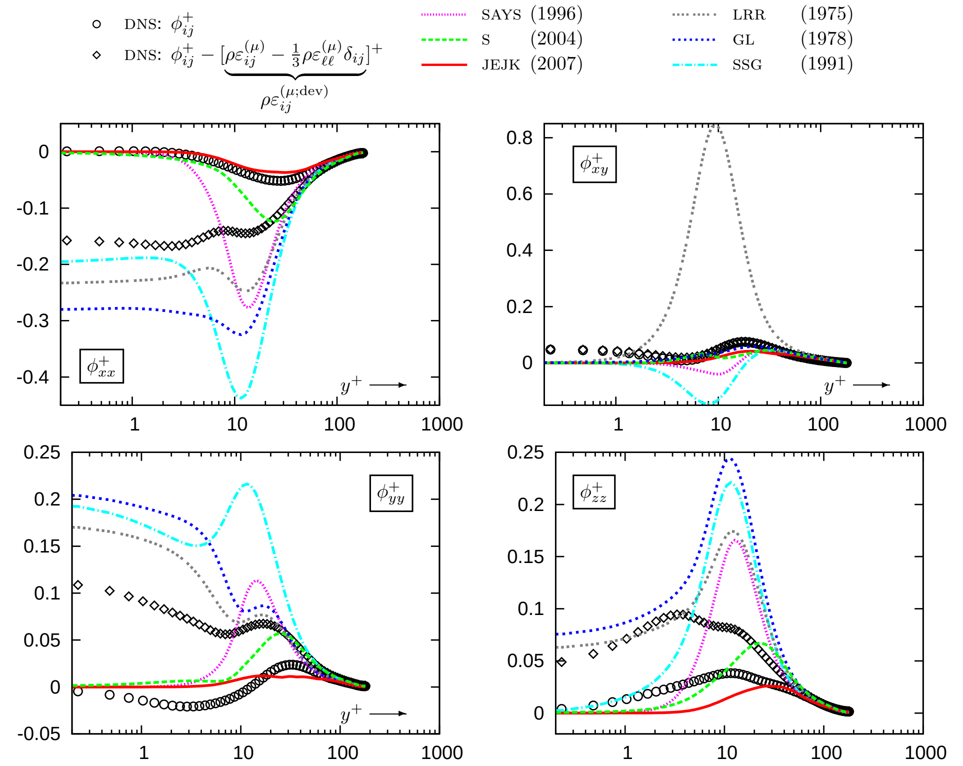

FIGURE 15. *A priori* comparison of various models (LRR: Launder *et al.* 1975; GL: Gibson & Launder 1978; SSG: Speziale *et al.* 1991; SAYS: So *et al.* 1996; S: Suga 2004; JEJK: Jakirlić *et al.* 2007) for the pressure-strain redistribution ϕ_{ij} with present DNS results for redistribution ϕ_{ij} and redistribution augmented by the anisotropy of dissipation $\phi_{ij} - \rho\varepsilon_{ij}^{(\mu;\text{dev})}$, in wall units, plotted against the nondimensional distance from the wall y^+ (in fully developed incompressible plane channel flow $\phi_{yz} = \phi_{zx}$).

JEJK (Jakirlić *et al.* 2007) closure gives the best results, followed by SAYS (So *et al.* 1996) and S (Suga 2004). Notice that the global prediction of the SAYS (So *et al.* 1996) closure fits $\phi_{ij}^{(\text{s})}$ alone, while its volume part which is given by the quasi-homogeneous SSG closure fits $\phi_{ij}^{(\text{s};\mathfrak{V})} - 2\rho\varepsilon b_{\varepsilon_{ij}}$. As a consequence the wall-echo term $[\phi_{ij}^{(\text{s};w)}]_{\text{SAYS}}$ must be interpreted as cancelling out the dissipation anisotropy included in $[\phi_{ij}^{(\text{s};\mathfrak{V})}]_{\text{SSG}}$. Notice that the SSG (Speziale *et al.* 1991) closure, and to a lesser extend the LRR (Launder *et al.* 1975) and GL (Gibson & Launder 1978) models, perform reasonably well in predicting $\phi_{ij}^{(\text{s})} - 2\rho\varepsilon b_{\varepsilon_{ij}}$, and not $\phi_{ij}^{(\text{s})}$ (Fig. 14).

Concerning the global prediction of ϕ_{ij} (Fig. 15) the trends observed in the detailed predictions of $\phi_{ij}^{(\text{r})} = \phi_{ij}^{(\text{r};\mathfrak{V})} + \phi_{ij}^{(\text{r};w)}$ (Fig. 13) and $\phi_{ij}^{(\text{s})} = \phi_{ij}^{(\text{s};\mathfrak{V})} + \phi_{ij}^{(\text{s};w)}$ (Fig. 14) are confirmed, in that the JEJK (Jakirlić *et al.* 2007) closure gives the best prediction, followed by the S (Suga 2004) and SAYS (So *et al.* 1996) models. The SAYS (So *et al.* 1996) model does a very good job in correcting the quasi-homogeneous SSG (Speziale *et al.* 1991) closure (which also contains the anisotropy of dissipation) for near-wall turbulence, but closures whose volume part does not include the dissipation anisotropy $-2\rho\varepsilon b_{\varepsilon_{ij}}$ (such as JEJK: Jakirlić *et al.* 2007, and to a lesser extent S: Suga 2004) are much easier to adapt to near-wall turbulence modelling (Figs. 13–15).

Notice, however, that even the best models, which predict satisfactorily the behaviour of ϕ_{xx} (in plane channel flow $\overline{u'u'}$ is produced by $P_{xx} \overset{(4.3g)}{=} -2\overline{u'v'}\partial_y\bar{u}$), are less accurate in the approximation of the redistribution for the two other normal components, especially in the near-wall region ($y^+ \lessapprox 10$; Fig. 14).

4.4. *Typical models for $d_{ij}^{(p)}$*

There are relatively few models for pressure diffusion which were recently reviewed in Vallet (2007). We examine here most of these models (Hirt (1969); Lumley (1978); Fu (1993); DRDL: Demuren *et al.* 1996; Vallet (2007)). Notice that Suga (2004) has proposed a model for the rapid part of pressure diffusion $d_{ij}^{(p;\mathrm{r})}$, indeed for the rapid wall-echo $d_{ij}^{(p;\mathrm{r};w)}$, but the proposed model is identically 0 in fully developed plane channel flow, and cannot therefore be assessed in the present work. Straatman (1999) has studied the calibration of the coefficients of the model of Lumley (1978) (§4.4.2), using the tensorial form of Lumley (1978) to model the triple velocity correlations, and hence belongs to the same family as Lumley (1978) and Vallet (2007) (for $d_{ij}^{(p;\mathrm{s};\mathfrak{V})}$).

4.4.1. Hirt 1969

The early attempt of Hirt (1969) at modelling the slow volume part of $d_{ij}^{(p)}$ (3.1, 3.2) is a tensorially invariant generalization of the specific to boundary-layer flow proposal of Donaldson (1969). Hirt (1969) has no model coefficient (equivalently the model-coefficient is taken to be 1), while Daly & Harlow (1970) who used the same formulation include a model-coefficient, although both Donaldson (1969) and Daly & Harlow (1970) set the corresponding model-coefficient† to 0. This model reads

$$[d_{ij}^{(p)}]_{\mathrm{Hirt}} := [d_{ij}^{(p;\mathrm{s};\mathfrak{V})}]_{\mathrm{Hirt}} + [d_{ij}^{(p;\mathrm{s};w)}]_{\mathrm{Hirt}} + [d_{ij}^{(p;\mathrm{r};\mathfrak{V})}]_{\mathrm{Hirt}} + [d_{ij}^{(p;\mathrm{r};w)}]_{\mathrm{Hirt}} \tag{4.18a}$$

$$[d_{ij}^{(p;\mathrm{s};\mathfrak{V})}]_{\mathrm{Hirt}} := \frac{\partial}{\partial x_\ell}\left(c_{\mathrm{Hirt}}\rho\frac{\mathrm{k}^2}{\varepsilon}\Big(\frac{\partial\overline{u_i'u_m'}}{\partial x_m}\delta_{j\ell} + \frac{\partial\overline{u_j'u_m'}}{\partial x_m}\delta_{i\ell}\Big)\right) \tag{4.18b}$$

$$[d_{ij}^{(p;\mathrm{s};w)}]_{\mathrm{Hirt}} := 0 \tag{4.18c}$$

$$[d_{ij}^{(p;\mathrm{r};\mathfrak{V})}]_{\mathrm{Hirt}} := 0 \tag{4.18d}$$

$$[d_{ij}^{(p;\mathrm{r};w)}]_{\mathrm{Hirt}} := 0 \tag{4.18e}$$

$$c_{\mathrm{Hirt}} = 2c_{\mathrm{Lumley}}c_{\mathrm{DH}} \quad ; \quad c_{\mathrm{Lumley}} = \tfrac{1}{5} \quad ; \quad c_{\mathrm{DH}} = \tfrac{22}{100} \tag{4.18f}$$

Had we used a model-coefficient c_{Hirt} equal to 1 instead of (4.18*f*), as used by Hirt (1969) and suggested by Daly & Harlow (1970), the values for $d_{ij}^{(p)}$ would have been an order-of-magnitude too high compared to DNS data (Kim *et al.* 1987; Moser *et al.* 1999; Hoyas & Jiménez 2006; Gerolymos *et al.* 2010*c*). To compare the early (Donaldson 1969; Hirt 1969; Daly & Harlow 1970) tensorial form (4.18*b*) with later proposals we used the same coefficient (4.18*f*) as the one (4.21*f*) used in the model of Fu (1993), which has a similar although not identical tensorial representation (4.21*b*), but with the opposite sign.

---

† B_{D_2} (Donaldson 1969, (11,12), p. 273) and θ_{DH} (Daly & Harlow 1970, (16), p. 2637)

4.4.2. Lumley 1978

Lumley (1978) made analytical calculation in Fourier space to obtain a quasi-homogeneous expression for the slow volume part of the pressure-velocity correlation $\overline{p'u'_i}$, whose validity is limited to weakly inhomogeneous flows

$$\frac{1}{\rho}[\overline{p'u'_i}]^{(\mathrm{s};\mathfrak{V})}_{\mathrm{Lumley}} := -\tfrac{1}{5}\overline{u'_iu'_mu'_m} \tag{4.19}$$

$$[d_{ij}^{(p)}]_{\mathrm{Lumley}} :=[d_{ij}^{(p;\mathrm{s};\mathfrak{V})}]_{\mathrm{Lumley}} + [d_{ij}^{(p;\mathrm{s};w)}]_{\mathrm{Lumley}} + [d_{ij}^{(p;\mathrm{r};\mathfrak{V})}]_{\mathrm{Lumley}} + [d_{ij}^{(p;\mathrm{r};w)}]_{\mathrm{Lumley}} \tag{4.20a}$$

$$[d_{ij}^{(p;\mathrm{s};\mathfrak{V})}]_{\mathrm{Lumley}} :=\frac{\partial}{\partial x_\ell}\Big(c_{\mathrm{Lumley}}\rho\big(\overline{u'_iu'_mu'_m}\delta_{j\ell} + \overline{u'_ju'_mu'_m}\delta_{i\ell}\big)\Big) \tag{4.20b}$$

$$[d_{ij}^{(p;\mathrm{s};w)}]_{\mathrm{Lumley}} := 0 \tag{4.20c}$$

$$[d_{ij}^{(p;\mathrm{r};\mathfrak{V})}]_{\mathrm{Lumley}} := 0 \tag{4.20d}$$

$$[d_{ij}^{(p;\mathrm{r};w)}]_{\mathrm{Lumley}} := 0 \tag{4.20e}$$

$$c_{\mathrm{Lumley}} \overset{(4.18f)}{=} \tfrac{1}{5} \tag{4.20f}$$

In the present *a priori* assessment the proposal (4.19) of Lumley (1978) was evaluated using the DNS-computed triple velocity correlations, and not a model for $\overline{u'_iu'_ju'_k}$, as in previous studies (Fu 1993; Straatman 1999; Demuren *et al.* 1996; Sauret & Vallet 2007; Vallet 2007). Hence the model tested is not a SMC, but a third-moment closure (TMC) instead.

4.4.3. Fu 1993

Fu (1993) used the proposal (4.19) of Lumley (1978) combined with the Daly & Harlow (1970) model for the triple velocity correlations $\overline{u'_iu'_ju'_k}$, to model the slow volume part of the pressure-velocity correlation $\overline{p'u'_i}$

$$[d_{ij}^{(p)}]_{\mathrm{Fu}} :=[d_{ij}^{(p;\mathrm{s};\mathfrak{V})}]_{\mathrm{Fu}} + [d_{ij}^{(p;\mathrm{s};w)}]_{\mathrm{Fu}} + [d_{ij}^{(p;\mathrm{r};\mathfrak{V})}]_{\mathrm{Fu}} + [d_{ij}^{(p;\mathrm{r};w)}]_{\mathrm{Fu}} \tag{4.21a}$$

$$[d_{ij}^{(p;\mathrm{s};\mathfrak{V})}]_{\mathrm{Fu}} :=\frac{\partial}{\partial x_\ell}\left(- c_{\mathrm{Fu}}\rho\frac{\mathrm{k}}{\varepsilon}\Big(\overline{u'_iu'_m}\frac{\partial \mathrm{k}}{\partial x_m}\delta_{j\ell} + \overline{u'_ju'_m}\frac{\partial \mathrm{k}}{\partial x_m}\delta_{i\ell}\Big)\right) \tag{4.21b}$$

$$[d_{ij}^{(p;\mathrm{s};w)}]_{\mathrm{Fu}} :=0 \tag{4.21c}$$

$$[d_{ij}^{(p;\mathrm{r};\mathfrak{V})}]_{\mathrm{Fu}} :=0 \tag{4.21d}$$

$$[d_{ij}^{(p;\mathrm{r};w)}]_{\mathrm{Fu}} :=0 \tag{4.21e}$$

$$c_{\mathrm{Fu}} = c_{\mathrm{Hirt}} \overset{(4.18f)}{=} 2c_{\mathrm{Lumley}}c_{\mathrm{DH}} \tag{4.21f}$$

The model has been applied to the study of the plane/round jet anomaly (Fu 1993).

4.4.4. Demuren *et al.* 1996, DRDL

Contrary to the previous proposals, Demuren *et al.* (1996) include a model for the rapid-part of the pressure diffusion term. The slow part was modeled by using a non-local elliptic relaxation approach applied to a baseline local (single-point closure) model for the slow pressure transport $\overline{p'u'_i}$, obtained by applying the model (4.19) of Lumley

(1978) to the Mellor & Herring (1973) closure for the triple velocity correlations

$$[\overline{u_i'u_j'u_k'}]_{\text{MH}} := -c_{\text{MH}_s}\frac{\text{k}^2}{\varepsilon}\left(\frac{\partial\overline{u_i'u_j'}}{\partial x_k}+\frac{\partial\overline{u_j'u_k'}}{\partial x_i}+\frac{\partial\overline{u_k'u_k'}}{\partial x_j}\right) \tag{4.22a}$$

$$\frac{1}{\rho}[\overline{p'u_i'}]^{(\text{s};\mathfrak{V})}_{\text{L;MH}} := -c_{\text{Lumley}}[\overline{u_i'u_m'u_m'}]_{\text{MH}} \tag{4.22b}$$

$$c_{\text{Lumley}} \overset{(4.18f)}{=} \tfrac{1}{5} \quad;\quad c_{\text{MH}_s} = \tfrac{2}{3}c_{\text{HL}_s} \quad;\quad c_{\text{HL}_s} = \tfrac{11}{100} \tag{4.22c}$$

The Mellor & Herring (1973) closure for the triple velocity correlations (4.22*a*) can be obtained (Demuren & Sarkar 1993) by isotropisation of the Hanjalić & Launder (1972) closure, with the relation (4.22*c*) between the corresponding coefficients c_{MH_s} and c_{HL_s}. The initial estimate of pressure diffusion using (4.22*b*) in a plane mixing layer (Rogers & Moser 1994) motivated the non-local elliptic relaxation approach (Demuren *et al.* 1996), described by Demuren *et al.* (1994). The closure for the rapid part of pressure-diffusion models directly $d_{ij}^{(p;\text{r};\mathfrak{V})}$ as being proportional to the mean velocity gradients.

$$[d_{ij}^{(p)}]_{\text{DRDL}} := [d_{ij}^{(p;\text{s};\mathfrak{V})}]_{\text{DRDL}} + [d_{ij}^{(p;\text{s};w)}]_{\text{F}} + [d_{ij}^{(p;\text{r};\mathfrak{V})}]_{\text{DRDL}} + [d_{ij}^{(p;\text{r};w)}]_{\text{DRDL}} \tag{4.22d}$$

$$[d_{ij}^{(p;\text{s})}]_{\text{DRDL}} := -\frac{\partial}{\partial x_\ell}\left(\text{ER}_{\text{D}}\big([\overline{p'u_i'}]^{(\text{s};\mathfrak{V})}_{\text{L;MH}}\big)\delta_{j\ell} + \text{ER}_{\text{D}}\big([\overline{p'u_j'}]^{(\text{s};\mathfrak{V})}_{\text{L;MH}}\big)\delta_{i\ell}\right) \tag{4.22e}$$

$$[d_{ij}^{(p;\text{s};\mathfrak{V})}]_{\text{DRDL}} := -\frac{\partial}{\partial x_\ell}\left([\overline{p'u_i'}]^{(\text{s};\mathfrak{V})}_{\text{L;MH}}\delta_{j\ell} + [\overline{p'u_j'}]^{(\text{s};\mathfrak{V})}_{\text{L;MH}}\delta_{i\ell}\right) \tag{4.22f}$$

$$[d_{ij}^{(p;\text{s};w)}]_{\text{DRDL}} := [d_{ij}^{(p;\text{s})}]_{\text{DRDL}} - [d_{ij}^{(p;\text{s};\mathfrak{V})}]_{\text{DRDL}} \tag{4.22g}$$

$$[d_{ij}^{(p;\text{r};\mathfrak{V})}]_{\text{DRDL}} := c_{\text{DRDL}_r}\left(\overline{u_j'u_m'}\frac{\partial\bar{u}_m}{\partial x_\ell}\delta_{i\ell} + \overline{u_i'u_m'}\frac{\partial\bar{u}_m}{\partial x_\ell}\delta_{j\ell}\right) \tag{4.22h}$$

$$[d_{ij}^{(p;\text{r};w)}]_{\text{DRDL}} := 0 \tag{4.22i}$$

where ER_{D} is the elliptic relaxation operator of Durbin (1993), defined as (Demuren *et al.* 1994)

$$L_{\text{D}}^2\nabla^2\text{ER}_{\text{D}}(f) - \text{ER}_{\text{D}}(f) = f \quad;\quad \text{ER}_{\text{D}}(f)\Big|_w = 0 \tag{4.22j}$$

$$L_{\text{D}} := C_{\text{D}_L}\ell_{\text{T}}\max\left(1, C_{\text{D}_\eta}Re_{\text{T}}^{-\frac{3}{4}}\right) \quad;\quad C_{\text{D}_L} = \tfrac{3}{10} \quad;\quad C_{\text{D}_\eta} = 70 \tag{4.22k}$$

$$c_{\text{DRDL}_r} = \tfrac{1}{10} \tag{4.22l}$$

In the *a priori* tests the operator ER_{D} (4.22*g*) was computed by solving numerically the elliptic equation (4.22*g*) using $O(\Delta y^2)$ space discretization. Demuren *et al.* (1996) recommend $c_{\text{DRDL}_r} \in [\frac{1}{10}, \frac{3}{10}]$, and we have chosen the lowest value $c_{\text{DRDL}_r} = \frac{1}{10}$ (4.22*l*) because the model generally overestimates $d_{ij}^{(p;\text{r};\mathfrak{V})}$ (*cf* §4.5).

4.4.5. Vallet 2007

Vallet (2007) suggested a model for pressure-transport $\overline{p'u_i'}$ based on an associated model for the triple velocity correlations which contains both slow and rapid terms, following the analysis of Younis *et al.* (2000)

$$-[\overline{u_i'u_j'u_\ell'}]_{\text{Vallet}} := \underbrace{c_{\text{LSB}_{\text{s}_1}}\frac{\text{k}}{\varepsilon}\mathcal{G}^{(\text{s})}_{ij\ell} + c_{\text{LSB}_{\text{s}_2}}\frac{\text{k}}{\varepsilon}\left(\mathcal{G}^{(\text{s})}_{imm}\delta_{j\ell} + \mathcal{G}^{(\text{s})}_{jmm}\delta_{i\ell} + \mathcal{G}^{(\text{s})}_{\ell mm}\delta_{ij}\right)}_{-[\overline{u_i'u_j'u_\ell'}]^{(\text{s})}_{\text{Vallet}} := -[\overline{u_i'u_j'u_\ell'}]^{(\text{s})}_{\text{LSB}}}$$
$$+ \underbrace{c_{\text{Vallet}_{\text{r}_1}}\frac{\text{k}^3}{\varepsilon^2}\mathcal{G}^{(\text{r})}_{ij\ell} + c_{\text{Vallet}_{\text{r}_2}}\frac{\text{k}^3}{\varepsilon^2}\left(\mathcal{G}^{(\text{r})}_{imm}\delta_{j\ell} + \mathcal{G}^{(\text{r})}_{jmm}\delta_{i\ell} + \mathcal{G}^{(\text{r})}_{\ell mm}\delta_{ij}\right)}_{-[\overline{u_i'u_j'u_\ell'}]^{(\text{r})}_{\text{Vallet}}} \qquad (4.23a)$$

where the slow terms are based on the tensorial form of Lumley (1978)

$$\mathcal{G}^{(\text{s})}_{ij\ell} := \overline{u_i'u_k'}\frac{\partial\overline{u_j'u_\ell'}}{\partial x_k} + \overline{u_j'u_k'}\frac{\partial\overline{u_i'u_\ell'}}{\partial x_k} + \overline{u_k'u_\ell'}\frac{\partial\overline{u_i'u_j'}}{\partial x_k} \qquad (4.23b)$$

with the coefficients $c_{\text{LSB}_{\text{s}_1}}$ and $c_{\text{LSB}_{\text{s}_2}}$ (4.23*f*) optimised by Schwarz & Bradshaw (1994),† and the rapid terms introduced in Vallet (2007) are based on an analogous tensorial form

$$\mathcal{G}^{(\text{r})}_{ij\ell} := \bar{S}_{ki}\frac{\partial\overline{u_j'u_\ell'}}{\partial x_k} + \bar{S}_{kj}\frac{\partial\overline{u_\ell'u_i'}}{\partial x_k} + \bar{S}_{k\ell}\frac{\partial\overline{u_i'u_j'}}{\partial x_k} \qquad (4.23c)$$

By analogy to the relation (4.19) of Lumley (1978), slow and rapid pressure-transport terms are modelled as

$$\frac{1}{\rho}[\overline{p'u_i'}]^{(\text{s};\mathfrak{V})}_{\text{Vallet}} := -\,c_{\text{Vallet}_{\text{SP}}}[\overline{u_i'u_m'u_m'}]^{(\text{s})}_{\text{LSB}} \qquad (4.23d)$$
$$\frac{1}{\rho}[\overline{p'u_i'}]^{(\text{r};\mathfrak{V})}_{\text{Vallet}} := -\,c_{\text{Vallet}_{\text{SP}}}[\overline{u_i'u_m'u_m'}]^{(\text{r})}_{\text{Vallet}} \qquad (4.23e)$$

The model coefficients are (Vallet 2007)

$$\begin{aligned} c_{\text{LSB}_{\text{s}_1}} &= 0.0980 \quad ; \quad c_{\text{LSB}_{\text{s}_2}} = 0.01265 \\ c_{\text{Vallet}_{\text{r}_1}} &= 0.0001 \quad ; \quad c_{\text{Vallet}_{\text{r}_2}} = 0.0001 \\ c_{\text{Vallet}_{\text{SP}}} &:= 0.085\left(1 + \min\left(0.5, A^{\max(0.25, 2(1-6A))}\right)\right) \end{aligned} \qquad (4.23f)$$

Notice that $c_{\text{Vallet}_{\text{SP}}}$ is function of the flatness parameter A (4.5*a*) to accommodate the model to wall turbulence. The Vallet (2007) model reads

$$[d^{(p)}_{ij}]_{\text{Vallet}} := [d^{(p;\text{s};\mathfrak{V})}_{ij}]_{\text{Vallet}} + [d^{(p;\text{s};w)}_{ij}]_{\text{Vallet}} + [d^{(p;\text{r};\mathfrak{V})}_{ij}]_{\text{Vallet}} + [d^{(p;\text{r};w)}_{ij}]_{\text{Vallet}} \qquad (4.23g)$$

$$[d^{(p;\text{s};\mathfrak{V})}_{ij}]_{\text{Vallet}} := -\frac{\partial}{\partial x_\ell}\left([\overline{p'u_i'}]^{(\text{s};\mathfrak{V})}_{\text{Vallet}}\delta_{j\ell} + [\overline{p'u_j'}]^{(\text{s};\mathfrak{V})}_{\text{Vallet}}\delta_{i\ell}\right) \qquad (4.23h)$$

$$[d^{(p;\text{s};w)}_{ij}]_{\text{Vallet}} := 0 \qquad (4.23i)$$

$$[d^{(p;\text{r};\mathfrak{V})}_{ij}]_{\text{Vallet}} := -\frac{\partial}{\partial x_\ell}\left([\overline{p'u_i'}]^{(\text{r};\mathfrak{V})}_{\text{Vallet}}\delta_{j\ell} + [\overline{p'u_j'}]^{(\text{r};\mathfrak{V})}_{\text{Vallet}}\delta_{i\ell}\right) \qquad (4.23j)$$

$$[d^{(p;\text{r};w)}_{ij}]_{\text{Vallet}} := 0 \qquad (4.23k)$$

---

† LSB: Lumley (1978) and Schwarz & Bradshaw (1994)

Re_{τ_w}	$\bar{M}_{\text{CL}}$	$N_x \times N_y \times N_z$	L_x	L_y	L_z	Δx^+	Δy^+_w	$N_{y^+\leq 10}$	Δy^+_{CL}	Δz^+	Δt^+	$t^+_{\text{OBS}_{\text{GF}}}$	$\Delta t^+_{s_{\text{GF}}}$
179	0.34	$193 \times 129 \times 169$	$4\pi\delta$	2δ	$\frac{4}{3}\pi\delta$	11.7	0.22	20	4.9	4.4	6.47×10^{-3}	1648	6.47×10^{-1}

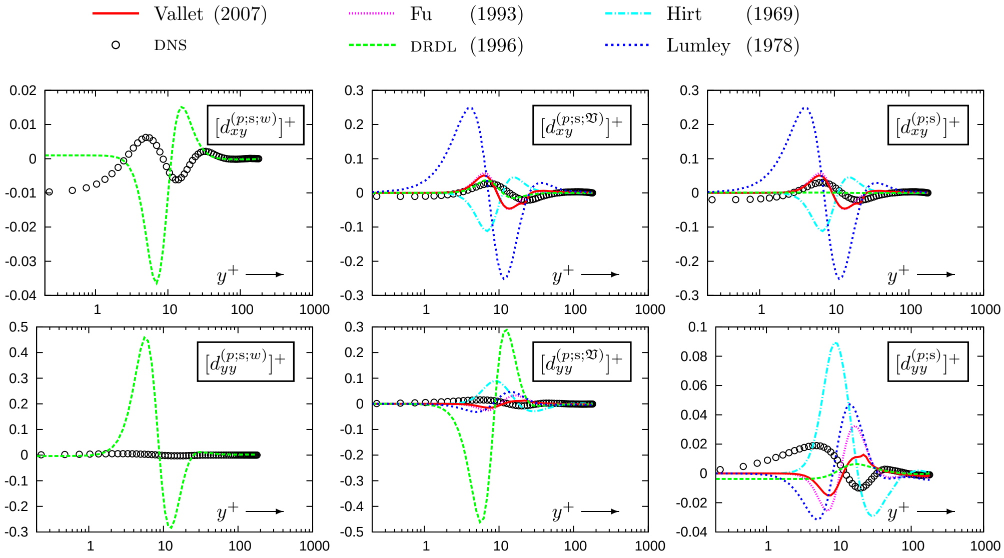

FIGURE 16. *A priori* comparison of various models (Hirt: Hirt 1969; Lumley: Lumley 1978; Fu: Fu 1993; DRDL: Demuren *et al.* 1996; Vallet: Vallet 2007) for the slow pressure diffusion $d_{ij}^{(p;\text{s})} = d_{ij}^{(p;\text{s};\mathfrak{V})} + d_{ij}^{(p;\text{s};w)}$ with present DNS results for the volume $d_{ij}^{(p;\text{s};\mathfrak{V})}$ and the wall-echo $d_{ij}^{(p;\text{s};w)}$ terms, in wall units, plotted against the nondimensional distance from the wall y^+ (in fully developed incompressible plane channel flow $d_{xx}^{(p)} = d_{yz}^{(p)} = d_{zz}^{(p)} = d_{zx}^{(p)}$).

4.5. A priori *assessment of typical models for* $d_{ij}^{(p)}$

With the exception of the proposal of Hirt (1969), all of the models for the slow part $d_{ij}^{(p;\text{s})}$ are based on the proposal of Lumley (1978) that pressure-transport $\overline{p'u'_i}$ is proportional to $-\overline{u'_i u'_m u'_m}$, *ie* to the transport of fluctuating turbulent kinetic energy. The TMC‡ *a priori* assessment (Fig. 16) of the proposal (4.19) of Lumley (1978), shows not only that the coefficient $c_{\text{Lumley}} = \frac{1}{5}$ (4.20*f*) is too high with reference to the DNS data for $d_{ij}^{(p;\text{s};\mathfrak{V})}$, but also that although the sign is correct for the shear component $d_{xy}^{(p;\text{s};\mathfrak{V})}$, it is incorrect for $d_{yy}^{(p;\text{s};\mathfrak{V})}$ (Fig. 16). A modification of the coefficient c_{Lumley} (4.20*f*) in (4.19), either using a smaller constant Straatman (1999) or a function (4.23*f*) of the flatness parameter A (Vallet 2007), can improve the predicted magnitude of $d_{ij}^{(p;\text{s};\mathfrak{V})}$ (*eg* the Vallet 2007 model in Fig. 16), but not the problem of sign. Hirt (1969) uses a different tensorial formulation (4.18*b*) resulting in the opposite sign for $d_{ij}^{(p;\text{s};\mathfrak{V})}$, compared to what is usually obtained from the relation (4.19) of Lumley (1978), but this does not solve the problem since for the model of Hirt (1969) the sign of $d_{yy}^{(p;\text{s};\mathfrak{V})}$ is correct but that of $d_{xy}^{(p;\text{s};\mathfrak{V})}$ is not (Fig. 16). The SMC closure of $\overline{p'_{(\text{s};\mathfrak{V})} u'_i}$ using a relation of the form (4.19), involves a model for the triple velocity correlations, which influences the final prediction. Fu (1993) uses the Daly & Harlow (1970) model for triple velocity correlations (4.21*b*, 4.21*f*) combined with the standard value of $c_{\text{Lumley}} = \frac{1}{5}$ (4.20*f*), and the underestimation of the y-gradients of the triple velocity correlations by the

---

‡ third-moment-closure using the DNS-computed triple velocity correlations $\overline{u'_i u'_j u'_k}$ in (4.19)

Re_{τ_w}	$\bar{M}_{\text{CL}}$	$N_x \times N_y \times N_z$	L_x	L_y	L_z	Δx^+	Δy_w^+	$N_{y^+\leq 10}$	Δy_{CL}^+	Δz^+	Δt^+	$t_{\text{OBS}_{\text{GF}}}^+$	$\Delta t_{s_{\text{GF}}}^+$
179	0.34	$193 \times 129 \times 169$	$4\pi\delta$	2δ	$\frac{4}{3}\pi\delta$	11.7	0.22	20	4.9	4.4	6.47×10^{-3}	1648	6.47×10^{-1}

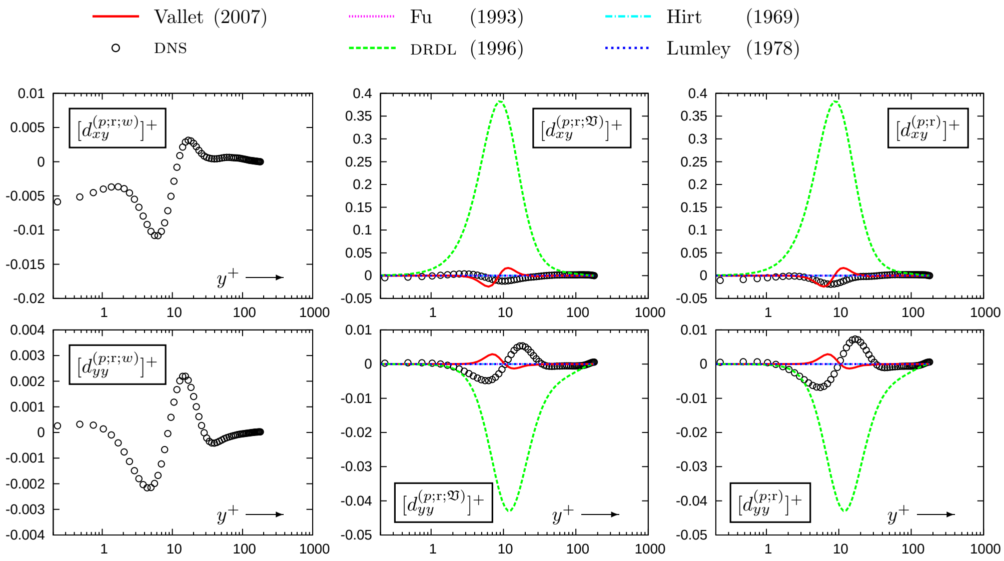

FIGURE 17. *A priori* comparison of various models (Hirt: Hirt 1969; Lumley: Lumley 1978; Fu: Fu 1993; DRDL: Demuren *et al.* 1996; Vallet: Vallet 2007) for the rapid pressure diffusion $d_{ij}^{(p;\text{r})} = d_{ij}^{(p;\text{r};\mathfrak{V})} + d_{ij}^{(p;\text{r};w)}$ with present DNS results for the volume $d_{ij}^{(p;\text{r};\mathfrak{V})}$ and the wall-echo $d_{ij}^{(p;\text{r};w)}$ terms, in wall units, plotted against the nondimensional distance from the wall y^+ (in fully developed incompressible plane channel flow $d_{xx}^{(p)} = d_{yz}^{(p)} = d_{zz}^{(p)} = d_{zx}^{(p)}$).

Re_{τ_w}	$\bar{M}_{\text{CL}}$	$N_x \times N_y \times N_z$	L_x	L_y	L_z	Δx^+	Δy_w^+	$N_{y^+\leq 10}$	Δy_{CL}^+	Δz^+	Δt^+	t_{OBS}^+	Δt_s^+
179	0.34	$193 \times 129 \times 169$	$4\pi\delta$	2δ	$\frac{4}{3}\pi\delta$	11.7	0.22	20	4.9	4.4	6.47×10^{-3}	2329	6.47×10^{-3}

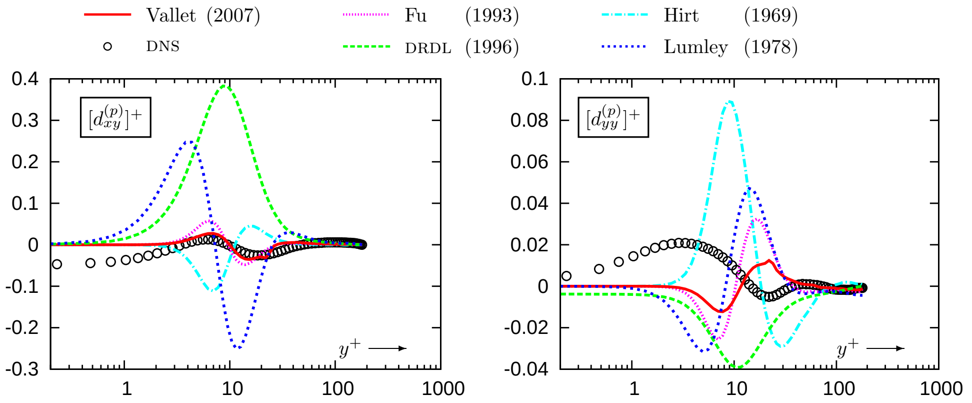

FIGURE 18. *A priori* comparison of various models (Hirt: Hirt 1969; Lumley: Lumley 1978; Fu: Fu 1993; DRDL: Demuren *et al.* 1996; Vallet: Vallet 2007) for the pressure diffusion $d_{ij}^{(p)} = d_{ij}^{(p;\mathfrak{V})} + d_{ij}^{(r;w)}$ with present DNS results, in wall units, plotted against the nondimensional distance from the wall y^+ (in fully developed incompressible plane channel flow $d_{xx}^{(p)} = d_{yz}^{(p)} = d_{zz}^{(p)} = d_{zx}^{(p)}$).

Daly & Harlow (1970) model yields a correct final level for $d_{ij}^{(p;\mathrm{s};\mathfrak{V})}$ (Fig. 16). On the other hand, Vallet (2007) uses the Lumley (1978) tensorial formulation for the slow part of the triple velocity correlations (4.23*a*) with the optimised coefficients of Schwarz & Bradshaw (1994), which yields slightly higher gradients for the triple velocity correlations, and recovers the correct level of $d_{ij}^{(p;\mathrm{s};\mathfrak{V})}$ (Fig. 16) by using a lower variable coefficient (4.23*f*) function of the flatness parameter A in (4.23*d*). Finally the model of Mellor & Herring (1973) for the triple velocity correlations combined with the standard model (4.19) of Lumley (1978), used for the slow volume part (4.22*a*–4.22*c*) of the DRDL (Demuren *et al.* 1996) model $[d_{ij}^{(p;\mathrm{s};\mathfrak{V})}]_{\mathrm{DRDL}}$ (4.22*f*), yields a very good prediction for the shear component $d_{xy}^{(p;\mathrm{s};\mathfrak{V})}$ but a very inaccurate one for the normal component $d_{yy}^{(p;\mathrm{s};\mathfrak{V})}$ (Fig. 16). The wall-echo term $[d_{ij}^{(p;\mathrm{s};w)}]_{\mathrm{DRDL}}$ (4.22*g*) added by the elliptic relaxation approach (4.22*j*–4.22*l*) in the DRDL (Demuren *et al.* 1996) model is designed to damp gradients. As a consequence, it adds a strong wall-echo term $d_{yy}^{(p;\mathrm{s};w)}$ to $d_{yy}^{(p;\mathrm{s};\mathfrak{V})}$ improving the global prediction of $d_{yy}^{(p;\mathrm{s})}$ (Fig. 16), but adds an equally strong wall-echo term $d_{xy}^{(p;\mathrm{s};w)}$ to the initially satisfactory volume term $d_{xy}^{(p;\mathrm{s};\mathfrak{V})}$ thus deteriorating the global prediction of $d_{xy}^{(p;\mathrm{s})}$ (Fig. 16).

Only two of the models (DRDL: Demuren *et al.* 1996; Vallet: Vallet 2007) include a closure for the rapid volume term $d_{ij}^{(p;\mathrm{r};\mathfrak{V})}$ (Fig. 17). The levels of $d_{ij}^{(p;\mathrm{r})}$ *a priori* predicted by the DRDL (Demuren *et al.* 1996) model (4.22*h*) are an order-of-magnitude too high (Fig. 17). The *a priori* assessment of the Vallet (2007) model (4.23*j*) gives reasonable magnitudes for $d_{ij}^{(p;\mathrm{r})}$, but the predicted normal component $d_{yy}^{(p;\mathrm{r})}$ has the wrong sign (Fig. 17).

A priori assessment of the global prediction of pressure diffusion $d_{ij}^{(p)}$ (Fig. 18) by the various models (§4.4) shows that the models of Vallet (2007) and Fu (1993) give the best prediction. The DRDL (Demuren *et al.* 1996) model is incorrectly dominated by its rapid part (Figs. 16–18) $d_{ij}^{(p;\mathrm{r})}$, which is responsible for the global unsatisfactory prediction (Fig. 16). The *a priori* assessment of the shear component $d_{xy}^{(p)}$ shows that the models of Vallet (2007) and Fu (1993) are quite satisfactory, except very near the wall ($y^+ \lessapprox 2$; Fig. 18). Notice nonetheless, that all of the models for ϕ_{xy} (Fig. 15) make the same error with the opposite sign in the near-wall region, so that the global prediction of $\Pi_{xy} \overset{(3.2)}{=} \phi_{xy} + d_{xy}^{(p)}$ is not affected by this discrepancy. On the contrary, the prediction of $d_{yy}^{(p)}$ (Fig. 18) is unsatisfactory, and although the models of Vallet (2007) and Fu (1993) are those having the smallest error, they yield, like all other models, the wrong sign for the normal component $d_{yy}^{(p)}$ (Fig. 18).

5. Conclusions

In the first part of the present paper (§2 and §3) we studied the influence of wall-blockage on turbulent pressure fluctuations p', in fully developed incompressible turbulent plane channel flow, using DNS (§2.1).

The instantaneous pressure fluctuations p' were separated (§2.2.1 and §2.2.2) into rapid, slow, ans Stokes terms ($p' = p'_{(\mathrm{r})} + p'_{(\mathrm{s})} + p'_{(\tau)}$) by solving the corresponding 1-D modified Helmholz equation (2.6) for each parallel-to-the-wall wavenumber, using the standard Green's function approach (*cf* Appendix) of Kim (1989). The new results in the present work concern the identification of the influence of wall-blockage (§2.2.3). To this end we define the quasi-homogeneous volume part of the slow and rapid fields ($p'_{(\mathrm{r};\mathfrak{V})}$ and $p'_{(\mathrm{s};\mathfrak{V})}$) as the solution of the corresponding 1-D modified Helmholz equation (2.6*a*), with the same source-terms but with different, freespace, boundary-conditions (boundedness at ∞), using the appropriate freespace Green's function (Tab. 2). The wall-echo fields are then identified as the difference of the complete and volume fields ($p'_{(\mathrm{r};w)} := p' - p'_{(\mathrm{r};\mathfrak{V})}$ and $p'_{(\mathrm{s};w)} := p' - p'_{(\mathrm{s};\mathfrak{V})}$).

The theoretical analysis (*cf* Appendix) of the Green's functions for the generic 1-D modified Helmholz equation (A 1) was applied (§2.2.4) to the determination of the error of the approximate method-of-images which replaces the exact boundary-conditions (2.6*b*) by using mirror images of the channel sources, one for each wall, demonstrating that the method-of-images is a high-wavenumber approximation. As long as the energy-containing wavenumbers of the source-terms are sufficiently high (equivalently the parallel-to-the-wall structure sizes $\ell_\kappa \lessapprox 4\delta$, δ being the channel halfheight) the method-of-images approximation is satisfactory, and in this case (§2.2.5) the interaction of wall-echo between upper and lower walls is negligible. When the relevant structure sizes are within this range ($\ell_\kappa \lessapprox 4\delta$), the wall-echo term, at the wall, is approximately equal (and of the same sign) as the corresponding volume term. These results are obtained by studying the Green's functions, and as such are independent of the particular distribution of the source-terms, depending only on the wavenumber.

This methodology for p'-splitting ($p' = p'_{(\mathrm{r};\mathfrak{V})} + p'_{(\mathrm{r};w)} + p'_{(\mathrm{s};\mathfrak{V})} + p'_{(\mathrm{s};w)} + p'_{(\tau)}$) was applied to DNS computations of low-Reynolds-number ($Re_{\tau_w} \approxeq 180$) fully developed plane channel flow (Tab. 1). The results for the rms-values of the 5 p'-fields verify, near the wall, the approximate equality of wall-echo and corresponding volume terms ($[p'_{(\mathrm{r};\mathfrak{V})}]_{\mathrm{rms}} \approxeq [p'_{(\mathrm{r};w)}]_{\mathrm{rms}}$ and $[p'_{(\mathrm{s};\mathfrak{V})}]_{\mathrm{rms}} \approxeq [p'_{(\mathrm{s};w)}]_{\mathrm{rms}}$ for $y^+ \lessapprox 3$). The rms-values of the wall-echo fields ($[p'_{(\mathrm{r};w)}]_{\mathrm{rms}}$ and $[p'_{(\mathrm{s};w)}]_{\mathrm{rms}}$) decay with increasing distance from the wall, always remaining much higher than the Stokes pressure ($[p'_{(\tau)}]_{\mathrm{rms}}$). The contribution of the 5 p'-fields to the correlations containing the fluctuating pressure, *viz* pressure diffusion $d_{ij}^{(p)}$ (§3.3), pressure-strain redistribution ϕ_{ij} (§3.4) and velocity/pressure-gradient $\Pi_{ij} = \phi_{ij} + d_{ij}^{(p)}$ (§3.5) shows that the approximate equality of wall-echo and corresponding volume terms, near the wall ($y^+ \lessapprox 3$), holds also for $d_{ij}^{(p)}$, ϕ_{ij} and Π_{ij}.†

Examination of the relative importance of each of the 5 p'-fields in the pressure-strain redistribution tensor ϕ_{ij} (§3.4) indicates, that for the ϕ_{xx} component the rapid volume term $\phi_{ij}^{(\mathrm{r};\mathfrak{V})}$ is the dominant contribution near the wall ($y^+ \lessapprox 10$), while the slow volume part $\phi_{ij}^{(\mathrm{s};\mathfrak{V})}$ is the dominant contribution in the buffer and outer regions ($y^+ \gtrapprox 20$). The opposite trend is observed for the ϕ_{zz} component, $\phi_{ij}^{(\mathrm{s};\mathfrak{V})}$ being the dominant contribution near the wall ($y^+ \lessapprox 10$) and $\phi_{ij}^{(\mathrm{r};\mathfrak{V})}$ being the dominant contribution in the buffer and outer regions ($y^+ \gtrapprox 20$). Finally, the Stokes term $\phi_{ij}^{(\tau)}$, which is generally small, is the dominant contribution to the shear component ϕ_{xy}, near the wall ($y^+ \lessapprox 8$), indicating that $p'_{(\tau)}$ is well-correlated with wall-shear. These results demonstrate that the relative importance of the rms-values of the 5 p'-fields does not determine the relative levels of the contribution of each field to $d_{ij}^{(p)}$ (§3.3), ϕ_{ij} (§3.4) and Π_{ij} (§3.5).

In the second part of the paper (§4) we use the DNS database generated in §3 for the *a priori* assessment of representative models for ϕ_{ij} and $d_{ij}^{(p)}$.

The models studied for the pressure-strain redistribution (§4.1) were chosen to be representative of modelling practices from the early developments (LRR: Launder *et al.* 1975;

---

† Notice that results using the approximate method-of-images should not be considered as a proof of this approximate equality, which is in-built in the method-of-images approximation (§2.2.5).

GL: Gibson & Launder 1978) through the more general quasi-homogeneous tensorial representation approaches (SSG: Speziale *et al.* 1991; SAYS: So *et al.* 1996) to more recent proposals (JEJK: Jakirlić *et al.* 2007), including a recent representative of the TCL family (S: Suga 2004). To provide a common representation of all these models we proposed (§4.2) a tensorial representation including a tensor $\boldsymbol{\eta}$ (4.15*a*), built as the deviator of the tensor product of the unit vector $\vec{e}_\eta$ (pointing in the dominant direction of turbulence inhomogeneity) by itself, along with the 3 generating tensors ($\mathbf{b}$, $\bar{\mathbf{S}}$ $\bar{\boldsymbol{\Omega}}$) used for the quasi-homogeneous case (Ristorcelli *et al.* 1995). The polynomial representation basis developed in the present work (§4.2) adds 14 new basis-tensors (4.16) to the 8 tensors (4.13) building the classical quasi-homogeneous basis. Furthermore, the rapid terms (containing mean velocity gradients) can be interpreted in terms of production by strain $P_{\bar{S}_{ij}}$ (4.3*i*) and production by rotation $P_{\bar{\Omega}_{ij}}$ (4.3*j*), whose difference is the tensor $D_{ij} := P_{\bar{S}_{ij}} - P_{\bar{\Omega}_{ij}}$ (4.3*h*, 4.3*c*) appearing in the original formulation of several models (LRR: Launder *et al.* 1975; SAYS: So *et al.* 1996; S: Suga 2004).

The *a priori* assessment of the different models for ϕ_{ij} (§4.3) indicates that the JEJK (Jakirlić *et al.* 2007) model gives the best overall performance, followed by the S (Suga 2004) model. The design philosophy of these two models is fundamentally different. The JEJK (Jakirlić *et al.* 2007) model (Tab. 3) uses few of the representation basis tensors (based on the ideas of isotropisation-of-production and of both slow and rapid wall-echo terms with inhomogeneity-directionality information) with coefficients which are carefully optimised functions of the invariants (both of Reynolds-stress anisotropy b_{ij} and of dissipation-rate anisotropy $b_{\varepsilon_{ij}}$), demonstrating how such relatively compact models can be highly successful. On the other hand, the S (Suga 2004) model of the TCL-family, is built using a much greater number of reducible tensors, with an effort to have few non constant coefficients. Nonetheless, when projected onto the irreducible polynomial representation basis (Tab. 3) all the coefficients are functions of the invariants (in the present case of Reynolds-stress anisotropy b_{ij} only). Finally the LRR (Launder *et al.* 1975), GL (Gibson & Launder 1978), and SSG (Speziale *et al.* 1991) models include the anisotropy of dissipation, *ie* model $\phi_{ij} - 2\rho\varepsilon b_{\varepsilon_{ij}}$ (Lumley 1978).

There exist relatively fewer proposals for pressure diffusion $d_{ij}^{(p)}$ (§4.4). The *a priori* TMC assessment of the weakly-inhomogeneous proposal (4.19) of Lumley (1978), using the DNS-computed triple-velocity correlations shows that this closure cannot correctly model both $d_{xy}^{(p)}$ and $d_{yy}^{(p)}$, in wall turbulence, the later normal component $d_{yy}^{(p)}$ being predicted with the wrong sign. This issue notwithstanding, the models of Vallet (2007) and Fu (1993) give the best prediction of the DNS data (§4.5). Since both are based on some form of the proposal (4.19) of Lumley (1978), they require improvement by the addition of some other term in the representation of either $\overline{p'u'_i}$ or $d_{ij}^{(p)}$ directly.

The *a priori* assessment shows that all of the models for ϕ_{ij} (§4.3) and for $d_{ij}^{(p)}$ (§4.5) are unsatisfactory in the very-near-wall region ($y^+ \lessapprox 3$) where they all return nearly 0-values, contrary to the DNS data. This problem does not necessarily affect the global RSM model performance, since in this region ($y^+ \lessapprox 3$) ϕ_{ij} and $d_{ij}^{(p)}$ cancel one another, so that the prediction of $\Pi_{ij} = \phi_{ij} + d_{ij}^{(p)}$ (3.2), which is the term appearing in Reynolds-stress transport (3.1), is not necessarily unsatisfactory, with the exception of Π_{zz} which goes to 0 much slower than the other components. Away from the wall, where ϕ_{ij} and $d_{ij}^{(p)}$ do not cancel one another, there are reasons to believe that pressure diffusion $d_{ij}^{(p)}$ plays an important role in the prediction of shear layer entrainment and should be modelled separately (Demuren *et al.* 1996; Vallet 2007).

Future work will concentrate in extending the wall-echo DNS database to higher Reynolds numbers, and in using the data to improve near-wall modelling of the pressure correlations.

The authors are listed alphabetically. We are particularly grateful to Prof. B.A. Younis for many enlightening discussions, and for hosting one of the authors (CL) for one year at the University of California at Davis. Computations were performed using HPC resources from GENCI–IDRIS (Grant 2010–022139). Sourcefiles of the code used and computer routines for the splittng are available as par of the freeware project aerodynamics (Gerolymos & Vallet 2009, `http://sourceforge.net/projects/aerodynamics`). Tabulated data are available at `http://www.aerodynamics.fr/DNS_database/CT_chnnl`. The present work was partly supported by the EU-funded research project ProBand, (STREP–FP6 AST4–CT–2005–012222).

Appendix. Green's functions

As discussed in §2.2, we have to solve the generic modified Helmholtz (Cheng *et al.* 2006) equation

$$\frac{d^2q(y;\kappa)}{dy^2} - \kappa^2 q(y;\kappa) = Q(y;\kappa) \qquad y \in (L_-, L_+) \tag{A 1}$$

with associated boundary-conditions at $y \in \{L_-, L_+\}$, for the complex-valued function $q : \mathbb{R} \longrightarrow \mathbb{C}$, $Q(y)$ being a given complex-valued function $Q : \mathbb{R} \longrightarrow \mathbb{C}$, and $\kappa \in \mathbb{R}_{\geq 0}$. Notice that there is no loss of generality in assuming $\kappa \in \mathbb{R}_{\geq 0}$ because (A 1) depends on κ^2 and is therefore independent of the sign of κ. The general method of solution (Bender & Orszag 1978) of the linear ODE (A 1) is based on the determination of the appropriate Green's function $G(y, Y; \kappa)$, solution of

$$\frac{\partial^2 G(y,Y;\kappa)}{\partial y^2} - \kappa^2 G(y,Y;\kappa) = \delta(y - Y) \tag{A 2a}$$

$$\lim_{\epsilon \to 0^+} \left[\frac{\partial G}{\partial y}(Y+\epsilon, Y; \kappa) - \frac{\partial G}{\partial y}(Y-\epsilon, Y; \kappa) \right] = 1 \tag{A 2b}$$

$$G(y,Y;\kappa) \in C^0(L_-, L_+) \tag{A 2c}$$

$$G(y,Y;\kappa) \in C^1(L_-, L_+) \setminus \{Y\} \tag{A 2d}$$

so that

$$q(y;\kappa) := \int_{L_-}^{L_+} G(y,Y;\kappa) Q(Y;\kappa) dY \tag{A 3}$$

satisfies (A 1) because of (A 2). The Green's function satisfies the symmetry (reciprocity) condition

$$G(y,Y;\kappa) = G(y,Y;\kappa) \qquad \forall y, Y \in (L_-, L_+) \qquad \forall \kappa \in \mathbb{R}_{\geq 0} \tag{A 4}$$

because the modified Helmholz operator $[d^2_{yy}(\cdot) - \kappa^2(\cdot)]$ is a self-adjoint linear differential operator (Ince 1926; Courant & Hilbert 1953). As shown in Bender & Orszag (1978), the general solution of (A 2) is

$$G(y,Y;\kappa)=\begin{cases} A_1(Y;\kappa)q_1(y;\kappa)+A_2(Y;\kappa)q_2(y;\kappa) & y<Y \\ \left(A_1(Y;\kappa)-\dfrac{q_2(Y;\kappa)}{[W(q_1,q_2)](Y;\kappa)}\right)q_1(y;\kappa) & \\ +\left(A_2(Y;\kappa)+\dfrac{q_1(Y;\kappa)}{[W(q_1,q_2)](Y;\kappa)}\right)q_2(y;\kappa) & y>Y \end{cases} \tag{A 5}$$

where $q_1(y;\kappa)$ and $q_2(y;\kappa)$ are 2 linearly independent solutions of the homogeneous equation $q''(y)-\kappa q(y)=0$,

$$[W(q_1,q_2)](y;\kappa):=\det\begin{bmatrix} q_1(y;\kappa) & q_2(y;\kappa) \\ q_1'(y;\kappa) & q_2'(y;\kappa)\end{bmatrix}\neq 0 \tag{A 6}$$

is the Wronskian ($\cdot'$ in (A 6) denotes differentiation by y, κ being a parameter), which is $\neq 0$ iff the 2 solutions are linearly independent. The functions $A_1(Y;\kappa)$ and $A_2(Y;\kappa)$ are determined by the boundary-conditions. The cases $\kappa\neq 0$ and $\kappa=0$ are fundamentally different, not only because the 2 linearly independent solutions of the homogeneous equation $q''(y)-\kappa q(y)=0$ differ, but principally because $\kappa=0$ is a characteristic number (eigenvalue) of (A 1), *viz* $q''(y)-\kappa q(y)\overset{\kappa=0}{=}q''(y)=0$ with homogeneous Neumann boundary-conditions admits the constant function as an eigensolution (Ince 1926; Courant & Hilbert 1953).

A.1. $\kappa\neq 0$

When $\kappa\neq 0$ we have

$$q_1(y;\kappa\neq 0)=\mathrm{e}^{+\kappa y} \tag{A 7a}$$

$$q_2(y;\kappa\neq 0)=\mathrm{e}^{-\kappa y} \tag{A 7b}$$

$$[W(q_1,q_2)](y;\kappa\neq 0)=\det\begin{bmatrix} \mathrm{e}^{+\kappa y} & \mathrm{e}^{-\kappa y} \\ +\kappa\mathrm{e}^{+\kappa y} & -\kappa\mathrm{e}^{-\kappa y}\end{bmatrix}=-2\kappa\neq 0 \tag{A 7c}$$

so that solution (A 5) reads

$$G(y,Y;\kappa\neq 0)=\begin{cases} A_1(Y;\kappa)\mathrm{e}^{+\kappa y}+A_2(Y;\kappa)\mathrm{e}^{-\kappa y} & y<Y \\ A_1(Y;\kappa)\mathrm{e}^{+\kappa y}+A_2(Y;\kappa)\mathrm{e}^{-\kappa y} & \\ \qquad +\dfrac{1}{\kappa}\sinh[\kappa(y-Y)] & y>Y\end{cases} \tag{A 8}$$

The functions $A_1(Y;\kappa)$ and $A_2(Y;\kappa)$ are determined so as to satisfy the boundary-conditions.

A.1.1. $G_{\mathrm{Kim}}(y,Y;\kappa\neq 0)$

Kim (1989) solves for the homogeneous Neumann boundary-conditions (2.6*b*)

$$\frac{\partial G_{\mathrm{Kim}}}{\partial y}\left(y=\pm\frac{L_y}{2},Y;\kappa\right)=0 \overset{\text{(A 3)}}{\Longleftrightarrow} \frac{\partial q_{\mathrm{Kim}}}{\partial y}\left(y=\pm\frac{L_y}{2};\kappa\right)=0 \tag{A 9a}$$

Straightforward calculations yield the functions $A_1(Y;\kappa)$ and $A_2(Y;\kappa)$ in (A 8) which satisfy (A 9*a*), giving

$$G_{\mathrm{Kim}}(y,Y;\kappa\neq 0)=-\frac{\cosh[\kappa(L_y-|y-Y|)]+\cosh[\kappa(y+Y)]}{2\kappa\sinh\kappa L_y} \tag{A 9b}$$

This if-less expression, which highlights the symmetry condition (A 4), is equivalent to the form in Kim (1989, (8), p. 440), written here using dimensional variables

$$G_{\text{Kim}}(y,Y;\kappa\neq 0)=\begin{cases} -\dfrac{\cosh[\kappa(\frac{1}{2}L_y-Y)]\cosh[\kappa(\frac{1}{2}L_y+y)]}{\kappa\sinh\kappa L_y} & y<Y \\[2ex] -\dfrac{\cosh[\kappa(\frac{1}{2}L_y-y)]\cosh[\kappa(\frac{1}{2}L_y+Y)]}{\kappa\sinh\kappa L_y} & y>Y \end{cases} \tag{A 9c}$$

because using well-known identities† (Harris & Stocker 1998, p. 249)

$$\begin{aligned} 2\cosh[\kappa(\tfrac{1}{2}L_y-Y)]\cosh[\kappa(\tfrac{1}{2}L_y+y)] &= \cosh[\kappa(L_y-Y+y)]+\cosh[\kappa(-Y-y)] \\ &= \cosh[\kappa(L_y-|y-Y|)]+\cosh[\kappa(y+Y)] \\ &\quad \forall y<Y \qquad \text{(A 9}d\text{)} \\ 2\cosh[\kappa(\tfrac{1}{2}L_y-y)]\cosh[\kappa(\tfrac{1}{2}L_y+Y)] &= \cosh[\kappa(L_y-y+Y)]+\cosh[\kappa(-y-Y)] \\ &= \cosh[\kappa(L_y-|y-Y|)]+\cosh[\kappa(y+Y)] \\ &\quad \forall y>Y \qquad \text{(A 9}e\text{)} \end{aligned}$$

A.1.2. *Accommodating the boundary-conditions ($\kappa\neq 0$)*

To take into account normal gradients $d_y q(y=\pm\frac{1}{2}L_y;\kappa\neq 0)=B_\pm(\kappa\neq 0)\neq 0$ at the channel walls, corresponding to the Stokes pressure (2.3, 2.6), Chang *et al.* (1999) superpose a boundary-condition q_{BC} term to the solution of Kim (1989)

$$q(y;\kappa\neq 0,B_\pm)=\int_{L_-}^{L_+}G_{\text{Kim}}(y,Y;\kappa\neq 0)Q(Y;\kappa\neq 0)dY+q_{\text{BC}}(y;\kappa\neq 0,B_\pm) \tag{A 10a}$$

$$\frac{d^2q(y;\kappa\neq 0,B_\pm)}{dy^2}-\kappa^2q(y;\kappa\neq 0,B_\pm)=Q(y;\kappa\neq 0) \qquad y\in(-\tfrac{1}{2}L_y,+\tfrac{1}{2}L_y) \tag{A 10b}$$

$$\frac{d^2q_{\text{BC}}(y;\kappa\neq 0,B_\pm)}{dy^2}-\kappa^2q_{\text{BC}}(y;\kappa\neq 0,B_\pm)=0 \qquad y\in(-\tfrac{1}{2}L_y,+\tfrac{1}{2}L_y) \tag{A 10c}$$

$$\frac{dq}{dy}(y=\pm\tfrac{1}{2}L_y;\kappa\neq 0,B_\pm)\overset{\text{(A 9}a\text{)}}{=}\frac{dq_{\text{BC}}}{dy}(y=\pm\tfrac{1}{2}L_y;\kappa\neq 0,B_\pm)=B_\pm(\kappa\neq 0) \tag{A 10d}$$

By (A 3, A 9), the superposition (A 10*a*) is the solution to (A 10*b*), with boundary-conditions (A 10*d*). The solution of (A 10*c*) with boundary-conditions (A 10*d*) is readily obtained by direct integration (Chang *et al.* 1999), and reads

$$q_{\text{BC}}(y;\kappa\neq 0,B_\pm)=\frac{B_+\cosh[\kappa(\frac{1}{2}L_y+y)]-B_-\cosh[\kappa(\frac{1}{2}L_y-y)]}{\kappa\sinh\kappa L_y} \tag{A 11}$$

A.1.3. *Freespace Green's function $G_{\mathfrak{V}}(y,Y;\kappa\neq 0)$*

The freespace Green's function is directly obtained from the general solution (A 8) by requiring that the solution should tend to 0 as $y\to\pm\infty$, which is equivalent to

$$\lim_{y\to\pm\infty}q_{\mathfrak{V}}(y;\kappa\neq 0)=0 \overset{\text{(A 3)}}{\iff} \lim_{y\to\pm\infty}G_{\mathfrak{V}}(y,Y;\kappa\neq 0)=0 \qquad \forall Y\in\mathbb{R}\setminus\{y\} \tag{A 12}$$

Using (A 12) to determine the functions $A_1(Y;\kappa)$ and $A_2(Y;\kappa)$ in (A 8) readily gives

$$G_{\mathfrak{V}}(y,Y;\kappa\neq 0)=-\frac{\mathrm{e}^{-\kappa|y-Y|}}{2\kappa} \tag{A 13}$$

---

† $\cosh(a+b)=\cosh a\cosh b+\sinh a\sinh b \qquad \cosh(a-b)=\cosh a\cosh b-\sinh a\sinh b$

A.1.4. *Upper/lower wall Green's functions* $G_\pm(y,Y;\kappa\neq 0)$

These Green's functions correspond to the problems where the domain of interest is $(-\infty,\frac{1}{2}L_y)$ (isolated upper-wall influence; G_+) or $(-\frac{1}{2}L_y,+\infty)$ (isolated lower-wall influence; G_-), *ie* they are halfspace problems ($\pm y \in (-\infty,\frac{1}{2}L_y)$). For each of these problems only one of the walls is present. The associated boundary-conditions are 0-gradient at the wall of the problem, and bounded influence at the infinity of the problem, *ie* in terms of Green's functions

$$G_+(y,Y;\kappa\neq 0) \text{ satisfies (A 2)} \Longleftrightarrow \text{(A 3)} \tag{A 14a}$$

$$\frac{\partial G_+}{\partial y}(y=+\tfrac{1}{2}L_y,Y;\kappa\neq 0)=0 \tag{A 14b}$$

$$\lim_{y\to-\infty} G_+(y,Y;\kappa\neq 0)=0 \quad \forall Y\in\mathbb{R}\setminus\{y\} \tag{A 14c}$$

to study the virtual influence of the upper wall, and

$$G_-(y,Y;\kappa\neq 0) \text{ satisfies (A 2)} \Longleftrightarrow \text{(A 3)} \tag{A 15a}$$

$$\frac{\partial G_-}{\partial y}(y=-\tfrac{1}{2}L_y,Y;\kappa\neq 0)=0 \tag{A 15b}$$

$$\lim_{y\to+\infty} G_-(y,Y;\kappa\neq 0)=0 \quad \forall Y\in\mathbb{R}\setminus\{y\} \tag{A 15c}$$

to study the virtual influence of the lower wall. By (A 3), boundary-conditions (A 14b, A 15b) imply 0-gradient at the wall of the problem (upper for G_+ and lower for G_-). Boundary-conditions (A 14c, A 15c) ensure boundedness at infinity for the halfspace corresponding to each problem. Straightforward computation of the functions $A_1(Y;\kappa)$ and $A_2(Y;\kappa)$ in (A 8) yields

$$G_-(y,Y;\kappa\neq 0)=-\frac{\mathrm{e}^{-\kappa|y-Y|}}{2\kappa}-\frac{\mathrm{e}^{-\kappa(L_y+y+Y)}}{2\kappa} \qquad y,Y\in[-\tfrac{1}{2}L_y,+\infty) \tag{A 16a}$$

$$G_+(y,Y;\kappa\neq 0)=-\frac{\mathrm{e}^{-\kappa|y-Y|}}{2\kappa}-\frac{\mathrm{e}^{-\kappa(L_y-y-Y)}}{2\kappa} \qquad y,Y\in(-\infty,+\tfrac{1}{2}L_y] \tag{A 16b}$$

which by (A 13) reads

$$G_-(y,Y;\kappa\neq 0)=G_{\mathfrak{V}}(y,Y;\kappa\neq 0)-\frac{\mathrm{e}^{-\kappa(L_y+y+Y)}}{2\kappa} \qquad y,Y\in[-\tfrac{1}{2}L_y,+\infty) \tag{A 17a}$$

$$G_+(y,Y;\kappa\neq 0)=G_{\mathfrak{V}}(y,Y;\kappa\neq 0)-\frac{\mathrm{e}^{-\kappa(L_y-y-Y)}}{2\kappa} \qquad y,Y\in(-\infty,+\tfrac{1}{2}L_y] \tag{A 17b}$$

ie the presence of a single wall in any of the 2 halfspace problems induces an additive correction to the freespace Green's function, the wall-echo $G_{w_\pm}(y,Y;\kappa\neq 0)$

$$G_{w_\pm}(y,Y;\kappa\neq 0):=G_\pm(y,Y;\kappa\neq 0)-G_{\mathfrak{V}}(y,Y;\kappa\neq 0) \tag{A 18}$$

A.1.5. *Accommodating the boundary-conditions for the halfspace problems ($\kappa\neq 0$)*

To take into account normal gradients $d_yq(y=\pm\frac{1}{2}L_y;\kappa)=B_\pm(\kappa)\neq 0$ at the wall for each of the halfspace problems of §A.1.4 we may proceed exactly as in §A.1.2, by superposing a boundary-condition $q_{\text{BC}_\pm}$ term to the corresponding solution (A 15) with

0-gradient condition, *viz*

$$q(y;\kappa\neq 0,B_-)=\int_{L_-}^{L_+}G_-(y,Y;\kappa\neq 0)Q(Y;\kappa\neq 0)dY+q_{\text{BC}_-}(y;\kappa\neq 0,B_-) \tag{A 19a}$$

$$\frac{d^2q(y;\kappa\neq 0,B_-)}{dy^2}-\kappa^2q(y;\kappa\neq 0,B_-)=Q(y;\kappa\neq 0)\qquad y\in(-\tfrac{1}{2}L_y,+\infty) \tag{A 19b}$$

$$\frac{d^2q_{\text{BC}_-}(y;\kappa\neq 0,B_-)}{dy^2}-\kappa^2q_{\text{BC}_-}(y;\kappa,B_-)=0\qquad y\in(-\tfrac{1}{2}L_y,+\infty) \tag{A 19c}$$

$$\frac{dq}{dy}(y=-\tfrac{1}{2}L_y;\kappa\neq 0,B_-)\overset{(\text{A }15b)}{=}\frac{dq_{\text{BC}_-}}{dy}(y=-\tfrac{1}{2}L_y;\kappa\neq 0,B_-)=B_-(\kappa\neq 0) \tag{A 19d}$$

$$\lim_{y\to+\infty}q_{\text{BC}_-}(y;\kappa\neq 0,B_-)=0 \tag{A 19e}$$

to study the virtual influence of the lower wall boundary-condition on the solution, and

$$q(y;\kappa\neq 0,B_+)=\int_{L_-}^{L_+}G_+(y,Y;\kappa\neq 0)Q(Y;\kappa\neq 0)dY+q_{\text{BC}_+}(y;\kappa\neq 0,B_+) \tag{A 20a}$$

$$\frac{d^2q(y;\kappa\neq 0,B_+)}{dy^2}-\kappa^2q(y;\kappa\neq 0,B_+)=Q(y;\kappa\neq 0)\qquad y\in(-\infty,+\tfrac{1}{2}L_y) \tag{A 20b}$$

$$\frac{d^2q_{\text{BC}_+}(y;\kappa\neq 0,B_+)}{dy^2}-\kappa^2q_{\text{BC}_+}(y;\kappa\neq 0,B_+)=0\qquad y\in(-\infty,+\tfrac{1}{2}L_y) \tag{A 20c}$$

$$\frac{dq}{dy}(y=+\tfrac{1}{2}L_y;\kappa\neq 0,B_+)\overset{(\text{A }14b)}{=}\frac{dq_{\text{BC}_+}}{dy}(y=+\tfrac{1}{2}L_y;\kappa\neq 0,B_+)=B_+(\kappa\neq 0) \tag{A 20d}$$

$$\lim_{y\to-\infty}q_{\text{BC}_+}(y;\kappa\neq 0,B_+)=0 \tag{A 20e}$$

to study the virtual influence of the upper wall boundary-condition on the solution. By (A 15), the superposition (A 19*a*) is the solution to (A 19*b*), with boundary-conditions (A 19*d*, A 19*e*). By (A 14), the superposition (A 20*a*) is the solution to (A 20*b*), with boundary-conditions (A 20*d*, A 20*e*). Straightforward computation yields

$$q_{\text{BC}_\pm}(y;\kappa\neq 0,B_\pm)=\pm\frac{B_\pm}{\kappa}\mathrm{e}^{-\kappa(\frac{1}{2}L_y\mp y)} \tag{A 21}$$

A.2. $\kappa=0$

When $\kappa=0$ (A 1) becomes a Poisson equation (Katz & Plotkin 1991)

$$\frac{d^2q(y;\kappa=0)}{dy^2}=Q(y;\kappa=0)\qquad y\in(-\tfrac{1}{2}L_y,\tfrac{1}{2}L_y) \tag{A 22}$$

The limits as $\kappa\to 0$ of the solutions obtained in §A.1 for $\kappa\neq 0$ are all singular, as can be easily verified by straightforward computation, contrary to the case of the same problem with Dirichlet boundary-conditions (Zauderer 2006). This is related to the existence of solutions of (A 22) with Neumann boundary-conditions at $y=\pm\frac{1}{2}L_y$, because integrating (A 22) yields

$$\frac{dq}{dy}(+\tfrac{1}{2}L_y;\kappa=0)-\frac{dq}{dy}(-\tfrac{1}{2}L_y;\kappa=0)=\int_{-\frac{1}{2}L_y}^{+\frac{1}{2}L_y}Q(Y;\kappa=0)dY \tag{A 23}$$

implying that (A 22) with gradient boundary-conditions $q'(\pm\frac{1}{2}L_y,\kappa=0)=B_\pm$ can only be solved iff the compatibility condition (A 23) is satisfied by the integral of the source-term and the boundary-conditions.

In the particular case of homogeneous Neumann boundary-conditions $B_\pm = 0$, which is the most important since $B_\pm \neq 0$ is only concerned with Stokes pressure (2.3, 2.6), the homogeneous equivalent of equation (A 22), $q''(y, \kappa = 0) = 0$, admits any constant function as solution, *ie* any constant function is an eigenfunction (Ince 1926; Courant & Hilbert 1953; Myint-U & Debnath 2007) of the homogeneous equivalent of (A 22), $q''(y, \kappa = 0) = 0$, with boundary-conditions $q'(\pm\frac{1}{2}L_y, \kappa = 0) = 0$, and $\kappa = 0$ is a characteristic number of the homogeneous equivalent of (A 1), $q''(y, \kappa) - \kappa^2 q(y, \kappa) = 0$ with boundary-conditions $q'(\pm\frac{1}{2}L_y, \kappa) = 0$. Therefore a solution only exists provided the corresponding compatibility relation (Ince 1926; Courant & Hilbert 1953) holds, *ie* the integral in (A 23) is equal to 0. This is analogous to the 3-D compatibility relation for the Poisson equation with Neumann boundary-conditions (Ockendon *et al.* 2003; Zauderer 2006).

A.2.1. $G_{\text{Kim}}(y, Y; \kappa = 0)$

In this case (2.3*b*, 2.6*b*) 0-gradient boundary-conditions apply on both walls ($y = \pm\frac{1}{2}L_y$). Assuming that the compatibility relation

$$\int_{-\frac{1}{2}L_y}^{+\frac{1}{2}L_y} Q(Y; \kappa = 0) dY = 0 \tag{A 24}$$

holds, there are 2 different ways for constructing a modified Green's function (Courant & Hilbert 1953; Zauderer 2006) for solving (A 22) with homogeneous Neumann boundary-conditions. The first method described in Courant & Hilbert (1953) makes explicit use of the eigensolution of (A 22) in a modified definition of the problem (A 2) for calculating the modified Green's function which satisfies the boundary-conditions, but has also to modify (A 3). The second method (Zauderer 2006) which leads to the Green's function used by Kim (1989) uses the standard definition of the Green's function (A 2) along with the standard integral solution (A 3). In this latter case however the boundary-conditions are not included in the solution but are obtained because of the compatibility relation (A 24).

Hence assuming that the compatibility relation (A 24) holds, so that (A 9*a*) for $\kappa = 0$ may be satisfied, the Green's function corresponding to (A 22) satisfies

$$\frac{\partial^2 G_{\text{Kim}}(y, Y; \kappa = 0)}{\partial y^2} = \delta(y - Y) \tag{A 25a}$$

$$\lim_{\epsilon \to 0^+} \left[\frac{\partial G_{\text{Kim}}}{\partial y}(Y + \epsilon, Y; \kappa = 0) - \frac{\partial G_{\text{Kim}}}{\partial y}(Y - \epsilon, Y; \kappa = 0) \right] = 1 \tag{A 25b}$$

$$G_{\text{Kim}}(y, Y; \kappa = 0) \in C^0(-\tfrac{1}{2}L_y, +\tfrac{1}{2}L_y) \tag{A 25c}$$

$$G_{\text{Kim}}(y, Y; \kappa) \in C^1(-\tfrac{1}{2}L_y, +\tfrac{1}{2}L_y) \setminus \{Y\} \tag{A 25d}$$

It is therefore made up by 2 straight lines joined together at Y, since by (A 25*a*) $\partial^2_{yy} G(y, Y; \kappa = 0) = 0 \ \forall y \neq Y$. If we further admit that $G_{\text{Kim}}(y, Y; \kappa = 0) = G_{\text{Kim}}(Y, y; \kappa = 0)$ (A 4), as expected because of the self-adjointedness of the the operator $[d^2_{yy}(\cdot)]$ (Ince 1926; Courant & Hilbert 1953), we must have (Katz & Plotkin 1991) $G_{\text{Kim}}(y, Y; \kappa = 0) = G_{\text{Kim}}(|y - Y|; \kappa = 0)$ so that

$$G_{\text{Kim}}(y, Y; \kappa = 0) = \frac{|y - Y|}{2} + c \tag{A 26}$$

The factor $\frac{1}{2}$ is required to satisfy (A 25*b*), and $c \in \mathbb{R}$ is a constant. The value of c has no influence whatsoever on the solution (A 3) because of the compatibility condition (A 24).† The simplest choice $c = 0$ corresponding to the reasonable situation $G_{\mathrm{Kim}}(y, y; \kappa = 0) = 0$ is made

$$G_{\mathrm{Kim}}(y, Y; \kappa = 0) = \frac{|y - Y|}{2} \tag{A 27}$$

and we have

$$\begin{aligned} \frac{dq_{\mathrm{Kim}}}{dy}(\pm\tfrac{1}{2}L_y; \kappa = 0) &\overset{\text{(A 3)}}{=} \int_{-\frac{1}{2}L_y}^{+\frac{1}{2}L_y} \frac{\partial G_{\mathrm{Kim}}}{\partial y}(y, Y; \kappa = 0)\, Q(Y; \kappa = 0) dY \\ &\overset{\text{(A 27)}}{=} \pm\tfrac{1}{2} \int_{-\frac{1}{2}L_y}^{+\frac{1}{2}L_y} Q(Y; \kappa = 0) dY \overset{\text{(A 24)}}{=} 0 \end{aligned} \tag{A 28}$$

Notice that in this case it is the compatibility relation (A 24), and not the Green's function alone which is responsible for satisfying the boundary-conditions.

A.2.2. *Accommodating the boundary-conditions ($\kappa = 0$)*

Finally, the solution of the boundary-conditions problem (required for $p'_{(\tau)}$) can be obtained directly by integrating

$$\frac{d^2 q_{\mathrm{BC}}(y; \kappa = 0, B_+, B_-)}{dy^2} = 0 \qquad y \in (-\tfrac{1}{2}L_y, +\tfrac{1}{2}L_y) \tag{A 29a}$$

$$\frac{dq_{\mathrm{BC}}}{dy}(y = \pm\tfrac{1}{2}L_y; \kappa = 0, B_+, B_-) = B_\pm(\kappa = 0) \tag{A 29b}$$

The solution exists iff

$$B_-(\kappa = 0) = B_+(\kappa = 0) \tag{A 30}$$

and is obviously a straight line, defined up to an additive constant

$$q_{\mathrm{BC}}(y; \kappa = 0, B_-, B_+) = \tfrac{1}{2}B_- y + \tfrac{1}{2}B_+ y + q_{\mathrm{BC}_0} \tag{A 31}$$

where by (A 31) $q_{\mathrm{BC}}(y = 0; \kappa = 0) = q_{\mathrm{BC}_0}$ is the solution at centerline.

A.2.3. *Freespace Green's function $G_{\mathfrak{V}}(y, Y; \kappa = 0)$*

The solution for the freespace Green's function $G_{\mathfrak{V}}(y, Y; \kappa = 0)$ is obtained exactly in the same way as for $G_{\mathrm{Kim}}(y, Y; \kappa = 0)$ (§A.2.1), yielding by (A 27)

$$G_{\mathfrak{V}}(y, Y; \kappa = 0) = G_{\mathrm{Kim}}(y, Y; \kappa = 0) = \frac{|y - Y|}{2} \tag{A 32}$$

Again, the sources $Q(y; \kappa = 0)$ must satisfy the compatibility condition (A 24) to ensure boundedness as $|y| \to \infty$

$$\begin{aligned} &\lim_{|y| \to \infty} \int_{-\frac{1}{2}L_y}^{+\frac{1}{2}L_y} G_{\mathfrak{V}}(y, Y \kappa = 0)\, Q(Y; \kappa = 0) dY \overset{\text{(A 32)}}{=} \\ &\lim_{|y| \to \infty} \left\{ \left(\int_{-\frac{1}{2}L_y}^{+\frac{1}{2}L_y} Q(Y; \kappa = 0) dY \right) \frac{|y|}{2} \right\} \overset{\text{(A 24)}}{=} 0 \quad \forall Y \in \mathbb{R} \setminus \{y\} \end{aligned} \tag{A 33}$$

---

† $\displaystyle\int_{-\frac{1}{2}L_y}^{+\frac{1}{2}L_y} \left(\frac{|y - Y|}{2} + c \right) Q(Y; \kappa = 0) dY = \int_{-\frac{1}{2}L_y}^{+\frac{1}{2}L_y} \frac{|y - Y|}{2} Q(Y; \kappa = 0) dY + c \int_{-\frac{1}{2}L_y}^{+\frac{1}{2}L_y} Q(Y; \kappa = 0) dY$ $\displaystyle\overset{\text{(A 24)}}{=} \int_{-\frac{1}{2}L_y}^{+\frac{1}{2}L_y} \frac{|y - Y|}{2} Q(Y; \kappa = 0) dY$

which is 0 iff (A 24) holds.

A.2.4. *Upper/lower wall Green's functions* $G_\pm(y,Y;\kappa=0)$

The solution for $G_\pm(y,Y;\kappa=0)$ is again obtained in exactly the same way as for $G_{\text{Kim}}(y,Y;\kappa=0)$ (§A.2.1), yielding by (A 32)

$$G_\pm(y,Y;\kappa=0)=G_{\mathfrak{V}}(y,Y;\kappa=0)=G_{\text{Kim}}(y,Y;\kappa=0)=\frac{|y-Y|}{2} \tag{A 34}$$

The boundary-conditions for the gradient at the wall $y=\mp\frac{1}{2}L_y$, and for boundedness at $\pm\infty$, are again satisfied by relations analogous to (A 28, A 33), iff the compatibility relation (A 24) holds.

A.2.5. *Accommodating the boundary-conditions for the halfspace problems ($\kappa=0$)*

Finally, the solution of the boundary-conditions (required for $p'_{(\tau)}$), in the case of the halfspace problems, can be obtained directly by integrating

$$\frac{d^2 q_{\text{BC}_\pm}(y;\kappa=0,B_\pm)}{dy^2}=0 \qquad \mp y\in(-\tfrac{1}{2}L_y,+\infty) \tag{A 35a}$$

$$\frac{dq_{\text{BC}_\pm}}{dy}(y=\pm\tfrac{1}{2}L_y;\kappa=0,B_\pm)=B_\pm(\kappa=0) \tag{A 35b}$$

The solution is obviously a straight line of slope $B_\pm(\kappa=0)$, and is bounded as $|y|\to\infty$ iff the compatibility condition

$$B_\pm(\kappa=0)=0\Longrightarrow q_{\text{BC}_\pm}(y;\kappa=0,B_\pm)=0 \tag{A 36}$$

holds.

A.3. *Approximation error in the method of images*

One interesting application of the halfspace problems is that, by superposition, they give the solution obtained by the method of images (Manceau *et al.* 2001). Indeed the method of images corresponds to applying the freespace Green's function on the domain $y\in(-\frac{1}{2}L_y,+\frac{1}{2}L_y)$, and on 2 ghost domains $y\in(-\frac{3}{2}L_y,-\frac{1}{2}L_y)\cup(+\frac{1}{2}L_y,+\frac{3}{2}L_y)$, with appropriately reflected source-terms

$$Q_{\text{MWL}}(y;\kappa)=Q(-L_y-y;\kappa) \qquad y\in(-\tfrac{3}{2}L_y,-\tfrac{1}{2}L_y) \tag{A 37a}$$

$$Q_{\text{MWL}}(y;\kappa)=Q(y;\kappa) \qquad y\in(-\tfrac{1}{2}L_y,+\tfrac{1}{2}L_y) \tag{A 37b}$$

$$Q_{\text{MWL}}(y;\kappa)=Q(+L_y-y;\kappa) \qquad y\in(+\tfrac{1}{2}L_y,+\tfrac{3}{2}L_y) \tag{A 37c}$$

and the approximation to the solution obtained by the method of images used by Manceau *et al.* (2001)† is

$$q_{\text{MWL}}(y;\kappa)=\int_{-\frac{3}{2}L_y}^{+\frac{3}{2}L_y} G_{\mathfrak{V}}(y,Y;\kappa)\,Q_{\text{MWL}}(Y;\kappa)\,dY \tag{A 38}$$

It is straightforward to construct a kernel $G_{\text{MWL}}(y,Y;\kappa)$ which applied on the source-terms in the actual computational domain $y\in(-\frac{1}{2}L_y,-\frac{1}{2}L_y)$ will return the method of images, because, defining $Y_\pm := \pm L_y - Y$, we have

---

† Although Manceau *et al.* (2001) neglect $q_{\text{BC}}(y;\kappa,B_\pm)$, this can be added to $q_{\text{MWL}}(y;\kappa)$ (A 38) to obtain the approximation of the complete solution (A 10a).

$$\begin{aligned}
q_{\mathrm{MWL}}(y;\kappa) - q_{\mathrm{BC}}(y;\kappa,B_\pm) &= \int_{-\frac{3}{2}L_y}^{+\frac{3}{2}L_y} G_{\mathfrak{V}}(y,Y;\kappa)\; Q_{\mathrm{MWL}}(Y;\kappa)\; dY \\
&\overset{(\mathrm{A}\,37),(\mathrm{A}\,38)}{=} \int_{-\frac{3}{2}L_y}^{-\frac{1}{2}L_y} G_{\mathfrak{V}}(y,Y;\kappa)\; Q(-L_y - Y;\kappa)\; dY \\
&\quad + \int_{-\frac{1}{2}L_y}^{+\frac{1}{2}L_y} G_{\mathfrak{V}}(y,Y;\kappa)\; Q(Y;\kappa)\; dY \\
&\quad + \int_{+\frac{1}{2}L_y}^{+\frac{3}{2}L_y} G_{\mathfrak{V}}(y,Y;\kappa)\; Q(+L_y - Y;\kappa)\; dY \\
&= - \int_{+\frac{1}{2}L_y}^{-\frac{1}{2}L_y} G_{\mathfrak{V}}(y,-L_y - Y_-;\kappa)\; Q(Y_-;\kappa)\; dY_- \\
&\quad + \int_{-\frac{1}{2}L_y}^{+\frac{1}{2}L_y} G_{\mathfrak{V}}(y,Y;\kappa)\; Q(Y;\kappa)\; dY \\
&\quad - \int_{+\frac{1}{2}L_y}^{-\frac{1}{2}L_y} G_{\mathfrak{V}}(y,L_y - Y_+;\kappa)\; Q(Y_+;\kappa)\; dY_+
\end{aligned} \tag{A 39}$$

yielding

$$q_{\mathrm{MWL}}(y;\kappa) = \int_{-\frac{1}{2}L_y}^{+\frac{1}{2}L_y} G_{\mathrm{MWL}}(y,Y;\kappa)\; Q(Y;\kappa)\; dY \tag{A 40a}$$

$$G_{\mathrm{MWL}}(y,Y;\kappa) := G_{\mathfrak{V}}(y,Y;\kappa) + G_{\mathfrak{V}}(y,-L_y - Y;\kappa) + G_{\mathfrak{V}}(y,L_y - Y;\kappa) \tag{A 40b}$$

and by (A 13)

$$G_{\mathrm{MWL}}(y,Y;\kappa \neq 0) \overset{(\mathrm{A}\,13)}{=} -\frac{\mathrm{e}^{-\kappa|y-Y|}}{2\kappa} - \frac{\mathrm{e}^{-\kappa|L_y+y+Y|}}{2\kappa} - \frac{\mathrm{e}^{-\kappa|L_y-y-Y|}}{2\kappa} \tag{A 40c}$$

Notice that (A 40) gives† the solution by integrating the sources in the actual domain $Y \in [-\frac{3}{2}L_y, -\frac{1}{2}L_y]$ with an approximate Green's functions $G_{\mathrm{MWL}}(y,Y;\kappa)$ (A 40*b*). This representation (A 40) readily yields the approximation error of the method of images, by comparison with the exact solution (A 9*b*) obtained using $G_{\mathrm{Kim}}(y,Y;\kappa)$. If we consider the actual domain $y, Y \in [-\frac{1}{2}L_y, +\frac{1}{2}L_y]$, we have

$$\left.\begin{array}{l} -\frac{1}{2}L_y \le y \le +\frac{1}{2}L_y \\ -\frac{1}{2}L_y \le Y \le +\frac{1}{2}L_y \end{array}\right\} \Longrightarrow \left\{\begin{array}{l} L_y + (y+Y) \ge 0 \\ L_y - (y+Y) \ge 0 \end{array}\right. \tag{A 41a}$$

---

† (A 40) is the 1-D equivalent of (Manceau *et al.* 2001, (4.2), p. 314)

so that

$$\begin{aligned}
G_{\text{MWL}}(y,Y;\kappa\neq 0) &\overset{(\text{A}\,40c,\ \text{A}\,41)}{=} -\frac{\mathrm{e}^{-\kappa|y-Y|}}{2\kappa} \\
&\qquad -\frac{\mathrm{e}^{-\kappa(L_y+y+Y)}}{2\kappa} \\
&\qquad -\frac{\mathrm{e}^{-\kappa(L_y-y-Y)}}{2\kappa} \qquad \forall y,Y\in[-\tfrac{1}{2}L_y,+\tfrac{1}{2}L_y] \qquad (\text{A}\,41b) \\
&\overset{(\text{A}\,13,\ \text{A}\,17)}{=} G_{\mathfrak{V}}(y,Y;\kappa\neq 0) \\
&\qquad +\underbrace{G_{-}(y,Y;\kappa\neq 0)-G_{\mathfrak{V}}(y,Y;\kappa\neq 0)}_{G_{w_-}(y,Y;\kappa\neq 0\ (\text{A}\,18))} \\
&\qquad +\underbrace{G_{+}(y,Y;\kappa\neq 0)-G_{\mathfrak{V}}(y,Y;\kappa\neq 0)}_{G_{w_+}(y,Y;\kappa\neq 0)\ (\text{A}\,18)} \\
&\qquad\qquad \forall y,Y\in[-\tfrac{1}{2}L_y,+\tfrac{1}{2}L_y] \qquad (\text{A}\,41c)
\end{aligned}$$

ie, the images problem (Manceau *et al.* 2001) is equivalent to adding to the freespace Green's function an independent wall-echo correction for each wall, the wall-echo correction for the upper (lower) wall being exactly the wall-echo of the halfspace problem with only the upper (lower) wall present (§A.1.4). Notice that by (A 34) $G_{w_-}(y,Y;\kappa=0)=G_{w_+}(y,Y;\kappa=0)=0$ so that (A 41*c*) holds $\forall\kappa\in\mathbb{R}_{\geq 0}$.

By (A 9*b*, A 41*b*) we may directly compute the error made when approximating the Green's function by the method of images

$$\begin{aligned}
&\frac{1}{L_y}\Big(G_{\text{MWL}}(y,Y;\kappa\neq 0)-G_{\text{Kim}}(y,Y;\kappa\neq 0)\Big) \overset{(\text{A}\,9b,\ \text{A}\,41b)}{=} \\
&\frac{\mathrm{e}^{-\kappa L_y}}{2\kappa L_y\sinh\kappa L_y}\Big(\cosh\kappa|y-Y|+\mathrm{e}^{-\kappa L_y}\cosh\kappa(y+Y)\Big) \qquad (\text{A}\,42) \\
&\qquad\qquad \forall y,Y\in[-\tfrac{1}{2}L_y,+\tfrac{1}{2}L_y]
\end{aligned}$$

where (A 42) was made nondimensional by dividing the Green's functions by L_y. Obviously

$$y,Y\in[-\tfrac{1}{2}L_y,+\tfrac{1}{2}L_y]\Longrightarrow \left.\begin{array}{l} 0\leq|y-Y|\leq L_y \\ 0\leq|y+Y|\leq L_y \end{array}\right\}\Longrightarrow\left\{\begin{array}{l} 0\leq\cosh\kappa|y-Y|\leq\cosh\kappa L_y \\ 0\leq\cosh\kappa|y+Y|\leq\cosh\kappa L_y \end{array}\right. \qquad (\text{A}\,43)$$

since $\cosh x=\cosh|x|$ is positive ans strictly increasing $\forall|x|\in\mathbb{R}_{\geq 0}$. Hence†

$$\begin{aligned}
&\frac{1}{L_y}\left(\max_{y,Y\in[-\frac{1}{2}L_y,+\frac{1}{2}L_y]}\Big|G_{\text{MWL}}(y,Y;\kappa)-G_{\text{Kim}}(y,Y;\kappa)\Big|\right)\leq \\
&\qquad\qquad \underbrace{\frac{\mathrm{e}^{-\kappa L_y}(1+\mathrm{e}^{-\kappa L_y})\cosh\kappa L_y}{2\kappa L_y\sinh\kappa L_y}}_{E_{\text{MWL}}(\kappa L_y)} \qquad (\text{A}\,44)
\end{aligned}$$

showing that the approximation error made by the method of images is a function of the nondimensional (outer scaling) wavenumber κL_y (Fig. 4).

---

† notice also that by (A 42) $G_{\text{MWL}}(y,Y;\kappa\neq 0)-G_{\text{Kim}}(y,Y;\kappa\neq 0)\geq 0\ \forall y,Y\in[-\tfrac{1}{2}L_y,+\tfrac{1}{2}L_y]$

REFERENCES

Al-Sharif, S. F., Cotton, M. A. & Craft, T. J. 2010 Reynolds stress transport models in unsteady and non-equilibrium turbulent flows. *Int. J. Heat Fluid Flow* **31**, 401–408.

del Álamo, J. C. & Jiménez, J. 2003 Spectra of the very large anisotropic scales in turbulent channels. *Phys. Fluids* **15** (6), L41–L44.

del Álamo, J. C., Jiménez, J., Zandonade, P. & Moser, R. D. 2004 Scaling of the energy spectra of turbulent channels. *J. Fluid Mech.* **500**, 135–144.

Balakumar, B. J. & Adrian, R. J. 2007 Large- and very-large scale motions in channel and boundary-layer flows. *Phil. Trans. Roy. Soc. London A* **365**, 665–681.

Batten, P., Craft, T. J., Leschziner, M. A. & Loyau, H. 1999 Reynolds-stress-transport modeling for compressible aerodynamics applications. *AIAA J.* **37** (7), 785–797.

Bender, C. M. & Orszag, S. A. 1978 *Advanced Mathematical Methods for Scientists and Engineers*, pp. 16–19 (Green's function for ODEs). New York [NY, USA]: Springer.

Briggs, W. L. & Henson, V. E. 1995 *The DFT: An Owner's Manual for the Discrete Fourier Transform*, pp. 144–150 (2–D DFT). Philadelphia [PA, USA]: SIAM.

Chang, III, P. A., Piomelli, U. & Blake, W. K. 1999 Relations between wall-pressure and velocity-field sources. *Phys. Fluids* **11** (11), 3434–3448.

Cheng, H., Huang, J. & Leiterman, T. J. 2006 An adaptive fast solver for the modified helmholtz equation in 2-D. *J. Comp. Phys.* **211**, 616–637.

Chou, P. Y. 1945 On velocity correlations and the solutions of the equations of turbulent fluctuations. *Quart. Appl. Math.* **3**, 38–54.

Corcos, G. M. 1964 The structure of the turbulent pressure field in boundary-layer flows. *J. Fluid Mech.* **18**, 353–378.

Courant, R. & Hilbert, D. 1953 *Methods of Mathematical Physics I*, pp. 351–358 (Green's function for ODEs), 371–377 (examples of Green's function for ODEs). New York [NY, USA]: Interscience.

Craft, T. J. 1998 Developments in a low-Reynolds-number second-moment closure and its application to separating and reattaching flows. *Int. J. Heat Fluid Flow* **19**, 541–548.

Craft, T. J. & Launder, B. 1996 A Reynolds-stress model designed for complex geometries. *Int. J. Heat Fluid Flow* **17**, 245–254.

Daly, B. J. & Harlow, F. H. 1970 Transport equations in turbulence. *Phys. Fluids* **13**, 2634–2649.

Demuren, A. O., Lele, S. K. & Durbin, P. 1994 Role of pressure diffusion in non-homogeneous shear flows. Studying Turbulence Using Numerical Simulation Databases - V, Proceeding of the CTR Summer Program 1996, Center for Turbulence Reasearch, NASA Ames/Stanford University [USA].

Demuren, A. O., Rogers, M. M., Durbin, P. & Lele, S. K. 1996 On modelling pressure diffusion in non-homogeneous shear flows. Studying Turbulence Using Numerical Simulation Databases - VI, Proceeding of the CTR Summer Program 1996, Center for Turbulence Reasearch, NASA Ames/Stanford University [USA].

Demuren, A. O. & Sarkar, S. 1993 Perspective : Systematic study of Reynolds closure models in the computations of plane channel flows. *ASME J. Fluids Eng.* **115**, 5–12.

Donaldson, C. duP. 1969 A computer study of an analytical model of boundary-layer transition. *AIAA J.* **7** (2), 271–278.

Durbin, P. A. 1993 A Reynolds-stress model for near-wall turbulence. *J. Fluid Mech.* **249**, 465–498.

Foysi, H., Sarkar, S. & Friedrich, R. 2004 Compressibility effects and turbulence scalings in supersonic channel flow. *J. Fluid Mech.* **509**, 207–216.

Fu, S. 1988 Computational modelling of turbulent swirling flows with second-moment closures. Phd thesis, University of Manchester Institute of Science and Technology, Manchester [GBR].

Fu, S. 1993 Modelling of the pressure-velocity correlation in turbulence diffusion. *Comp. Fluids* **22**, 199–205.

Fu, S. & Wang, C. 1997 Second-moment closure modelling of turbulence in a noninertial frame. *Fluid Dyn. Res.* **20**, 43–65.

Gerolymos, G. A., Joly, S., Mallet, M. & Vallet, I. 2010*a* Reynolds-stress model flow prediction in aircraft-engine intake double-S-shaped duct. *J. Aircraft* **47** (4), 1368–1381.

Gerolymos, G. A., Lo, C. & Vallet, I. 2010*b* Tensorial representations of Reynolds-stress redistribution. *ArXiv* **2010**, 1012.2865v1(1–4), (submitted for publication).

Gerolymos, G. A., Neubauer, J., Sharma, V. C. & Vallet, I. 2002 Improved prediction of turbomachinery flows using near-wall Reynolds-stress model. *ASME J. Turbom.* **124** (1), 86–99.

Gerolymos, G. A., Sauret, E. & Vallet, I. 2004 Contribution to the single-point-closure Reynolds-stress modelling of inhomogeneous flow. *Theor. Comp. Fluid Dyn.* **17** (5–6), 407–431.

Gerolymos, G. A., Sénéchal, D. & Vallet, I. 2009 Very-high-order weno schemes. *J. Comp. Phys.* **228**, 8481–8524.

Gerolymos, G. A., Sénéchal, D. & Vallet, I. 2010*c* Performance of very-high-order upwind schemes for dns of compressible wall-turbulence. *Int. J. Num. Meth. Fluids* **63**, 769–810.

Gerolymos, G. A. & Vallet, I. 2001 Wall-normal-free near-wall Reynolds-stress closure for 3-D compressible separated flows. *AIAA J.* **39** (10), 1833–1842.

Gerolymos, G. A. & Vallet, I. 2002 Wall-normal-free Reynolds-stress model for rotating flows applied to turbomachinery. *AIAA J.* **40** (2), 199–208.

Gerolymos, G. A. & Vallet, I. 2009 aerodynamics (a library and software package for computational aerodynamics). http://sourceforge.net/projects/aerodynamics.

Gibson, M. M. & Launder, B. E. 1978 Ground effects on pressure fluctuations in the atmospheric boundary-layer. *J. Fluid Mech.* **86**, 491–511.

Hamba, F. 1999 Effects of pressure fluctuations on turbulence growth in compressible homogeneous shear flow. *Phys. Fluids* **11** (6), 1623–1635.

Hanjalić, K. 1994 Advanced turbulence closure models: A view of current status and future prospects. *Int. J. Heat Fluid Flow* **15**, 178–203.

Hanjalić, K. & Jakirlić, S. 1993 A model of stress dissipation in second-moment closures. *Appl. Sci. Res.* **51**, 513–518.

Hanjalić, K. & Jakirlić, S. 1998 Contribution towards the second-moment closure modelling of separating turbulent flows. *Comp. Fluids* **27**, 137–156.

Hanjalić, K. & Launder, B. E 1972 A Reynolds stress model of turbulence and its application to thin shear flows. *J. Fluid Mech.* **52**, 609–638.

Harris, J. W. & Stocker, H. 1998 *Handbook of Mathematics and Computational Science*. New York [ny, usa]: Springer Verlag.

Hirt, C. W. 1969 Generalized turbulence transport equations. Int Sem. of Int. Center for Heat and Mass Transfer, Herceg Novi, Yugoslavia.

Hoyas, S. & Jiménez, J. 2006 Scaling of the velocity fluctuations in turbulent channels up to $Re_\tau = 2003$. *Phys. Fluids* **18**, 011702(1–4).

Hoyas, S. & Jiménez, J. 2008 Reynolds number effects on the Reynolds-stress budgets in turbulent channels. *Phys. Fluids* **20**, 101511(1–8).

Hu, Z. W., Morfey, C. L. & Sandham, N. D. 2002 Aeroacoustics of wall-bounded turbulent flow. *AIAA J.* **40** (3), 465–473.

Hu, Z. W., Morfey, C. L. & Sandham, N. D. 2006 Wall pressure and shear stress spectra from direct simulations of channel flow. *AIAA J.* **44** (7), 1541–1549.

Hu, Z. W. & Sandham, N. D. 2001 dns databases for turbulent Couette and Poiseuille flow. Tech. Rep. AFM–01–04. afm Research Group, School of Engineering Sciences, University of Southampton.

Hutchins, N. & Marusic, I. 2007 Evidence of very long meandering features in the logarithmic region of turbulent boundary-layers. *J. Fluid Mech.* **579**, 1–28.

Ince, I. L. 1926 *Ordinary Differential Equations*, 1st edn., pp. 123–126 (adjoint linear differential operator), 254–263 (Green's functions), 266–269 (compatibility conditions). New York [ny, usa]: Dover.

Jakirlić, S., Eisfeld, B., Jester-Zürker, R. & Kroll, N. 2007 Near-wall reynolds-stress model calculations of transonic flow configurations relevant to aircraft aerodynamics. *Int J. Heat Fluid Flow* **28**, 602–615.

Jakirlić, S. & Hanjalić, K. 2002 A new approach to modelling near-wall turbulence energy and stress dissipation. *J. Fluid Mech.* **459**, 139–166.

Jovanović, J. 2004 *The Statistical Dynamics of Turbulence*. Berlin [d]: Springer.

Katz, J. & Plotkin, A. 1991 *Low-Speed Aerodynamics: From Wing Theory to Panel Methods*, pp. 52–57 (kernel solution of the Laplace equation). New York [ny, usa]: McGraw-Hill.

Kim, J. 1989 On the structure of pressure fluctuations in simulated turbulent channel-flow. *J. Fluid Mech.* **205**, 421–451.

Kim, J., Moin, P. & Moser, R. 1987 Turbulence statistics in fully developed channel flow at low-Reynolds-number. *J. Fluid Mech.* **177**, 133–166.

Launder, B. E., Reece, G. J. & Rodi, W. 1975 Progress in the development of a Reynolds-stress turbulence closure. *J. Fluid Mech.* **68**, 537–566.

Launder, B. E. & Shima, N. 1989 2-moment closure for the near-wall sublayer: Development and application. *AIAA J.* **27** (10), 1319–1325.

Lumley, J. L. 1978 Computational modeling of turbulent flows. *Adv. Appl. Mech.* **18**, 123–176.

Manceau, R., Wang, M. & Laurence, D. 2001 Inhomogeneity and anisotropy effects on the redistribution term in Reynolds-averaged Navier-Stokes modelling. *J. Fluid Mech.* **438**, 307–338.

Mansour, N. N., Kim, J. & Moin, P. 1988 Reynolds-stress and dissipation-rate budgets in a turbulent channel flow. *J. Fluid Mech.* **194**, 15–44.

Mellor, G. L. & Herring, H. J. 1973 A survey of the mean turbulent field closure models. *AIAA J.* **11** (5), 590–599.

Moin, P. & Mahesh, K. 1998 Direct numerical simulation: A tool in turbulence research. *Ann. Rev. Fluid Mech.* **30**, 539–578.

Monin, A. S. & Yaglom, A. M. 1971 *Statistical fluid mechanics: Mechanics of turbulence*, vol. 1. Cambridge [ma, usa]: MIT Press.

Moser, R. D., Kim, J. & Mansour, N. N. 1999 Direct numerical simulation of turbulent channel flow up to $Re_\tau = 590$. *Phys. Fluids* **11** (4), 943–945.

Myint-U, T. & Debnath, L. 2007 *Linear Partial Differential Equations for Scientists and Engineers*, 4th edn., pp. 310–317 (Green's function). Boston [ma, usa]: Birkhäuser.

Naka, Y., Omori, T., Obi, S. & Masuda, S. 2006 Simultaneous measurements of fluctuating velocity and pressure in a turbulent mixing layer. *Int. J. Heat Fluid Flow* **27**, 737–746.

Naot, D., Shavit, A. & Wolfshtein, M. 1970 Interactions between components of the turbulent velocity correlation tensor due to pressure fluctuations. *Israel J. Techn.* **8** (3), 259–269.

Naot, D., Shavit, A. & Wolfshtein, M. 1973 2-point-correlation model and the redistribution of Reynolds-stresses. *Phys. Fluids* **16** (6), 738–743.

Oceni, A. G., Manceau, R. & Gatski, T. B. 2008 A hierarchy of explicit algebraic models for wall-bounded flows. In *Proceedings 7. ERCOFTAC International Symposium on Engineering Turbulence Modelling and Measurements (ETMM7), 4–6 jun 2008, Limassol, [cyp]* (ed. M. A. Leschziner, S. Kassinos, J. P. Bonnet, D. Laurence, W. Rodi, A. Tomboulides & C. Tropea), , vol. 1, pp. 83–88.

Ockendon, J., Howison, S., Lacey, A. & Movchan, A. 2003 *Applied Partial Differential Equations*, revised edn., pp. 163–166 (well–posedness for Poisson equation), 169–174 (Green's function). Oxford [gbr]: Oxford University Press.

Panton, R. L. & Linebarger, J. H. 1974 Wall pressure spectra calculations for equilibrium boundary-layers. *J. Fluid Mech.* **65**, 261–287.

Patel, V. C., Rodi, W. & Scheuerer, G. 1985 Turbulence models for near-wall and low-Reynolds-number flows: A review. *AIAA J.* **23**, 1308–1319.

Piquet, J. 1999 *Turbulent Flows — Models and Physics*. Berlin [d]: Springer Verlag.

Pope, S. B. 2000 *Turbulent Flows*. Cambridge [gbr]: Cambridge University Press.

Reynolds, W. C. 1974 Recent advances in the computation of turbulent flows. *Adv. Chem. Eng.* **9**, 193–246.

Ristorcelli, J. R., Lumley, J. L. & Abid, R. 1995 A rapid-pressure covariance representation consistent with the Taylor-Proudman theorem materially frame indifferent in the 2-D limit. *J. Fluid Mech.* **292**, 111–152.

Rivlin, R. S. 1955 The theory of matrix polynomials and its application to the mechanics of isotropic continua. *Indiana Univ. Math. J.* **4**, 681–702.

Rivlin, R. S. & Ericksen, J. L. 1955 Stress-deformation relations for isotropic materials. *Indiana Univ. Math. J.* **4**, 323–425.

Rogers, M. M. & Moser, R. D. 1994 Direct simulation of a self-similar turbulent mixing layer. *Phys. Fluids* **6** (2), 903–923.

Rotta, J. 1951*a* Statistische Theorie nichthomogener Turbulenz — 1. Mitteilung. *Z. Phys.* **129**, 547–572.

Rotta, J. 1951*b* Statistische Theorie nichthomogener Turbulenz — 2. Mitteilung. *Z. Phys.* **131**, 51–77.

Sambasivam, A., Girimaji, S. S. & Poroseva, S. V. 2004 Realizability of the reynolds-stress and rapid pressure-strain correlation to turbulence modelling. *J. Turb.* **5**, 000006(1–22).

Sauret, E. & Vallet, I. 2007 Near-wall turbulent pressure diffusion modelling and influence in 3-D secondary flows. *ASME J. Fluids Eng.* **129** (5), 634–642.

Schiestel, R. 2007 *Modelling and Simulation of Turbulent Flows*. John Wiley and Sons.

Schwarz, W. R. & Bradshaw, P. 1994 Term-by-term tests of stress-transport turbulence models in a 3-D boundary-layer. *Phys. Fluids A* **6** (2), 986–998.

Shih, T. H. & Lumley, J. L. 1993 Critical comparison of 2-order closures with direct numerical simulations of homogeneous turbulence. *AIAA J.* **31** (4), 663–670.

Shima, N. 1988 A Reynolds-stress model for near-wall and low-Reynolds-number regions. *ASME J. Fluids Eng.* **110**, 38–44.

Shima, N. 1993*a* Prediction of turbulent boundary-layer flows with a 2-moment closure — Part 1 — Effects of periodic pressure gradient, wall transpiration, and free-stream turbulence. *ASME J. Fluids Eng.* **115**, 56–63.

Shima, N. 1993*b* Prediction of turbulent boundary-layer flows with a 2-moment closure — Part 2 — Effects of streamline curvature and spanwise rotation. *ASME J. Fluids Eng.* **115**, 64–69.

Shir, C. C. 1973 A preliminary numerical study of atmospheric turbulent flows in the idealized planetary boundary-layer. *J. Atm. Sci.* **30**, 1327–1339.

Simonsen, A. J. & Krogstad, P. Å. 2005 Turbulent stress invariant analysis: Classification of existing terminology. *Phys. Fluids* **17**, 088103(1–4).

Smith, G. F. 1971 On isotropic functions of symmetric tensors, skew-symmetric tensors and vectors. *Int. J. Eng. Sci.* **9**, 899–916.

So, R. M. C., Aksoy, H., Yuan, S. P. & Sommer, T. P. 1996 Modeling Reynolds-number effects in wall-bounded turbulent flows. *ASME J. Fluids Eng.* **118**, 260–267.

So, R. M. C., Lai, Y. G., Zhang, H. S. & Hwang, B. C. 1991 2-order near-wall turbulence closures: A review. *AIAA J.* **29**, 1819–1835.

Spencer, A. J. M. & Rivlin, R. S. 1959 The theory of matrix polynomials and its application to the mechanics of isotropic continua. *Arch. Rat. Mech. Anal.* **2**, 309–336.

Speziale, C. G., Sarkar, S. & Gatski, T. B. 1991 Modelling the pressure-strain correlation of turbulence: An invariant dynamical systems approach. *J. Fluid Mech.* **227**, 245–272.

Straatman, A. G. 1999 A modified model for diffusion in second-moment turbulence closures. *ASME J. Fluids Eng.* **121** (4), 747–756.

Suga, K. 2004 Modeling the rapid part of the pressure-diffusion process in the Reynolds stress transport equation. *ASME J. Fluids Eng.* **126**, 634–641.

Townsend, A. A. 1956 *The structure of turbulent shear flow*. Cambridge [gbr]: Cambridge University Press.

Vallet, I. 2007 Reynolds-stress modelling of 3-D secondary flows with emphasis on turbulent diffusion closure. *ASME J. Appl. Mech.* **74** (6), 1142–1156.

Vallet, I. 2008 Reynolds-stress modelling of $M = 2.25$ shock-wave/turbulent-boundary-layer interaction. *Int. J. Num. Meth. Fluids* **56** (5), 525–555.

Wallin, S. & Johansson, A. V. 2000 An explicit algebraic reynolds-stress model for incompressible and compressible turbulent flows. *J. Fluid Mech.* **403**, 89–132.

Younis, B. A., Gatski, T. B. & Speziale, C. G. 2000 Towards a rational model for the triple velocity correlations of turbulence. *Proc. Royal Society Lon. A* **456**, 909–920.

Zauderer, E. 2006 *Partial Differential Equations of Applied Mathematics*, pp. 446–447 (Green's function for odes), 451–454 (modified Green's function). Hoboken [nj, usa]: Wiley.